Contribution of the Fronto-parietal Cortical Dynamics to Grip Force Control

By

Nishant Rao

A thesis/dissertation submitted to the Department of Health and Human Performance,

College of Liberal Arts and Social Sciences

In partial fulfillment of the requirements for the degree of

Doctor of Philosophy

in Kinesiology

Chair of the Committee: Dr. Pranav J. Parikh (HHP, UH)

Committee Members: Dr. Stacey Gorniak (HHP, UH)

Dr. Charles Layne (HHP, UH)

Dr. Jose L. Contreras-Vidal (ECE, UH)

Dr. Sheng Li (UTHealth, TIRR Memorial Hermann)

University of Houston

May 2022

DEDICATION/EPIGRAPH

This work is dedicated to the tireless efforts, persistent support, and constant goodwill of all those who make this journey worthwhile.

ACKNOWLEDGEMENTS

I am extremely grateful to my advisor, mentor, and guru Dr. Pranav J. Parikh for imparting a diligent training in research as well as in professional fronts. His balanced outlook towards PhD education has been pivotal in leading me where I am today. I am thankful for all the insightful discussions and thoughtful perspectives we shared that have inspired me to push my boundaries. Thanks to the grants including the NIH NM4R grant (PI: PJP), the UH High Priority Area Research Seed Grant (PI: PJP), the SfN TPD Award (to NR), the Cullen fellowships (NR) and Department of Health and Human Performance Doctoral Student Research Award (NR) for funding our studies. I would like to thank Dr. Contreras-Vidal from the ECE department particularly for his commitment towards my EEG training, providing critical insights to my research, his generous support, and introducing me to several interesting opportunities that helped me expand my professional outlook. I am glad also to be a part of the ongoing collaboration and build upon the research study conducted by Dr. Andrew Paek and team. Thanks, Dr. Paek, for introducing me to the project. I thank my committee members Dr. Gorniak, Dr. Layne, and Dr. Li for their valuable feedback on my dissertation and throughout my PhD journey. Special thanks to John Kass, Landon, and Grace for your assistance at various stages of the study. It has been a pleasure working with all the Parikh lab members, and of course the fellow HHP grad students – you all make the PhD pursuit bearable. A big shout out to the HHP staff for all your help. To all my friends and family – thanks for adding fun atop your constant support. I am thankful to my parents for their encouragement throughout my journey. Finally, Taruna – my wife and a fellow science-enthusiast, is to thank for having a steadfast belief in me and keeping my life flavorful.

ABSTRACT

While holding a coffee mug filled to the brim, we strive to avoid spilling the coffee. This ability relies on the interaction between the control of finger forces on a moment-to-moment basis and the visual information about the object. Such sensorimotor interaction is affected in patients with stroke, Parkinson's disease, and cerebral palsy. Studies investigating force control have shown that fluctuations in the exerted force are not mere noise but arise from systematic physiological processes. Most recent evidence points toward a link between neural activity within the fronto-parietal brain regions including primary motor cortex (M1) and the fluctuations in grip force. However, specific contribution of the cortical activity to regulation of grip force remains unclear. This is a significant research gap because it limits our understanding about how the brain enables efficient control of grip forces during grasping. The current dissertation focused on bridging this research gap using noninvasive neuromodulation and neuroimaging approaches via two specific aims. In Aim-1, we determined the causal involvement of M1 in regulating grip force variability using transcranial magnetic stimulation (TMS) among healthy young individuals. Consistent with our hypothesis, temporary disruption of M1 resulted in upregulation of the grip force variability when compared to that post sham (placebo) stimulation. Interestingly, this upregulation was observed when visual feedback of the exerted grip force was available, but not when the visual feedback of the exerted grip force was removed, indicating the critical role of M1 in integrating visuomotor information for regulating grip force variability. In Aim-2, we examined the dependence of lateralized fronto-parietal neural activity on grip force magnitude during a grip force control task using noninvasive electroencephalography (EEG). Accumulating evidence suggests mechanistic role of neural variability in cognitive

processes that scale with task demands. Consequently, we hypothesized laterally specific modulation in EEG variability with increasing magnitude of the grip force exerted during an isometric grip force control task in healthy young individuals. Consistent with our hypothesis, the neural variability was found to be lateralized, topographically constrained, and functionally dependent on the grip force magnitude thereby, showcasing the influence of force-dependent behavioral processes on neural variability. Taken together, this dissertation underscores the integral role of M1 and associated fronto-parietal cortical activity during grip force control. We highlight the relevance of these findings to the rehabilitation of upper extremity motor functions among patients with sensorimotor deficits and propose directions for future studies investigating neural correlates of digit force control.

TABLE OF CONTENTS

LIST OF TABLES

LIST OF FIGURES

Chapter 1. Introduction

1.1. Chapter overview

This section is organized to convey the central problem statement in a brief, succinct description encompassing key findings from the previous studies leading to the identified research gaps. Noting the critical findings on physiological processes that characterize digit force control, we highlight the currently unclear contribution of specific cortical circuits in the fronto-parietal brain regions which underlie moment-to-moment force control. After an overview of our approach to bridge the research gaps, we describe the significance of the studies in the context of broader clinical biomedical research. The flowchart showing overview for this chapter is depicted in Figure 1.

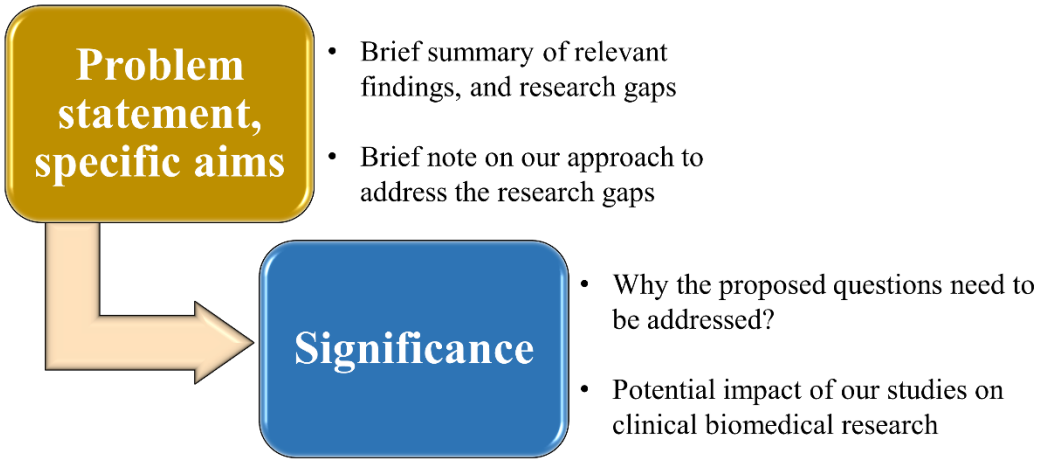

Figure 1: Flowchart of information organized in Chapter 1

1.2. Background and Problem statement

Efficient moment-to-moment force control ensures that we do not accidentally spill the coffee while drinking from a coffee mug filled to the brim. The seemingly simple task belies the underlying physiological complexity that is evident from aberrant moment-to-moment force control among patients with sensorimotor ailments (e.g. stroke, Parkinson's disease, cerebral palsy, and focal hand dystonia; Figure 2 (Fellows and Noth, 2003; Olivier et al., 2007; Chu and Sanger, 2009; Grafton, 2010; Lodha et al., 2013). Despite the ubiquitous nature of the task, mechanisms underlying moment-to-moment force control remain poorly understood.

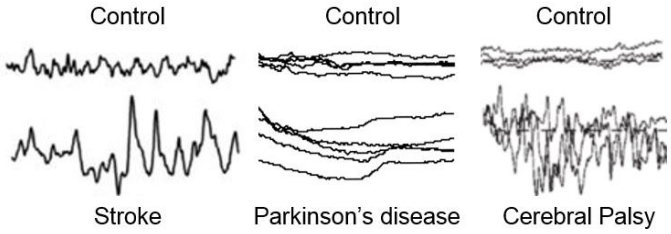

Figure 2: Force traces showing aberrant force variability among patients with stroke (Lodha et al. 2013), Parkinson's disease (Fellows and Noth 2003), and cerebral palsy (Chu et al. 2009)

Fluctuations (or variability) in grip forces during sustained isometric contractions are known to be a direct indicator of the regulation in grip forces (Lodha et al., 2013; Poon et al., 2013). Variability has been suggested to arise from the peripheral neuromuscular, subcortical, and cortical systems (Eisen et al., 1996; Bilodeau et al., 2000; Jones et al., 2002; Enoka et al., 2003; Vaillancourt et al., 2003a; Churchland et al., 2006a; Christou, 2011; Ko et al., 2015). Traditional views on the source of this variability primarily related it to motor noise whose amplitude increases with magnitude of the force exerted (Harris and Wolpert, 1998), attributing its origination to peripheral muscular processes (Galganski

et al., 1993; Slifkin and Newell, 1999; Slifkin et al., 2000; Enoka et al., 2003). However, recent modelling work has found marginal contribution of muscle dynamics and motor unit properties to force variability (Nagamori et al., 2021). For instance, modelling the population activity in motor units by incorporating motoneuron-motor unit discharge rate coupling, fusion of motor unit twitches, aponeurosis, and tendon elasticity failed to account for the experimentally observed trend in force variability with force magnitude (Nagamori et al., 2021). Similarly, the association between inter-spike interval variability in motor units and force fluctuations was found to be marginal (Feeney et al., 2018). On the other hand, these studies pointed out the contribution of variability in common synaptic inputs to motor neurons to force fluctuations, indicating significant contribution of central sources via descending tracts to motoneuronal pool in regulating force variability (Feeney et al., 2018; Nagamori et al., 2021). Our recent work found an association between the variability in corticospinal excitability to the variability in time to peak grip force rate during a similar isometric grip force production task (Rao and Parikh, 2019).

Importantly, the cortical activity within frontal and parietal regions may contribute to the variability in kinematic or kinetic features of motor output (Osborne et al., 2005; Churchland et al., 2006a; Fox et al., 2007; Hohl et al., 2013; Chaisanguanthum et al., 2014; Lisberger and Medina, 2015; Mizuguchi et al., 2016; Haar et al., 2017). Accumulating evidence is suggestive of central contributions to grip force variability (Jones et al., 2002; Vaillancourt et al., 2003b; Harris & Wolpert, 2004; Milner et al., 2007; Therrien et al., 2011, 2013; Poon et al., 2013; Lodha and Christou, 2017). Moreover, magnitude of grip forces is known to influence the associated neural activation specifically over the fronto-parietal brain regions (Ehrsson et al., 2000b, 2001; Poon et al., 2013) in addition to

inducing changes in the corticospinal excitability (Perez and Cohen, 2009; Bunday et al., 2014; Rao and Parikh, 2019). While the involvement of neural circuitry spanning prefrontal, premotor, primary motor (M1) and sensory cortices in digit force planning has been characterized earlier, the causal involvement of M1 in regulation of the grip force fluctuations **remains unclear**.

Studies aiming to understand the role of neural activation during grasping and digit force applications have primarily focused on the average neural activity (Aguirre et al., 1998; Ehrsson et al., 2000b; Vaillancourt et al., 2003b; Garrett et al., 2011a; Birn, 2012; Poon et al., 2013; Grady and Garrett, 2018). Importantly, averaging neural activation over multiple trials neglects the contribution of within-trial neural fluctuations to the task (Ehrsson et al., 2000b; Vaillancourt et al., 2003b; Garrett et al., 2011a; Poon et al., 2013). Recent evidence suggests critical role of fluctuations in neural activity (i.e., neural variability) during behavior (McIntosh et al., 2010; Garrett et al., 2011b; Grady and Garrett, 2014). For instance, recent human neuroimaging studies show that after controlling for average neural activity, neural variability across several brain regions increased while performing a cognitive task versus rest (Garrett et al., 2013a), and decreased with increasing difficulty in a fixation-based attentional task (Garrett et al., 2014). Researchers argue that neural variability adds complementary information about task-specific neural states, orthogonal from that inferred via average neural activity (Garrett et al., 2010, 2011b, 2013a, 2014). Importantly however, the contribution of neural variability to moment-to-moment grip force control **remains unknown**.

Taken together, these research gaps limit our understanding about neural processes that enable efficient moment-to-moment grip force control during grasping. Through this

dissertation, **we aimed at bridging these research gaps** using noninvasive neuromodulation and neuroimaging approach. The **overall hypothesis** of this dissertation is that the activity over the selected fronto-parietal regions critically underlie the moment-to-moment force control.

1.3. Specific aims

Aim-1 (neuromodulation): To determine the contribution of M1 to moment-to-moment grip force control at different force magnitudes. Grip force control is known to underlie physiological processes that maintain variations around the average force (as assessed by standard deviation, SD), as well as sequential variations over multiple timescales resulting from moment-to-moment sensorimotor corrections (quantified using multiscale sample entropy, MSE)(Slifkin and Newell, 1999; Vaillancourt and Newell, 2003; Lodha et al., 2013). These processes exhibit distinct relationship with grip force magnitude in presence (or absence) of visual feedback (Slifkin and Newell, 1999; Sosnoff et al., 2006). Notably, M1 is known to function as a 'central hub' in transforming motor commands critical for transient force applications(Ehrsson et al., 2001; Olivier et al., 2007; Davare et al., 2010; Grafton, 2010; Therrien et al., 2011; Parikh et al., 2014, 2020; Rao and Parikh, 2019). To test its causal involvement in the regulation of grip forces moment-to-moment, we employed transcranial magnetic stimulation (TMS)-based approach to temporarily induce inhibitory, excitatory, or sham (placebo) cortical plasticity over M1. Continuous or intermittent theta burst stimulation (cTBS, iTBS) are known to temporarily inhibit or facilitate M1 activity arguably via the long-term depression or potentiation-like mechanisms. The neuromodulation effects are known to last for ~25 minutes post stimulation (Huang et al., 2005; Teo et al., 2011; Vernet et al., 2013; Parikh et al., 2020).

Based on previous reports indicating reduction in force error following cTBS, and increased variability in thumb movement post iTBS (Voss et al., 2007; Teo et al., 2011), we hypothesized that: **Hypothesis 1a**- cTBS (or iTBS) over M1, when compared to sham, will decrease (or increase) sequential variations in MSE over multiple timescales in presence of visual feedback at each force magnitude, and that **Hypothesis 1b**- Sequence-independent component in grip force variability (assessed via SD, CV) will decrease (or increase) post cTBS (or iTBS) respectively when compared to sham over M1, at a given force magnitude in presence of visual feedback.

Aim-2 (neuroimaging): <u>To determine the contribution of variability in fronto-parietal neural activity to grip force fluctuations.</u> Neural variability has been shown to systematically modulate with task demands, cognitive states, and the involvement of associated neural resource. Despite the potential applicability and significance of brain signal variability to sensorimotor behavior, its contribution to the control of grip force remains unknown. Considering the evidence that fronto-parietal cortical processing for digit force control applications is spatially lateralized (Ehrsson et al., 2001; Vaillancourt et al., 2003b; Davare et al., 2008; Poon et al., 2012, 2013), we hypothesized that variability in electroencephalography (EEG) activity recorded over the fronto-parietal region will be lateralized and systematically modulated with increase in grip force magnitude. To characterize the modulation in sequential and sequence-independent components of neural variability over fronto-parietal regions with grip force magnitude, we recorded participants' EEG activity as they performed an isometric force production task (Figure 3). We performed SD and sE-based analyses of fronto-parietal electrocortical activity (via EEG) and grip force variability to test – **Hypothesis 2a**: sE in EEG activity recorded over

the fronto-parietal region will be greater in the left (contralateral) hemisphere and will be systematically modulated with grip force magnitude; and **Hypothesis 2b**: SD in fronto-parietal EEG variability will be greater in left (contralateral) and will show systematic changes depending upon the force magnitude.

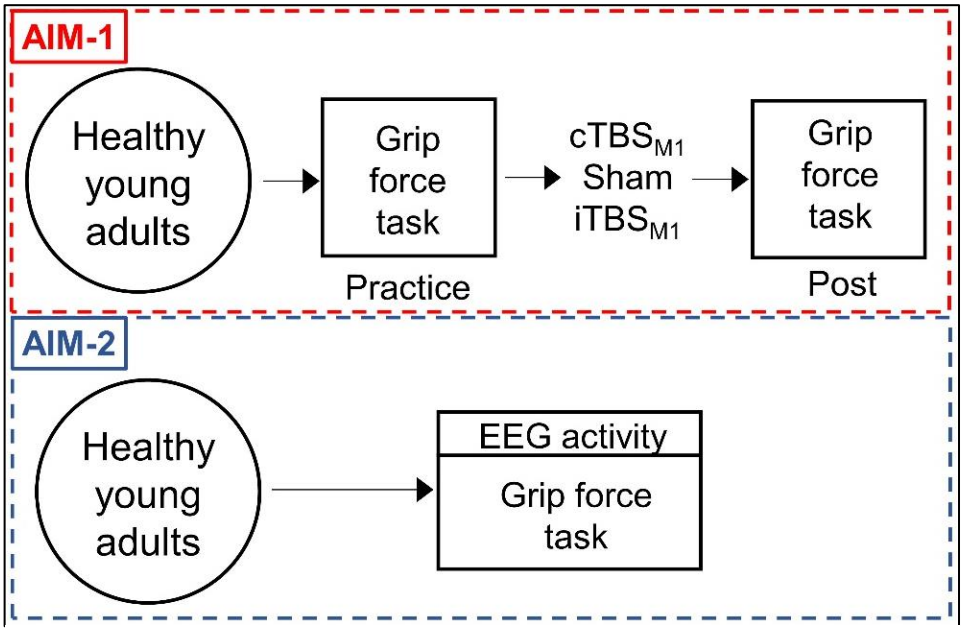

Figure 3: Schematic of experimental design for aim-1 (within-subject crossover design, each session conducted >4 days apart), and aim-2 (EEG session when subjects perform grip force task)

1.4. Complementary design of the dissertation studies

The two proposed studies were designed to address two critical questions related to the neural processes underlying grip force control. The first study aimed at understanding the causal role of primary motor cortex (M1) in regulating grip force variability with systematically altered availability of the visual feedback of the force. For this study, we used noninvasive neuromodulation-based approach to temporarily disrupt M1 activity and assessing its effect on grip force variability. The second study aimed at determining the modulation in neural variability in response to the increase in grip force task demand (viz. increase in force magnitude). In this study, we employed a noninvasive neuroimaging-

based approach to assess the modulation in EEG variability with increase in grip force magnitude. While the first study was designed to determine brain's influence on behavioral (grip force) variability, the second study was designed to assess the influence of behavioral (grip force) task demand on brain signal variability. Consequently, the two studies complemented the findings from corresponding approaches while highlighting the systematic involvement of variability at the neural and behavioral levels essential for grip force control.

1.5. Significance

Despite the knowledge that the activity within fronto-parietal brain regions is important for grasping, their specific contribution to moment-to-moment force control remains unclear. This is a significant knowledge gap because it limits our understanding about how brain enables efficient control of digit forces and restricts the design of current interventions for patients with sensorimotor deficits in the upper extremity. The current dissertation aimed at bridging the identified research gaps using noninvasive neuromodulation (TMS) and neuroimaging (EEG) approaches. Our findings highlight the critical role of M1 and associated fronto-parietal cortical circuitry in moment-to-moment force control. The new knowledge might significantly contribute to various aspects of clinical biomedical research by:

1) providing a mechanistic account of neural processing during unimanual precision grasping,

2) prompting the identification of cortical targets to aid the design of brain-machine interfaces for precision motor control, and

3) highlighting the potential of noninvasive neuromodulation and neuroimaging approaches in facilitating the rehabilitation research for patients with sensorimotor deficits and neurological disorders.

Chapter 2. Literature review

2.1 Section overview

In this section, we review literature critical to the understanding of digit force applications, factors associated with the grasping and dexterous manipulation, and the underlying neurophysiological mechanisms. In the process, we also present findings from our published, peer-reviewed manuscript to highlight the dependence of digit force modulation on digit placement during a grasping-and-lifting task (Rao et al., 2021). We further characterize the age-related deficits specific to associative learning mechanism to modulate digit placement in an anticipatory manner. After discussing candidate neural mechanisms underlying the age-related deficit, we focus on the central contribution to digit force application involving sensorimotor cortical regions in addition to the premotor and parietal cortices. The section is followed by a review of principles and techniques which facilitate the characterization of neural activity including the transcranial magnetic stimulation (TMS), and electroencephalography (EEG). The applicability of these techniques has spanned from understanding fundamental mechanisms modulating neurophysiological variability during digit force control to clinics and rehabilitation settings.

Next, we present our published, peer-reviewed manuscript highlighting the role of variability in corticospinal excitability in planning to exert a higher versus lower force prior to grasping an object. Importantly, we accounted for the variability in digit placement experimentally and confirmed it based on additional analysis. The study further showed how individual differences in modulating the variability in corticospinal excitability systematically explained behavioral variations during grip force application as a function of force magnitude.

With the characterization of individual and trial-to-trial variations in digit forces, we subsequently review previous research aimed at elucidating the mechanisms associated with within-trial variations in digit force application. The discussion is focused on probing the components of within-trial force variability that is dependent on or independent from the sequential temporal structure of digit force. We conclude this section by summarizing the critical aspects of the reviewed literature leading to the research gap in understanding the central contribution to within-trial force variability and the specific hypothesis of interest. Sequence of information in this chapter as shown in Figure 4.

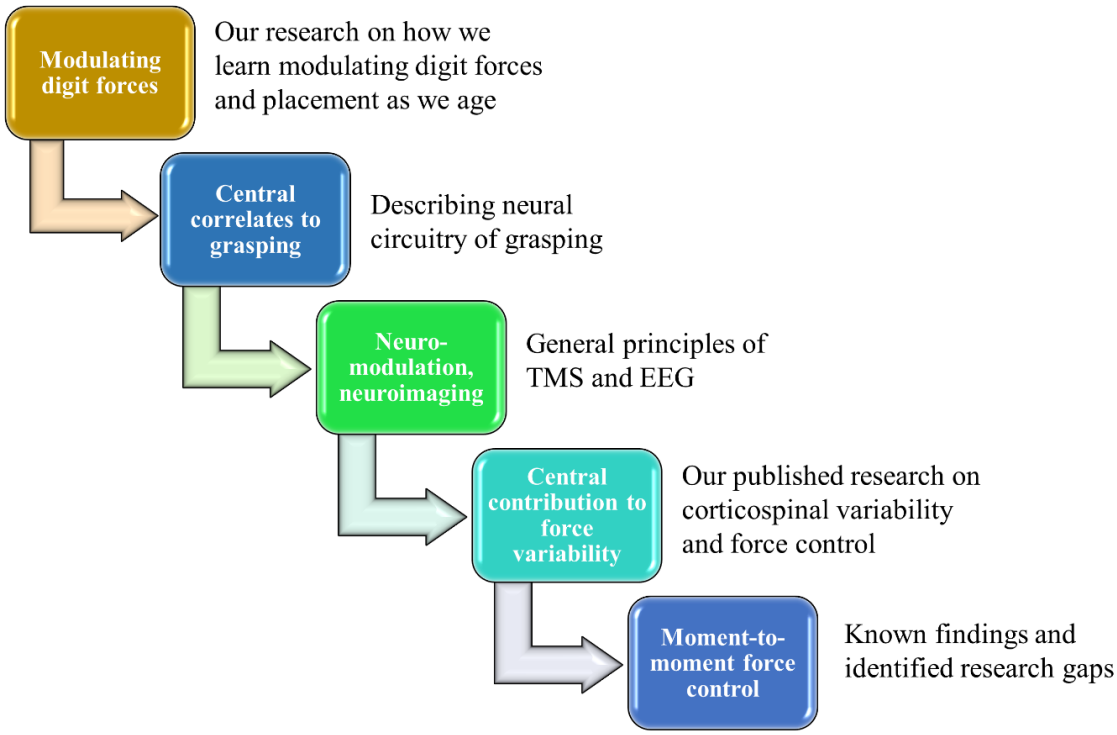

Figure 4: Organization of Chapter 2

The following content is a part of our published, peer-reviewed manuscript aimed at understanding the fundamental mechanisms of learning to modulate digit forces as a function of the digit placement on an object. The article further characterized deficits developed in the ability to learn digit placement and force modulation with normal aging. Findings from this study were pivotal in informing the subsequent research performed as a part of this dissertation.

2.2 How do we modulate digit forces for dexterous manipulation in routine life? (Published, peer-reviewed manuscript – Rao et al, 2021, *J. Appl. Phys.*)

2.2.1. New and Noteworthy

We studied whether older adults are able to predictively modulate digit position using arbitrary color cues indicating object center of mass location for dexterous manipulation. Older adults showed an impaired ability to modulate digit position using the color cues when compared with young adults. Interestingly, similar impairments were not found when same older individuals learned the task using implicit knowledge. Our findings suggest an age-related impairment specifically in the conditional learning mechanisms for dexterous manipulation.

2.2.2. Abstract

Explicit knowledge of object center of mass or CM location fails to guide anticipatory scaling of digit forces necessary for dexterous manipulation. We previously showed that allowing young adults to choose where to grasp the object entailed an ability to use arbitrary color cues about object CM location to gradually minimize object tilt across several trials. This conditional learning was achieved through accurate anticipatory modulation of digit position using the color cues. However, it remains unknown how aging affects the ability to use explicit color cues about object CM location to modulate digit placement for dexterous manipulation. We instructed healthy older and young adults to learn a manipulation task using arbitrary

color cues about object CM location. Subjects were required to exert clockwise, counterclockwise, or no torque on the object according to the color cue and lift the object while minimizing its tilt. Older adults produced larger torque error during conditional learning trials, resulting in a slower rate of learning than young adults. Importantly, older adults showed impaired anticipatory modulation of digit position when information of the CM location was available via explicit color cues. The older adults also did not modulate their digit forces to compensate for this impairment. Interestingly, however, anticipatory modulation of digit position was intact in the same individuals when information of object CM location was implicitly conveyed from trial-to-trial. We discuss our findings in relation to age-dependent changes in processes and neural network essential for learning dexterous manipulation using arbitrary color cue about object property.

2.2.3. Introduction

We can perform dexterous manipulation based on explicit information about object properties (Gordon et al., 1991; Cole and Rotella, 2002; Chouinard et al., 2005; Nowak et al., 2007, 2009; Lukos et al., 2008; Ameli et al., 2011; Parikh and Santello, 2017). For instance, subjects can accurately scale digit forces in an anticipatory manner based on arbitrary cues about object weight and texture within a few trials and this associative memory for digit force scaling would last for at least 24 hours (Nowak et al., 2007; Ameli et al., 2008). Interestingly, when subjects were asked to use visual instructional cues about object center of mass (CM) location to lift the object by preventing it from rolling, they failed to scale their digit forces leading to task failure (Salimi et al., 2003). These findings suggest that explicit visual cues of object CM

location are ineffective in guiding manipulation that primarily depends on accurate scaling of digit forces. Importantly, dexterous manipulation may also depend on the modulation of digit position based on object properties (Fu et al., 2010; Mojtahedi et al., 2015; Davare et al., 2019; Parikh et al., 2020). In the aforementioned association studies, subjects were directed to grasp at the same points on the object, which restricted a change in digit position from trial to trial. That is, an important component of dexterous manipulation – choice of digit position, was neglected. Remarkably, when subjects were given a choice regarding where to grasp the object, they were able to learn to use arbitrary color cues about object CM location to anticipatorily modulate their digit position to guide dexterous manipulation (Parikh and Santello, 2017).

Aging might influence the ability to modulate grasp parameters using arbitrary visual cues about object property for dexterous manipulation. Cole and Rotella (Cole and Rotella, 2002) instructed older adults to grip the object approximately at the center of contact surfaces and lift it using arbitrary cues about either object weight or texture. The authors found that older adults, unlike young adults, showed impaired learning to scale their digit forces using the arbitrary visual cues informing them about object weight and texture. It remains unknown whether allowing choice of digit placement would afford older adults an ability to use arbitrary visual cues about object CM location similar to that observed in young adults (Salimi et al., 2003). The aim of this study was to determine whether older adults can modulate their digit positions in an anticipatory manner based on arbitrary color cues about object CM location for successful object manipulation. We used our recently developed conditional visuomotor task that required subjects to associate an arbitrary color cue to the mass distribution of an object (Parikh

and Santello, 2017). On each trial, subjects had to select one of three possible responses (i.e., exertion of clockwise, counterclockwise, or no torque) according to the color cue and to lift the object while minimizing object tilt across 60 trials. The direction and magnitude of object tilt during the lift provided feedback to subjects about success or failure of their association. As older adults are known to have an impaired ability to learn using explicit cues (Salthouse, 1985; Vakil and Agmon-Ashkenazi, 1997; Fisk and Warr, 1998; Small et al., 1999; Cole and Rotella, 2002; Zhong and Moffat, 2016), we hypothesized that older adults will fail to use arbitrary color cues about object CM location to modulate their digit position in an anticipatory manner. A lack of modulation in digit position will result in a failure to accurately scale the compensatory torque based on color-CM association until the time of object liftoff (i.e., in an anticipatory manner) in older adults when compared with young adults.

2.2.4. Materials and Methods

Participants:

Twenty naïve participants were recruited across two groups: older adults (69 ±5 yr [mean ±SD], n=10, 4 females) and young adults (25 ±3 yr [mean ±SD], n=10, 5 females). All participants provided written informed consent to participate in the study. Participants had normal or corrected-to-normal vision and no history of neurological disease and musculoskeletal disorders or upper limb injury (self-reported). Participants appeared to be aware of their environment and current events based on their responses to questions designed to assess their cognitive status (Parikh and Cole, 2012). All participants followed the same experimental protocol. Tactile sensibility thresholds were obtained from the distal volar pads of the index finger using Semmes- Weinstein

pressure filaments (Smith and Nephew Roland, Menominee Falls, WI). We used a descending method of limits to establish a threshold (Parikh and Cole, 2012; Rao et al., 2020). The index finger was tested approximately midway between the center of the pad and the radial margin of the finger. A threshold was recorded for the smallest filament diameter (buckling that could be perceived on at least 70% of its applications). Both groups demonstrated normal for age tactile sensibility threshold measured using Semmes-Weinstein pressure filaments. The mean tactile sensibility threshold was 208 mg for older adults and 52 mg for young adults. The study was approved by the Institutional Review Board at the University of Houston.

Apparatus:

Grip device. A custom-designed inverted T-shaped device was outfitted with two six-dimensional force and torque transducers (Nano-25; ATI Industrial Automation, Garner, NC) (Parikh and Santello, 2017; Rao and Parikh, 2019). The surfaces of the grip device were covered with sandpaper (grit #320). This device measured grip and load forces (normal and tangential to the graspable surface) and the center of pressure of both thumb and index finger. The base of our grip device consisted of three compartments (left, center, and right). A 400-g mass was inserted in the left (LCM) or right (RCM) bottom compartment to shift the mass distribution of the grip device to the left or right of its vertical midline, respectively. This added mass to either the left or right base compartment generated a negative or positive external torque of 255 N·mm on the device, respectively, following the lift onset. When the added mass was placed in the center base compartment (CCM), the mass distribution remained symmetrical. To prevent visual identification of the location of the added mass, the view of the base

compartments was blocked by a lid. As an additional preventive measure, the base compartments were placed away from the participant. The total mass of the grip device with added mass was 790 g. The subject's hand rested on a table that was placed directly in front of their seat to ensure that the start position and arm posture were consistent throughout the experiment. An electromagnetic sensor (Polhemus FASTRAK; 0.05° resolution) was attached to the top of the device to measure the object roll. The roll of the object was defined as the angle between the gravitational vector and the vertical axis of the grip device, contained in the frontal plane of the grip device.

Experimental Procedure:

Conditional visuomotor task: This task was adopted from our previous work (Parikh and Santello, 2017). All experiments were conducted in a well-illuminated and quiet room. Subjects washed their hands with soap and water. They sat on a chair fitted with a platform designed to support their arm. The grip device was positioned 30 cm from the subject's right hand on a table in front of the chair. Subjects were instructed to reach and grasp the grip device at a self-selected speed using their thumb and index fingertips of the right hand. They were instructed to lift the object to a height of ~10 cm while attempting to minimize object tilt, hold it for ~1 s, and replace it on the table. A computer monitor positioned in front of the subject was used to provide subjects with cues. For each trial, a series of three cues was presented to the subject. First, a "ready" cue signaled the beginning of the trial. Next, a "CM" cue was presented at random delays (1-3 s) after the "ready" cue. For all but practice trials, this CM cue was a red, yellow, or blue in color and was arbitrarily associated with LCM, CCM, or RCM condition, respectively. For practice trials, the CM cue was always white in color and did not provide subjects

with any information regarding the location of CM. Lastly, a "go" cue appeared on the monitor 1s after the CM cue to instruct subjects to begin the task. The task required subjects to associate a color cue with CM and using this association, learn to exert a torque in the appropriate direction and magnitude to counter the torque exerted by the cued CM.

Experimental Protocol

Practice trials: Subject were familiarized with the experimental setup and the task by asking them to practice lifting the grip device and minimizing its roll. For the practice trials, the added mass (400 g) was placed in the right base compartment (RCM) of the grip device. Subjects were made aware that the added mass was going to be placed in the same compartment across all practice trials but the location of mass remained unknown to them. Subjects performed the task using a white cue which alerted the subjects about the upcoming task phase. Subjects performed 15 practice trials followed by a rest for ~10 min before proceeding with the conditional learning trials (Figure 5**)**.

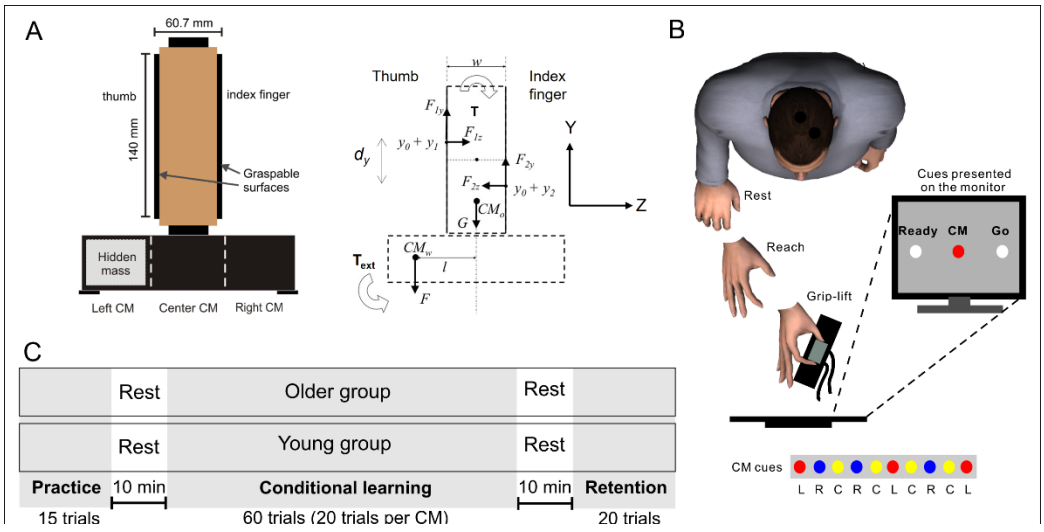

Figure 5: Experimental design. A: Grip device. B: Experimental setup. C: Experimental protocol. Adapted from Parikh PJ, Santello M. Role of human premotor dorsal region in learning a conditional visuomotor task. J Neurophysiol 117: 445–456, 2017.

Conditional learning trials: We altered the CM of the grip device on every trial by placing the mass in the right (RCM condition), center (CCM condition), or left compartment (LCM condition) at the base of the object. The trials were pseudorandomized to avoid presenting the same CM over two consecutive trials. Subjects were informed about the trial-by-trial change in the CM location, but they were not explicitly told in which compartment the added mass would be across trials. Subjects were informed of the change in CM location using arbitrary color cues which were shown on a monitor directly in the line of sight of each subject. By trial and error, subjects were required to learn to associate the color cue with the CM location and select one of three possible responses: exertion of a clockwise, counterclockwise, or no torque, as per the color cue, and to lift the grip device while minimizing its tilt. Subjects received feedback about whether they successfully associated or failed to associate their response with the color cues (the stimulus) based on the direction and magnitude of the object tilt. Each CM condition was repeated 20 times (total 60 conditional learning trials). Before each trial, the experimenter changed the location of the added mass out of view of the subject. Since the practice trials were all completed with the RCM condition, and the sequence of the conditions was designed to avoid presenting the same CM on consecutive trials, the RCM condition was not presented on the first trial of the conditional learning block. Subjects were able to rest for 30 s between trials and this period included the time to change the location of the added mass. Following 60 conditional learning trials, subjects rested for ~10 min before beginning the retention trials.

Retention trials: Subjects were told to perform the conditional visuomotor task similar to the task performed in the conditional learning trials – by using the learned color-CM association. The location of the CM was, again, changed without the subjects' knowledge by pseudorandom placement of the added mass in either of the three base compartments (right, center, and left) of the grip device. The condition presented in the last trial of the conditional learning block was not presented in the first trial of the retention block to avoid presentation of the same CM across two consecutive trials. Subjects rested between trials while the experimenters changed the location of the CM. The retention block consisted of 20 trials. Notably, the practice and conditional learning blocks embedded implicit and explicit knowledge-based mechanisms to learn to exert a torque in the appropriate direction and magnitude to counter the torque exerted by the external mass, respectively. In the case of practice trials, the learning was based on the knowledge of object CM location from trial-to-trial, using information from previous lifts. Similar paradigm has been previously studied within the context of grasp-and-lift tasks and has been shown to underlie formation of sensorimotor memory (Gordon et al., 1991; Johansson and Cole, 1992; Lukos et al., 2013; Schneider et al., 2019). On the contrary, the color cue-based association with the object CM location during the conditional learning block is known to underlie stages initiated by stimulus identification from trial-to-trial (Asaad et al., 1998; Parikh and Santello, 2017).

Data Acquisition and Analysis

Conditional visuomotor learning of anticipatory control of dexterous manipulation was quantified using measurement and analysis of digit forces and positions at lift onset (Parikh and Santello, 2017). Analysis of variables at object lift

onset allows the quantification of subjects' ability to coordinate digit forces and position based on recalling a force-position distribution associated with a specific color cue experienced in previous trials. After object lift onset, the object roll provides subjects with feedback about the extent to which the selected digit force and position were correctly associated with the color cue. The visual and haptic feedback about the magnitude and direction of object roll is used to drive the behavioral response on the next presentation of the same color cue. Across all practice trials, the CM location remained the same across consecutive trials (i.e., right center of mass) to allow subjects to use feedback of object roll to adjust digit force and placement on the following trial. The following variables were analyzed: [1] Digit load force (LF) was defined as the vertical force component parallel to the grip surface produced by each digit to lift the object; [2] Normal force (F_N) is the force component perpendicular to the grip surface; [3] Grip force (F_{GF}), is the average of the normal forces produced by each digit; and [4] Digit center of pressure for each digit was defined as the vertical coordinate of the point of resultant force application by the digit on the grip surface. Using these variables, the following two variables were computed: [5] Torque and [6] Torque error (TE). In accordance with previous studies (Parikh and Santello, 2017; Parikh et al., 2020), the torque (or compensatory torque as described previously) generated by the subject was computed as:

$$T = \left(\frac{w}{2}.d_{LF}\right) + (d_Y.F_{\mathrm{GF}})$$

where dLF is the difference between the LF of the thumb and index finger, dY is the vertical difference between the center of pressure of the thumb and index finger, FGF is the grip force, w is the grip width, and w/2 is the moment arm for the thumb and index

finger LF. When the external mass (400 g) was placed in the left (LCM) or right (RCM) compartment, it introduced a torque (Text) on the zy plane of -255 or 255 N·mm, respectively. When the mass was placed in the central compartment, the mass distribution remained symmetrical (i.e., Text was considered zero). The task goal of minimizing object tilt required subjects to apply a torque on the object of similar magnitude but opposite in direction. Thus, the target torques for LCM and RCM conditions were 255 and -255 N·mm, respectively. The torque error (TE) was defined as the absolute difference between the target torque (the torque required to counter the external torque; and the compensatory torque generated by the subject. If an individual exerts a torque on the object (i.e., actual torque or compensatory torque) that is closer to the target torque at the time of object lift onset, then the object would be lifted with minimal tilt. The measure of TE and compensatory torque when assessed specifically at the time of object lift onset is indicative of anticipatory control of digit position and digit forces (Lukos et al., 2008; Parikh et al., 2020). [7] Peak object roll was also computed as the maximum roll occurring ~150 ms after object lift-off. Erroneous anticipatory control of digit position and digit forces results in object roll ~150 ms after object lift-off, occurring before corrective responses to counter object roll can be made at reaction time latencies (Lukos et al., 2007)

All of the above variables, except peak roll, were computed at the time of object lift onset to quantify anticipatory control of manipulation (Parikh and Santello, 2017; Parikh et al., 2020). This is the time before subjects could perceive and react to the external torque (T_{ext}). Object lift onset was defined as the time at which the vertical

position of the grip device crossed and remained above a threshold (mean + 2SD of the baseline) for 200 ms (Zhang et al., 2010).

Statistical Analyses

For the conditional learning block, we averaged the TE and the object roll measurements across three successive learning trials (average of trials 1-3, average of trials 4-6, average of trials 7-9, etc.). For the retention block, we averaged the TE and the object roll measurements across three successive trials for the first 18 trials. For the practice block, we measured each subjects' ability to apply a torque to help minimize the roll of the grip device by comparing the first practice trial with the average of the last five practice trials. We performed repeated measures analysis of variance (ANOVA; $\boldsymbol{\alpha}$ = 0.05) on TE, roll, d_Y, d_{LF}, and F_{GF} with GROUP (Older, Young) as a between-subject factor and one or more of the following within subject factors: $Bin_{learning}$ (20 levels, $bin_{learning}$ 1 to 20), $Bin_{retention}$ (6 levels, $bin_{retention}$ 1 to 6), *CM* (LCM, RCM, CCM), *Trial* (1-20), and *Practice Trial* (first, average of the last 5 trials). For the conditional learning block, we performed a post hoc between-group comparisons for $bin_{learning}$ 1 and $bin_{learning}$ 20, which represent the first and last exposure to each CM condition, respectively. We applied Huynh-Feldt corrections when sphericity assumption was violated. Post hoc comparisons using paired t-tests were performed with Bonferroni corrections, if needed. ANOVA and posthoc analyses were performed using SPSS software version 22.0 (IBM, USA).

We also report estimation statistics that describe the magnitude and precision of the effect size (Cohen, 2016; Cumming and Calin-Jageman, 2016). A total of 5000 bootstrap samples were taken (with replacement), and the resampling distribution of

difference in mean (i.e., effect size) was determined (Ho et al., 2019). A bias-corrected bootstrap 95% confidence interval (CI) was constructed from the resampling distribution. The data was analyzed and figures were produced using the estimation coding software (Ho et al., 2019). The p-value obtained from the two-sided permutation t-test (α = 0.05) provided the likelihood of observing the effect size, if the null hypothesis of zero difference is true (**Table 1**).

Table 1: Estimation statistics organized by figure panel. The type of measurement, comparison, mean difference with 95% confidence interval (CI), and the p-value for the permutation two-sided test are provided.

Figure	Measure	Comparison	Mean difference [95% CI]	Permutation two-sided test p-value
Fig. 3A	T_{error} ($Bin_{learning}$ 1)	YA vs OA	-34.7537 [-54.1398, -15.9093]	0.0056
Fig. 3A	T_{error} ($Bin_{learning}$ 20)	YA vs OA	120.3494 [84.7709, 148.9389]	0
Fig. 3B	T_{error} (CCM)	YA vs OA	-11.2205 [-21.6519, 6.3999]	0.136
Fig. 3B	T_{error} (RCM)	YA vs OA	112.3767 [75.3912, 148.1285]	0
Fig. 3B	T_{error} (LCM)	YA vs OA	109.1967 [81.2220, 139.2750]	0
Fig. 5A	d_Y (CCM)	YA vs OA	-1.0875 [-3.1586, 1.4553]	0.365
Fig. 5A	d_Y (RCM)	YA vs OA	12.2412 [6.4696, 22.4727]	0.0012
Fig. 5A	d_Y (LCM)	YA vs OA	-14.1863 [-23.5683, -8.6982]	0.0002
Fig. 5B	d_{LF} (CCM)	YA vs OA	0.6267 [-1.3301, 1.7890]	0.4612
Fig. 5B	d_{LF} (RCM)	YA vs OA	-1.4561 [-3.5254, 0.2270]	0.1692
Fig. 5B	d_{LF} (LCM)	YA vs OA	1.1934 [-1.2901, 3.1041]	0.3258
Fig. 5C	GF (CCM)	YA vs OA	2.7146 [-3.1135, 7.7379]	0.3742
Fig. 5C	GF (RCM)	YA vs OA	-1.9468 [-9.1389, 3.7351]	0.5954
Fig. 5C	GF (LCM)	YA vs OA	-0.5076 [-6.4848, 4.4274]	0.865

2.2.3. Results

None of the subjects reported fatigue or discomfort during or after the task.

Conditional visuomotor learning in older adults.

Both young and older adults were instructed to perform a conditional visuomotor task using the object for which CM was altered on a trial-by-trial basis in a pseudorandom fashion, thus resulting in three CM conditions: RCM, CCM, and LCM (Figure 5). Participants were also informed about the change in CM of the object through arbitrary color cues where red, blue and yellow colors corresponded to LCM, RCM, and CCM conditions respectively. However, they had no *apriori* information about the color – object CM association. By trial and error, all adults were required to learn to associate the color cue with object CM and select accurate torque, according to the identified cue, and to lift the object while minimizing object tilt. Minimization of object tilt required application of torque on the object that approached the target external torque. The direction and magnitude of object tilt provided feedback to subjects about success or failure of their stimulus-response association. The trial sequence was designed to inform individuals about color-object CM association in the first three trials. As both young and older adults were unaware of the association between the color and object CM during the first two trials (LCM followed by RCM), they produced very large TE during these trials. On trial 3, we observed a sudden reduction in TE as compared to trial 1. Note that the same CM condition was not repeated over two consecutive trials. Therefore, presentation of the third color cue on trial 3 would have allowed subjects to infer, by elimination, the upcoming CM condition. However, an alternative explanation for the drop in TE on trial 3 is that subjects did not attempt to infer object CM location in the initial exposure to the color cues, but rather that they exerted, as a default, little to no torque in the early trials. Furthermore, although subjects were exposed to all color-object CM associations by trial 3, they continued to produce a fairly large TE. Young adults

gradually reduced TE over 60 learning trials. In contrast, older adults failed to reduce TE over 60 learning trials.

To quantify the time course of conditional learning, we focused our analysis on the trial 'bins' (average of 3 trials; (Parikh and Santello, 2017)). We found that the reduction in TE across the conditional learning trials was significantly smaller in older adults when compared with young adults (significant Group × $Bin_{learning}$ interaction: $F_{19, 342} = 9.74$, $p < 0.0001$, $\eta_p^2 = 0.35$; Figure 6). Specifically, at the end of learning trials (i.e., $bin_{learning}$ 20), we found that older adults showed significantly greater TE than young adults ($t_{18} = 6.98$; $p < 0.0001$; Figure 7). For $bin_{learning}$ 1, older adults showed significantly smaller TE than young adults ($t_{18} = 3.375$; $p = 0.003$). We also found a significant main effect of Group ($F_{1, 18} = 39.56$, $p < 0.0001$, $\eta_p^2 = 0.69$) and $Bin_{learning}$ ($F_{19, 342} = 37.76$, $p < 0.0001$, $\eta_p^2 = 0.68$). An exponential fit of the TE data averaged across subjects ($y = a \cdot e^{bx} + c$) resulted in a half-life of 45 trials and 252 trials in young and older adults, respectively (significant difference in exponential coefficients; $t_{18} = 4.22$; $p = 0.001$). These findings suggest that older adults were unable to learn to accurately produce the torque using color cues about CM location to the same extent as young adults by the 60^{th} conditional learning trial. We found that the reduction in peak roll across the conditional learning trials was significantly smaller in older adults when compared with young adults (significant Group × $Bin_{learning}$ interaction: $F_{19, 342} = 2.979$, $p < 0.0001$, $\eta_p^2 = 0.14$; Supplemental Fig. S1 (0). Specifically, at the end of learning trials (i.e., $bin_{learning}$ 20), we found that older adults showed significantly greater peak roll than young adults ($t_{18} = 2.47$; $p = 0.02$). For $bin_{learning}$ 1, there was no significant difference in peak roll between older and young adults ($t_{18} = 1.9$; $p = 0.07$). We also

found a significant main effect of $Bin_{learning}$ ($F_{19, 342} = 20.78$, $p < 0.0001$, $\eta_p^2 = 0.54$) but not Group ($F_{1, 18} = 0.099$, $p = 0.757$, $\eta_p^2 = 0.005$). Consistent with the torque findings, these findings suggest that older adults were unable to minimize peak roll to the same extent as young adults by the 60th conditional learning trial. These findings, along with previous studies (Lukos et al., 2007, 2008; Parikh and Santello, 2017; Parikh et al., 2020), demonstrated that compensatory torque is a valid predictor of manipulation

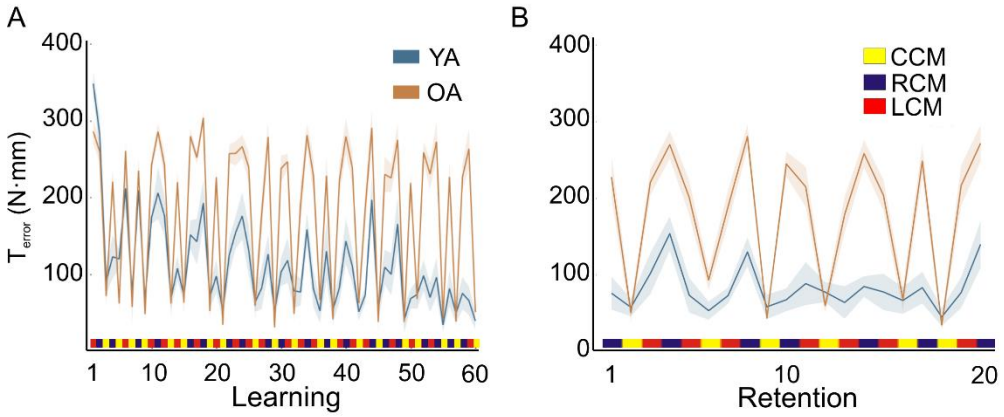

Figure 6: Conditional learning and retention. Torque error (TE) plotted as a function of trial, during conditional learning (A) and retention among older adults (OA) and young adults (YA) (B). The CM presented in a pseudorandom order across trials are denoted by different colors on the horizontal axis. Data are averages (± SE) of all subjects for both plots (n = 10 for both OA and YA, effects tested using a combination of repeated measures ANOVA and t tests). ANOVA, analysis of variance; CM, center of mass.

performance, i.e.,, object roll. Specifically, as subjects learn the appropriate compensatory torque required to minimize object roll, peak object roll negatively correlates with the magnitude of compensatory torque. Following the conditional learning trials, young adults were able to recall the association between arbitrary color cues and object CM to select the torque appropriate to a given CM learned during the task (see Figure 6 and Figure 7).

We expected the effect of aging on the production of torque (close to the target torque) during conditional learning to also vary across CM conditions. We found that

the reduction in TE for older and young adults differed across CM conditions (significant Group × CM interaction: $F_{2, 36} = 31.88$, $p < 0.0001$, $\eta_p^2 = 0.64$; Figure 6). Furthermore, we found that older adults demonstrated greater TE than young adults for the RCM ($t_{18} = 5.73$; $p < 0.0001$) and the LCM ($t_{18} = 6.94$; $p < 0.0001$) conditions, but not for the CCM condition ($t_{18} = 1.58$; $p = 0.14$).

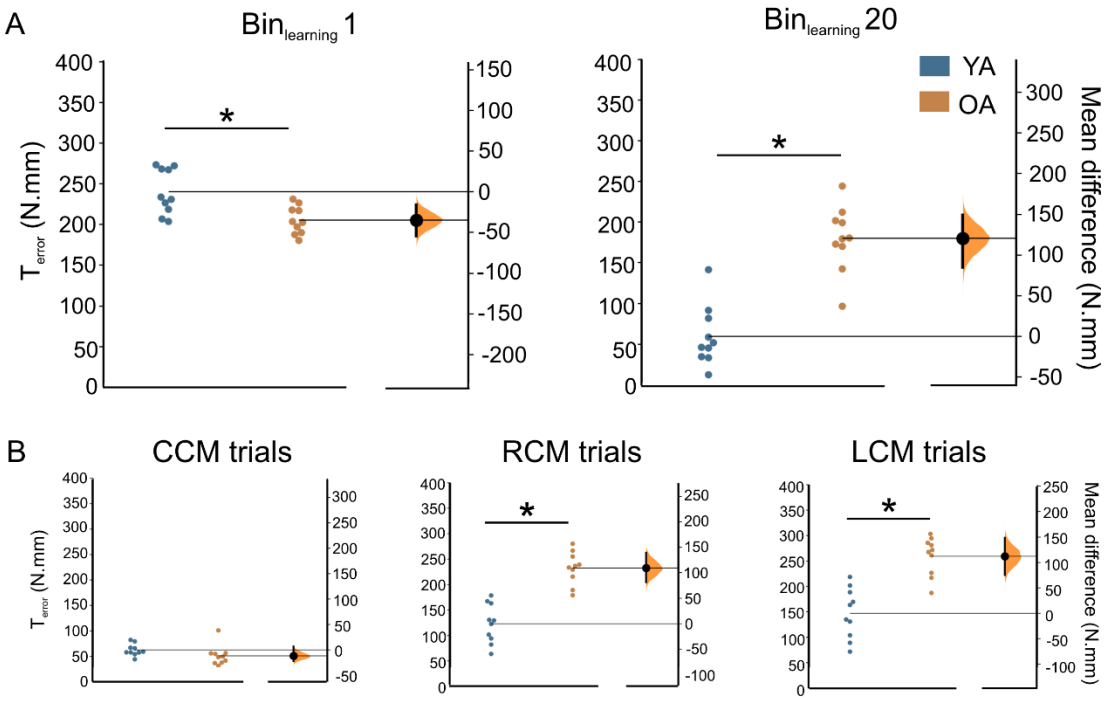

Figure 7: Estimation plots for torque error (TE). A: TE for $bin_{learning}$ 1 (left) and $bin_{learing}$ 20 (right) during conditional learning trials in older adults (OA) and young adults (YA). B: TE is shown for each object CM for older adults (OA) and young adults (YA), (n = 10 for both OA and YA). Data for individual subjects (solid circles) in both groups are plotted on the left axes and the mean difference between groups is plotted on the right axes as a bootstrap resampling distribution. The mean difference is depicted as a large black dot with the 95% confidence interval indicated by the ends of the vertical error bar. * Significant differences ($P < 0.05$). CM, center of mass.

Next, we present findings from the individual behavioral variables that constituted the torque exerted on the object (see equation 1) to further understand the effects of aging on conditional visuomotor learning.

Modulation of digit position during conditional learning:

Older adults failed to use the correct modulation of index finger and thumb based on the arbitrary color cues about object CM location when compared with young adults (Group × CM interaction: $F_{1.09., 19.62} = 12.89$, $p = 0.002$; $\eta_p^2 = 0.42$; but no main effect of Group: $F_{1, 18} = 0.57$, $p = 0.46$; Figure 8 and Figure 9). That is, young adults but

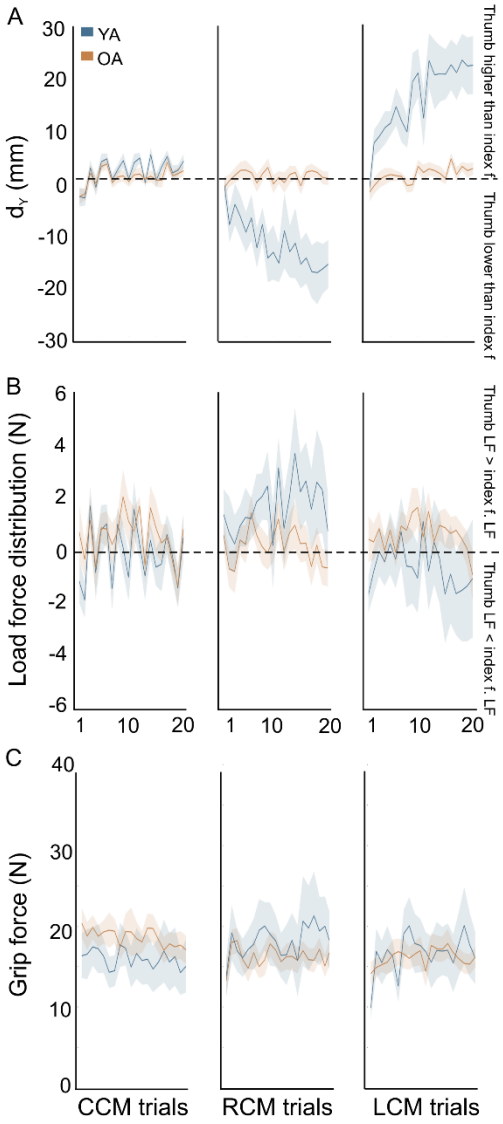

Figure 8: Digit placement, load force distribution, and grip force during conditional learning. A: vertical distance between thumb and index finger center of pressure (dY) is plotted as a function of trial for each object CM for older adults (OA) and young adults (YA) B: difference between thumb and index finger load force (dLF) is plotted as a function of trial for each object CM for OA and YA. C: grip force (GF) is plotted as a function of trial for each object CM for OA and YA; n = 10 for both OA and YA, effects tested using a combination of repeated measures ANOVA and t tests. Data are averages of all subjects (± SE). ANOVA, analysis of variance; CM, center of mass.

not older adults modulated the relative placement of the thumb and index finger on the object (d_Y) to the CM location during conditional learning. However, the modulation in d_Y across learning trials was mainly observed for the RCM and LCM conditions (significance CM × Trial interaction: $F_{6.04, 108.79} = 7.8$; $p < 0.0001$; main effect of Trials: $F_{19, 342} = 5.04$, $p < 0.0001$; $\eta_p^2 = 0.22$). For the CCM condition, both young and older adults placed their thumb and index finger at nearly same location on their corresponding graspable surfaces ($t_{18} = 0.89$; $p = 0.39$; Figure 8 and Figure 9). Importantly, for the RCM condition across the conditional learning trials, young adults chose to place their index finger higher than thumb on the object while older adults did not ($t_{18} = -3.02$; $p = 0.007$; Figure 6 and Figure 7). For the LCM condition, young adults chose to place their thumb higher than index finger on the object while older adults did not ($t_{18} = 3.72$; $p = 0.002$; Figure 8 and Figure 9). In young adults, the separation of thumb and index finger for RCM and LCM trials occurred at initial object contact and this modulation was not observed in older adults (Supplemental material, S2 and Fig. S2 (0)). That is, young adults but not older adults were able to choose digit position based on explicit visual cues about object CM location early on during the trial (i.e., before utilizing the somatosensory feedback regarding digit forces and/or position). Also, subjects in both groups modestly (statistically non-significant) repositioned their digits after initial object contact as they exerted forces on the object until object liftoff (Supplemental Fig. S3 (0)). The amount of this repositioning was similar across groups (Supplemental material, S3 **(**0)). The observed modulation of d_Y in young adults provide objective evidence of their ability to identify the CM of the object using color cues and modulate digit placement accordingly. Such CM location-dependent modulation of digit

placement was absent in older adults.

Modulation of digit forces during conditional learning

Although we observed significant interaction between Group and CM location for d_{LF} (Group × CM interaction: $F_{2, 36} = 3.38$; $p = 0.04$; $\eta_p^2 = 0.16$; but no main effect of Group: $F_{1, 18} = 0.024$; $p = 0.88$; Figure 6 and Figure 7), posthoc analyses failed to observe significant group differences for RCM ($t_{18} = 1.436$; $p = 0.17$), LCM ($t_{18} = -1.03$; $p = 0.32$), and CCM ($t_{18} = -0.78$; $p = 0.45$). The magnitude of d_{LF} changed across trials (main effect of Trials: $F_{19, 342} = 2.8$; $p < 0.0001$; $\eta_p^2 = 0.13$). However, the change in d_{LF} across trials was similar across CM conditions (no CM × Trial interaction: $F_{38, 684} = 1.33$; $p = 0.09$).

Similarly, although we observed significant interaction between Group and CM location for F_{GF} (Group × CM interaction: $F_{2, 36} = 10.21$; $p < 0.0001$; $\eta_p^2 = 0.36$; but no main effect of Group: $F_{1, 18} = 0.001$; $p = 0.98$), posthoc comparisons failed to observe significant differences between two groups (RCM: $t_{18} = 0.57$; $p = 0.58$, LCM: $t_{18} = 0.17$; $p = 0.86$, and CCM: $t_{18} = -0.91$; $p = 0.37$; Figure 8 and Figure 9). Grip force did not significantly change across trials (significant CM × Trial interaction: $F_{38, 684} = 1.91$, $p = 0.001$, $\eta_p^2 = 0.096$, but no main effect of Trial: $F_{19, 342} = 0.99$; $p = 0.47$). **Table 1** on estimation statistics reports the group mean difference with corresponding 95% CI (effect size), and the p-value for the permutation two-sided test. The findings of the estimation statistics were found to be consistent with the ANOVA findings.

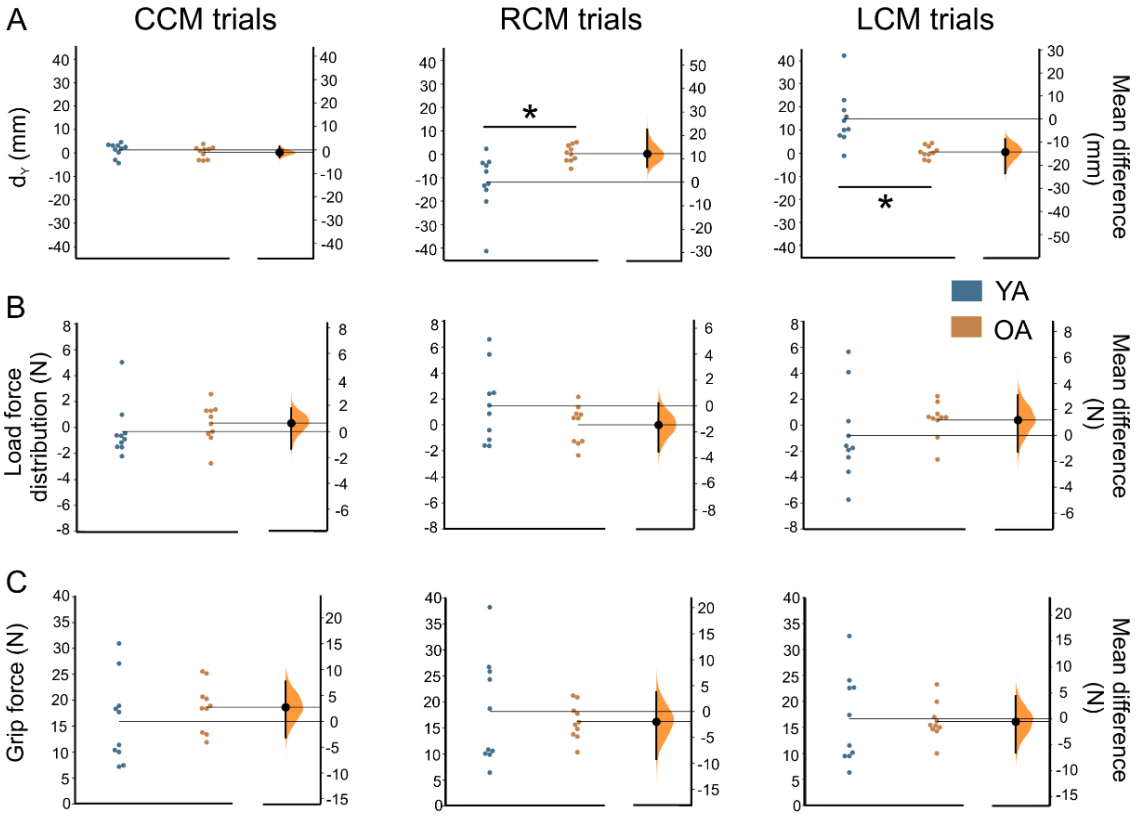

Figure 9: Estimation plots for digit placement, load force distribution, and grip force during conditional learning. A: vertical distance between thumb and index finger center of pressure (dY) is shown for each object CM for older adults (OA) and young adults (YA), n = 10 for both OA and YA. B: difference between thumb and index finger load force (dLF) is shown for each object CM for OA and YA. C: grip force (GF) is shown for each object CM for OA and YA. Data for individual subjects (solid circles) in both groups are plotted on the left axes and the mean difference between groups is plotted on the right axes as a bootstrap resampling distribution. The mean difference is depicted as a large black dot with the 95% confidence interval indicated by the ends of the vertical error bar. Asterisks denote significant differences (P 0.05). CM, center of mass.

Practice.

Both older and young adults practiced the conditional visuomotor task to familiarize with the task requirement of object roll minimization (RCM only). Subjects were required to produce a torque on the object prior to lift onset that had to be equal in magnitude but opposite in direction to the external torque generated by the added mass (target torque = −255 N·mm) to minimize object roll. That is, subjects were required to

anticipate, rather than react to, the external torque, through consecutive lifts. As they were unaware of the CM location on the first practice trial and because the object is visually symmetrical, both older and young adults exerted no or negligible torque on the object. This led to large torque error (TE - Young adults: 210 ±30.11 N·mm; Older adults: 276.5 ±15.6 N·mm) and object roll (Young adults: 12.18° ±2.9°; Older adults: 11.36° ±1.34°). Importantly, subjects were able to reduce TE and object roll over the remaining practice trials (TE - Young adults: 44.95 ±5.26 N·mm; Older adults: 118 ±10.2 N·mm and object roll - Young adults: 3.67° ±0.29°; Older adults: 3.12° ±0.33°). Both older adults and young adults were able to significantly reduce TE in a similar manner through practice (main effect of Practice Trial: $F_{1, 18} = 78.68$; $p < 0.001$, $\eta_p^2 = 0.81$; no significant Group × Practice Trial interaction: $p = 0.87$). However, across practice trials, older adults demonstrated significantly greater TE than young adults (main effect of Group: $F_{1, 18} = 15.75$; $p = 0.001$, $\eta_p^2 = 0.47$). Similar overall results were found for object roll (main effect of Practice Trial: $F_{1, 18} = 28.84$, $p < 0.0001$, $\eta_p^2 = 0.62$; no significant Group × Practice Trial interaction: $p = 0.93$; no main effect of Group: $p = 0.69$). For conciseness, we have included all figures pertaining to the practice trial in Supplemental document (Supplemental Fig. S4 (https://figshare.com/s/d06114e556877c8a9a8d)).

Both young and older adults modulated their digit position over the practice trials (main effect of Practice Trial: $F_{1, 18} = 5.99$; $p = 0.025$, $\eta_p^2 = 0.25$; no significant Group × Practice Trial interaction: $p = 0.48$; no main effect of Group: $p = 0.59$). On the first practice trial, all subjects placed their thumb and index finger at nearly same location on their corresponding graspable surfaces (Young adults: -1.41 ±1.41 mm and

Older adults: -1.44 ±1.56 mm). All subjects learned to position their index fingertip higher than the thumb with repeated exposure to the object with an external mass on the right side (Average of last five trials - Young adults: -7.3 ±3.75 mm and Older adults: -4.7 ±1.1 mm). Additionally, the vertical separation between thumb and index finger was observed at initial object contact (Supplemental material, S5 and S6 and Figs. S5 and S6). These findings suggest that both young and older adults showed the previous trial effect on digit positioning before the availability of somatosensory feedback regarding digit force and/or position. Similarly, both young and older adults learned to apply significantly higher load force with their index fingertip than the thumb over the practice trials (main effect of Practice Trial: $F_{1, 18} = 37.93$; $p < 0.001$, $\eta_p^2 = 0.68$; no significant Group × Practice Trial interaction: $p = 0.47$; no main effect of Group: $p = 0.07$). On the first trial, both groups exerted similar load force with their digits (Young adults: -0.76 ±0.87 N and Older adults: -0.75 ±0.6 N). During later practice trials, both groups applied higher load force with their index finger than the thumb (Young adults: -3.9 ±0.9 N and Older adults: -1.77 ±1.69 N). Both groups exerted greater grip force on the object with repeated practice (main effect of Practice Trial: $F_{1, 18} = 6.2$; $p = 0.023$, $\eta_p^2 = 0.26$; no significant Group × Practice Trial interaction: $p = 0.48$; no main effect of Group: $p = 0.12$). Young adults increased their grip force from 11.01 ±1.65 N to 14.07 ±1.62 N while older adults increased their grip force from 12.92 ±2.18 N to 18.47 ±1.83 N across the practice trials. These results indicate that both the groups showed an intact ability to modulate the components of TE i.e., digit position, load force, and grip force during practice trials. It is likely that higher TE among older adults could underlie small, non-significant differences in load force and grip force and their associated multiplicative

effects on the application of torque (see eq. 1).

2.2.4. Discussion

A novel finding of this study is that the older adults failed to learn to use arbitrary visual cues about object CM location for anticipatory control of digit position, when compared with young adults. Moreover, older adults also showed an impairment in modulating digit forces to account for the absence of accurate digit placement. A lack of modulation of digit position and the absence of digit force-to-position compensation in older adults were reflected in their impaired ability to minimize the error in compensatory torque exerted on the object across the conditional learning trials. Thus, we observed a slower rate of conditional visuomotor learning in older adults when compared with young adults. Importantly, this aging-related impairment in anticipatory modulation of digit position was specific to conditional learning, i.e., the same participants (older and young adults alike) successfully modulated their digit positions in an anticipatory manner when performing the similar task but using implicit knowledge of object property (i.e., absence of the color cues). We discuss these findings in the context of age-related deficits in processes essential for conditional visuomotor learning and bridge this understanding with previously reported neurophysiological mechanisms underlying dexterous manipulation.

Attentional Mechanisms, Aging, and Conditional Visuomotor Learning

The conditional learning paradigm necessitates formation of association between the stimulus and its predictive relevance in a given task (Parikh and Santello, 2017; Mutter et al., 2019). This process is argued to rely on the modulation of attentional

mechanisms to extract the predictive information from the relevant stimulus while ignoring irrelevant or distracting stimuli (Stevens et al., 2008; Mutter et al., 2019). Consequently, an impairment in the ability to modulate attention could impair conditional learning. In our study, however, it is less likely that older adults were impaired in attending to the visual color cues about object CM location. The experimenters ensured subjects' compliance with instructional cues during the sessions, e.g. initiating a reach only after the presentation of *go* cue. The practice trials gave subjects an opportunity to familiarize themselves with the visual cues, the experimental setup and the laboratory ambience. Both young and older adults were able to follow the instructional cues (*ready, task, go)* to successfully perform the object manipulation task during practice trials. After every associative visuomotor learning trial, subjects were made aware of the change in the location of external mass because these changes were done in their presence, although hidden from their view. Importantly, subjects accurately reported the change in color of the *task* cue after every learning trial. Moreover, a recent study systematically investigated whether an impairment in attentional network with aging could affect conditional learning by instructing healthy older and younger adults to perform category learning and dot-probe tasks (Mutter et al., 2019). Despite lower accuracy in predicting association pairs on the category learning task, older adults learned to modulate their attention toward predictive stimuli while directing it away from the irrelevant ones, similar to the young adults. The findings from the dot-probe task provided more direct evidence during which the older adults rapidly responded to the dot probe when cued by a predictive stimulus versus a non-predictive stimulus. Thus, the ability to modulate attentional processes to derive predictive information from the

arbitrary cues was found to be intact in older adults (Mutter et al., 2019). Our study involved a similar process of associating a color cue-based stimulus to the object CM location relevant to accomplish the task requirement. It is, therefore, likely that the age-related impairment in the anticipatory modulation of digit position found in this study was due not to older adults' inability to modulate the attentional mechanisms during conditional learning.

Connecting the dots: Effects of Aging on Conditional Visuomotor Learning during Dexterous manipulation

We found that older adults were slower in learning novel color-torque associations to lift the object while minimizing object tilt (significant *Group* × *Conditional learning bins* interaction effect). This is in agreement with studies demonstrating impaired learning using explicit cues in older adults (Salthouse, 1985; Vakil and Agmon-Ashkenazi, 1997; Fisk and Warr, 1998; Small et al., 1999; Cole and Rotella, 2002; Zhong and Moffat, 2016). Such an impairment might have functional implications on the daily lives of older adults due to their difficulty in associating an appropriate motor behavior with arbitrary cues such as a particular color of light blinking on the phone or color of the work file. In our study, the observed impairment in the application of compensatory torque on the object in older adults during conditional learning trials was not due to poor motor execution as these adults, similar to young adults, successfully learned to apply accurate compensatory torque on the object during practice trials (significant learning effect but no *Group* × *Practice trials* interaction effect). We consider possible mechanisms underlying the age-dependent impairment in conditional learning during dexterous manipulation.

During conditional learning trials, subjects had to select one of three possible responses (i.e., exertion of clockwise, counterclockwise, or no torque) to lift the object while minimizing its tilt across 60 trials. Selection of a response depends on a visual identification of the color cue that provides knowledge about the object's CM location (Asaad et al., 1998; Parikh and Santello, 2017). It is possible that this visual identification of object CM location was impaired, which might have affected the selection of accurate compensatory torque. Alternatively, the identification of visual cue was intact but the subsequent transformation of this information into motor commands was impaired in older adults (Parikh and Cole, 2012). That is, older adults could have failed to act upon changes in CM condition despite having the knowledge of CM location based on the visual cue from trial-to-trial. During the conditional learning trials, older adults exerted erroneous compensatory torque on the object across the conditional learning trials. The erroneous compensatory torque was primarily observed for the RCM and LCM trials and not for the CCM trials. The application of accurate torque, a requirement during the RCM and LCM trials, during our conditional learning trials is a function of correct spatial distribution of digit contact points (d_Y) (Parikh and Santello, 2017). Young adults were found to place the index fingertip higher than the thumb when cued about a right CM, and lower than the thumb when cued about a left CM as conditional learning progressed, a finding consistent with (Parikh and Santello, 2017). This result is important as it indicates that young adults could correctly identify object CM location, an ability that would have allowed them to exert a torque with the appropriate direction on the object. In contrast, older adults failed to show modulation of digit position using arbitrary visual cues about object CM location throughout the

conditional learning trials (Figure 6 and Figure 7). That is, older adults placed their thumb and index finger at nearly same location on their corresponding graspable surfaces irrespective of object CM location and did not demonstrate a tendency to learn the anticipatory modulation of digit position using color cues over the learning trials. Moreover, this age-related impairment in modulating digit position during conditional learning was present at early contact. Absence of digit position modulation using relevant color cues over the learning trials is a novel and important finding as the same group of older adults were able to learn to successfully and anticipatorily modulate their digit contact points based on implicit knowledge of object property during practice trials. For all practice trials, the external mass remained in the right compartment of the base of object. Thus, the CM condition during practice trials was analogous to the CM condition (i.e., RCM) during conditional learning trials, except that the latter condition introduced the color-coded cue associations which were interspersed with the other two object CM conditions (LCM and CCM). Importantly, the finding from the practice trials are consistent with our previous report (Parikh and Cole, 2012) of intact ability of older adults to modulate grasp parameters based on somatosensory and visual information about task performance. It should be noted that practice with right-sided mass did not provide an undue advantage during conditional learning trials because the deficits in digit position modulation were similar across RCM and LCM conditions Figure 6 and Figure 7).

Both older and young adults failed to scale their digit forces based on color cues about object CM location, the latter finding is consistent with (Salimi et al., 2003). Additionally, our results point toward a deficit in older adults pertaining to an important

feature of dexterous manipulation using the color cues, i.e., modulation of digit forces as a function of digit position. In young adults, digit force modulation (e.g. more positive d_{LF} for later RCM trials and more negative for later LCM trials; see Figure 6) was found to compensate for large modulation of digit position (e.g. more negative d_Y for later RCM trials and more positive for later LCM trials). The unusually large modulation of digit position, if left uncorrected, would have resulted in larger than necessary compensatory torque application, thus tilting the object in the opposite direction. The accurate modulation of digit forces was likely guided by somatosensory information about digit position (Davare et al., 2019; Parikh et al., 2020). In contrast, older adults failed to modulate digit forces to account for the lack of anticipatory control of digit position during conditional learning trials. The age-related tactile sensory impairment might have compromised their ability to sense digit position information for the modulation of digit forces during conditional learning trials. Our earlier work found that older adults are able to use somatosensory information following initial object contact but prior to lift off to sense the digit position for digit force modulation, however their reliance on this strategy was imperfect as there was resultant unwanted torque acting on the object (Parikh and Cole, 2012). Overall, the inability to modulate digit position using the color cues about object CM location and the lack of digit force-to-position compensation during conditional learning trials led to erroneous application of compensatory torque on the object in older adults. Our recent study (Parikh et al., 2020) showed that primary motor (M1) and primary somatosensory (S1) cortices are crucial for the control of digit position during dexterous manipulation using implicit knowledge of the object CM. Importantly M1 neurons in non-human primates are known to be

involved in developing novel representations of behaviorally relevant features such as arbitrary color cues during conditional learning (Zach et al., 2008). It is likely that the age-dependent altered activation within M1 and S1, as reported by several studies (Hutchinson et al., 2002; Heuninckx et al., 2008; Bernard and Seidler, 2012; Hirsiger et al., 2016; Gagnon et al., 2019), could underlie the impaired modulation of digit position thereby, affecting response selection in older adults during the conditional learning block.

The selected response during conditional learning needs to be monitored so that feedback about the behavioral consequences of the current response could inform subsequent responses for similar stimulus presentations – either by modifying it on future stimulus presentations if a selection error was made, or repeating it if the selected response was correct (Cole and Rotella, 2002; Parikh and Santello, 2017). Object tilt occurring after lift onset provides subjects with feedback about the extent to which the selected force-position distribution was correctly associated with the color cue. Visual and haptic feedback about the magnitude and direction of object roll is then used to drive the response on the next presentation of the same color cue. In case of practice trials where the CM condition (i.e., RCM) remained the same across consecutive trials, older and young adults alike could use feedback of object tilt to control digit placement and force distribution on the subsequent trial. This finding suggests that older adults had an intact ability to monitor behavioral consequences of the response during learning trials, a finding consistent with (Parikh and Cole, 2012). However, the CM conditions were pseudorandomized during conditional learning trials, which required the subjects to remember this information and use it during next presentation of the same color cue. It

is possible that older adults were unable to store this information in memory and/or retrieve this information to guide behavior on subsequent stimulus presentations. The hippocampal connection with prefrontal cortex is found to be critical for aiding the formation of novel associations during a conditional learning task (Brincat and Miller, 2015). Neurophysiological evidence based on non-human primates suggests that aging accompanies reduction in working memory capacity due to reduced hippocampal activity over the lifespan (Asaad et al., 1998; Fisk and Warr, 1998; Cole and Rotella, 2002). An age-related reduction in bold-related activity in prefrontal regions has been found during the formation of sensorimotor mappings (Dennis et al., 2009) Additionally, our previous study (Parikh and Santello, 2017) using a similar conditional visuomotor paradigm showed that contralateral dorsal premotor cortex (PMd) plays an important role during the formation of novel associations in young adults. Mainly, disruption of PMd using continuous theta burst transcranial magnetic stimulation led to a slower rate of learning but did not affect the recall of a learned conditional visuomotor behaviour. The age-related decrement in the acquisition of novel associations might be linked to age-related changes in hippocampus, basal ganglia, prefrontal, premotor and motor regions (Jernigan et al., 2001; Woodruff-Pak et al., 2001; Pitcher et al., 2002; Oliviero et al., 2006; Dennis et al., 2009; Seidler et al., 2011; Gallen et al., 2016). Future studies investigating a broader constellation of factors (Hess, 2005) influencing the age-dependent modulation in memory mechanisms hold promise to elucidate the holistic impact of aging on conditional visuomotor learning.

Conditional learning is believed to be complete when the error in motor response selection cued by an arbitrary stimulus is reduced and reaches a plateau (Cole

and Rotella, 2002; Parikh and Santello, 2017). Using this learned stimulus-response association, subjects are able to select an effective motor response when a familiar stimulus is presented. Although we are not able to comment on older adults' ability to recall as the conditional visuomotor task was not learned, there is evidence for absence of deficit in recalling a learned behavior. Fisk and Warr (Fisk and Warr, 1998) have shown that the older adults were able to accurately recall previously learned associations despite being impaired in acquiring new associations between individual cursor movements and the corresponding keys over a number of learning trials as indicated by the greater number of incorrect attempts when compared with young adults. Similarly, older adults were found to be impaired in acquiring novel stimulus-response association and not in the retention of learned associations (Small et al., 1999).

Overall, our findings suggest that the older adults' inability to predictively modulate digit position based on arbitrary color cues about object property likely resulted from age-related alterations in conditional learning processes such as stimulus identification, response selection, and/or memory formation. These processing decrements might be due to age-related changes in the cortical-subcortical network involving prefrontal, premotor, sensorimotor, hippocampus, and basal ganglia regions. Findings from this study further inform the systematic physiological underpinnings to age-related sensorimotor deficits that often manifest as reduced dexterity among older adults.

2.2.5. Acknowledgement

We thank the reviewers for their constructive comments on an earlier version of the manuscript. We thank Eesha Kundra and Kevin Nguyen for assistance with data

collection. This work was supported by the University of Houston, Division of Research High Priority Area Research Seed Grant to PJP.

Endnote

Supplemental information is available at:

URL - https://figshare.com/s/d06114e556877c8a9a8d.

Data pertaining to this manuscript may be found at http://dx.doi.org/10.17632/jh9ct4w4wz.1.

2.3 Central contribution to digit force application during grasping

Multiple studies have identified specific brain regions involved in processing information critical for grasping an object. A noteworthy neural network that is critical for successful planning and execution of a grasp (also referred to as the 'grasping circuit') involves the primary motor (M1), sensory (S1), dorsal and ventral premotor (PMd, and PMv respectively), the supplementary motor area (SMA), anterior intraparietal sulcus (aIPS), along with a network of prefrontal, and posterior parietal cortical regions (Grafton, 2010). While the primary motor cortex is known to act as a 'central hub' processing motor commands necessary for execution of a movement, a combination of associated regions including S1, PMd, PMv, and aIPS are involved in processing sensory information prior to, during, as well as after a movement execution. These regions are known to facilitate the motor planning, motor learning, adaptation, and retention of the sensorimotor memories among other functions in grasping. The corticospinal tract that is critical to relay cortical signals to the muscles originates mainly from M1 and connects to the contralateral hand muscles via the spinal cord. Various properties within this tract are known to systematically modulate in preparation, execution and in the

wake of uncertainty in upcoming actions during a grasping task (Davare et al., 2006, 2008; Lukos et al., 2007; Parikh and Santello, 2017).

2.4 Electroencephalography (EEG)

Electroencephalography (or EEG) is a noninvasive neuroimaging technique consisting of a cap of electrodes to assess the electrical activity from the scalp. Its general principle of function involves recording the electrical potential difference that exists at a particular scalp location to quantify the underlying neural activity. The recorded activity can be sampled at millisecond resolution to capture temporal variations in the scalp potentials (and therefore underlying cortical activity) over prolonged duration. The advantages of using EEG over (functional) magnetic resonance imaging (MRI) is its improved temporal resolution and portability. However, EEG systems are limited by their spatial resolution compared to that from MRI (Veldman et al., 2018).

2.5 Transcranial magnetic stimulation (TMS)

Transcranial magnetic stimulation is a noninvasive technique to deliver controlled magnetic pulse by placing a figure-of-8 coil over a cortical region of interest (Di Lazzaro et al., 2005). The general principle of its function involves inducing electric field in the underlying cortical tissue by providing a magnetic pulse over the scalp region. This technique could be used to probe the properties of the corticospinal tract during various phase of a task to assess its functional modulation, including corticospinal excitability, latency, and variability. Additionally, TMS could also be used to temporarily (~25-30 minutes) induce inhibitory or excitatory neural plasticity, or induce temporary disruption in the cortical tissue to assess its role in a task of interest. Due to its wide applicability and noninvasive nature, TMS

has been used in clinic for treatment of several neurological, psychological, and cognitive disorders (Huang et al., 2007; Davare et al., 2008; Siebner et al., 2009; Rao et al., 2019). In the subsequent section, we will go through the mechanisms by which variability in the corticospinal tract (as assessed by TMS) is modulated prior to the grasp onset, and its contribution to the grip force application in healthy young adults.

2.6 Trial-to-trial variability in corticospinal excitability and digit force application (published, peer-reviewed manuscript – Rao et al 2019, *Front. Syst. Neurosci*)

2.6.1. Abstract

Neuronal firing rate variability prior to movement onset contributes to trial-to-trial variability in primate behavior. However, in humans, whether similar mechanisms contribute to trial-to-trial behavioral variability remains unknown. We investigated the time-course of trial-to-trial variability in corticospinal excitability (CSE) using transcranial magnetic stimulation (TMS) during a self-paced reach-to-grasp task. We hypothesized that CSE variability will be modulated prior to the initiation of reach and that such a modulation would explain trial-to-trial behavioral variability. Able-bodied individuals were visually cued to plan their grip force before exertion of either 30% or 5% of their maximum pinch force capacity on an object. TMS was delivered at six time points (0.5, 0.75, 1, 1.1, 1.2, and 1.3 s) following a visual cue that instructed the force level. We first modeled the relation between CSE magnitude and its variability at rest (n = 12) to study the component of CSE variability pertaining to the task but not related to changes in CSE magnitude (n = 12). We found an increase in CSE variability from 1.2 to 1.3 s

following the visual cue at 30% but not at 5% of force. This effect was temporally dissociated from the decrease in CSE magnitude that was observed from 0.5 to 0.75 s following the cue. Importantly, the increase in CSE variability explained at least ~40% of inter-individual differences in trial-to-trial variability in time to peak force rate. These results were found to be repeatable across studies and robust to different analysis methods. Our findings suggest that the neural mechanisms underlying modulation in CSE variability and CSE magnitude are distinct. Notably, the extent of modulation in variability in corticospinal system prior to grasp within individuals may explain their trial-to-trial behavioral variability.

2.6.2. Introduction

Trial-to-trial variability is an inherent feature of motor behavior (Stein et al., 2005; Faisal et al., 2008). Intertrial variability in motor output reflects the presence of stochastic noise in the sensorimotor system and may interfere with one's ability to perform a given movement consistently (Harris and Wolpert, 1998; Slifkin and Newell, 1999; Stein et al., 2005; Faisal et al., 2008). Another perspective suggests that the intertrial motor output variability provides the sensorimotor system an ability to explore the motor workspace for optimizing motor learning (Tumer and Brainard, 2007; Wu et al., 2014).

Several studies have found central correlates of variability in kinematic or kinetic features of motor output (Osborne et al., 2005; Churchland et al., 2006a; Fox et al., 2007; Hohl et al., 2013; Chaisanguanthum et al., 2014; Lisberger and Medina, 2015; Mizuguchi et al., 2016; Haar et al., 2017). In monkeys, variable activity of sensory neuronal populations within extrastriate MT region explained variability in execution of smooth-pursuit eye movement (Hohl et al., 2013). Firing rates of neurons within primate primary

motor (M1) and premotor cortices during movement preparation explained intertrial variability in peak reach velocity (Churchland et al., 2006a). In humans, variation in fMRI responses within inferior parietal lobule observed during motor execution has been shown to explain differences in intertrial variability in reach kinematics across individuals (Haar et al., 2017). However, in humans, the contribution of planning related central mechanisms to variability in motor output remains to be known.

Motor evoked potentials (MEP) elicited non-invasively using transcranial magnetic stimulation (TMS) can provide information regarding the neural mechanisms at cortical, subcortical, and spinal levels, i.e., corticospinal excitability (CSE), during various phases of a task (Bestmann and Krakauer, 2015). For instance, CSE is modulated by activity within inferior parietal lobule and caudal intraparietal sulcus while planning a contralateral reach (Koch et al., 2008). The modulation in intertrial variability in CSE assessed during movement preparation has been shown to encode value-based decision-making processes and differentiate fast versus slow reaction time responses (Klein-Flugge et al., 2013). These findings suggest that the temporal unfolding of CSE variability from trial-to-trial may provide information regarding planning-related neural processes. However, whether intertrial CSE variability during the planning phase of a task explains variability in motor output remains to be known. In the current study, we studied the time course of intertrial CSE variability during grasp force planning and whether the modulation in CSE variability explains intertrial variability in their grip force application. We studied a grasping task because our earlier work has found CSE to be a sensitive measure to investigate grasp planning related mechanisms (Parikh et al, 2014). We investigated the time course of CSE variability while able-bodied individuals prepared to

perform a self-paced, isometric grip force production task and studied whether the modulation in CSE variability explained differences in trial-to-trial variability in the application of grip force across individuals. Subjects were instructed to first reach for an instrumented object, grasp it, and apply grip force. They were cued to exert either 30% or 5% of the maximal pinch force during the task. We delivered TMS pulses over M1 at different time points during the planning phase of the task to assess the temporal unfolding of CSE variability. Intertrial variability in CSE assessed in this manner may be related to intrinsic changes in MEP amplitude, a phenomenon that has been studied before (Stein et al., 2005; Darling et al., 2006; Faisal et al., 2008; Bestmann and Krakauer, 2015). Therefore, we modeled a relation between CSE variability and its amplitude in absence of a task during a separate session (Darling et al., 2006; Klein-Flugge et al., 2013). This allowed us to study the component of CSE variability that was beyond the intrinsic changes in CSE magnitude. We hypothesized that the planning related CSE variability would be modulated while preparing to perform the force production task. As CSE variability may represent neural variability and as the latter is known to explain behavioral variability during task planning in primates (Churchland et al., 2006a), we expect that individuals with greater modulation in CSE variability would exhibit a greater intertrial variability in their grip force application. We expected differences in these findings for the two force levels because the neural activity might be dependent on the magnitude of force (Dettmers et al., 1996; Ehrsson et al., 2001; Hendrix et al., 2009; Perez and Cohen, 2009; Parikh et al., 2014).

2.6.3. Materials and Methods

Subjects

Thirteen young, healthy, right-handed subjects (Oldfield, 1971) aged between 18 and 36 years (mean ± SD: 25.30 ± 3.59 years; 4 females) provided written informed consent to participate in this study. Subjects eligible for the protocol had a normal or corrected-to-normal vision, no upper limb injury, and no history of neurological diseases or musculoskeletal disorders. They were screened for potential risks or adverse reactions to TMS using the TMS Adult Safety Screen questionnaire (Keel et al., 2001; Rossi et al., 2009b). The study was approved by the Institutional Review Board of the University of Houston.

Experimental apparatus

Subjects were instructed to grasp a custom-designed inverted T-shaped grip device using their index finger and thumb. Two six-dimensional force/torque transducers (Nano-25; ATI Industrial Automation, Garner, NC), mounted on the grip device, measured the force and moments exerted by their index finger and thumb on the object (Figure 10). Force data were acquired using 12-bit analog-to-digital converter boards (sampling frequency 1 kHz; model PCI-6225; National Instruments, Austin, TX).

Electromyography (EMG)

We recorded muscle activity from first dorsal interosseous (FDI), abductor policis brevis (APB), and abductor digiti minimi (ADM) using differential surface electrodes (band-pass filter with a cut-off frequency range of 20–450 Hz; Delsys Bagnoli EMG System, Boston, MA). EMG data were sampled at 5 kHz using CED data acquisition board (Micro1401, Cambridge, England). Both force and EMG data were analysed using custom-made MATLAB script (R2016b; Mathworks, Natick, MA).

Transcranial Magnetic Stimulation (TMS)

Single-pulse TMS was used to assess CSE during the experiment (Parikh et al., 2014; Davare et al., 2019; Goel et al., 2019; Rao et al., 2019). We first estimated the resting motor threshold (rMT) by delivering suprathreshold single monophasic TMS pulses (Magstim 200, Whitland, UK) with the TMS coil held tangential to the scalp and perpendicular to the presumed direction of the central sulcus, 45° from the midsagittal line, with the handle pointing backward, inducing current in the posteroanterior direction. The coil position was adjusted to optimize the motor-evoked potential (MEP) in all recorded muscles. Following this procedure, the rMT was estimated as the minimum TMS-intensity to elicit motor evoked potential (MEP) with an amplitude of ~50 μV (peak-to-peak) for at least 5 of the 10 consecutive trials in the FDI muscle (Klein-Flugge et al., 2013; Parikh et al., 2014; Rossini et al., 2015; Rao et al., 2019). The TMS coil was stabilized using a coil holder mounted on the TMS chair (Rogue Research). The TMS coil was traced on the subject's scalp using a surgical marker pen. The coil location was regularly checked for any displacement that might have occurred during a session. The average rMT across subjects (mean ± SE) was 41 ± 3% of the maximum stimulator output.

Experimental design

Eleven of thirteen subjects participated in two experiments performed at least 24 hours apart. Two subjects were able to participate in one of the two experiments. The two experimental sessions were counterbalanced across subjects.

Experiment 1 (at rest; n = 12*).* We established a relation between the variability in MEP and its amplitude at rest. We delivered single pulse TMS at the following TMS intensities: 0.9, 1, 1.1, 1.2, 1.3, 1.4, 1.5, 1.6 or 1.7 times the rMT (Darling et al., 2006) with ten

consecutive pulses delivered at each intensity in a randomized order. Subjects neither performed a task nor received a stimulus except TMS.

Experiment 2 (the force task; n = 12*).* During this session, we asked subjects to perform an isometric force production task using their index finger and thumb of the right hand. The distance between the grip device and the hand was ~30 cm at the beginning of each trial. Subjects were instructed to reach for the grip device, grasp the device at the same locations, and exert grip force to match a target on computer monitor using their index finger and thumb (Figure 10).

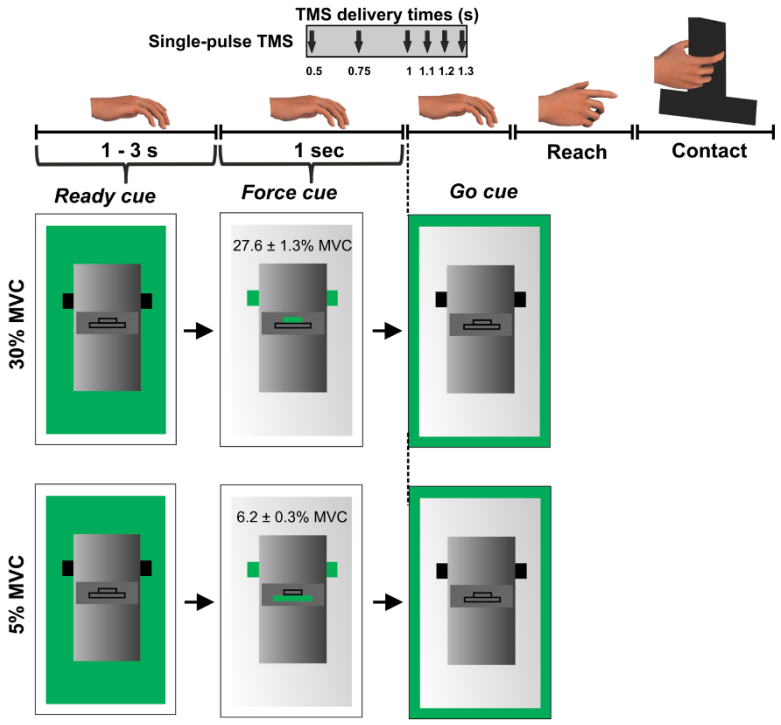

Figure 10: Experimental protocol. Figure adapted from *Parikh PJ, Davare M, McGurrin P, Santello M (2014) Corticospinal excitability underlying digit force planning for grasping in humans. Journal of Neurophysiology, 111: 2560–2569.*

We introduced two different force levels (30% and 5% of maximal pinch force) to investigate modulation in MEP variability at different force magnitudes. To rule out differential planning of digit position from trial-to-trial, we instructed subjects to grasp

the device at marked locations on every trial. This location was denoted by a black tape attached on the front panel of the grip device (Parikh et al., 2014). Self-selection of digit contact points during object grasping would require subjects to plan digit placement (Davare et al., 2019) making it challenging to isolate the digit force planning component embedded in the reach-to-grasp task. A computer monitor placed behind the device displayed three sequential visual cues on every trial: 'ready', 'force' and 'go'. The 'ready' cue signalled the beginning of a trial. The 'force' cue informed the subject about whether the upcoming force task required 5% or 30% of grip force application. Finally, the 'go' cue instructed subjects to initiate the reach and perform the force production task. The 'ready' and 'force' cues were separated by a randomly varying interval between 1-3s while 'force' and 'go' cues were separated by 1s (**Fig. 1**). Subjects were instructed to apply grip force to reach the target (displayed on the computer monitor during the 'force' cue presentation) at a self-selected speed and maintain that force for 3s using their right hand. Visual feedback of subject's grip force was provided during each trial. Subjects practiced the force production task to get familiarized with the experimental task before the session. At the beginning of the session, we measured maximum voluntary contraction (MVC) for each subject by asking them to apply maximum pinch force only using right thumb and index finger. We selected the largest force of three MVC trials to set the force target. The variability in MEP is sensitive to the magnitude of background EMG activity (Darling et al., 2006). Thus, during all reach and grasp trials, subjects were instructed to maintain their muscles in a relaxed state until the 'go' cue. This allowed comparable EMG activity

across trials and minimized the confounding effect of background muscle activity on MEP variability.

While subjects performed the *force task*, single TMS pulses at 120% of rMT were delivered to the scalp location for FDI marked earlier at 1 of the 6 latencies in a randomized order: 0.5, 0.75, 1 ('go'), 1.1, 1.2, or 1.3 s following the 'force' cue (Figure 10). Each subject performed 15 trials per TMS time point and force level in a randomized sequence. As there were six TMS time points across two force levels, subjects performed 180 trials across four blocks with 45 trials per block and with ~5 min of rest between the blocks. The minimum time interval between successive TMS pulses was ~15 sec. For this experimental setup, our earlier study has shown that the reach is not initiated at least until 0.4 s after the 'go' cue (i.e., 1.4 s following the 'force' cue) (Parikh et al., 2014). Therefore, the TMS pulse delivered at 6 different time points (one TMS pulse per trial) following the 'force' cue would represent planning related corticospinal activity.

Data processing and Statistical analysis

Behavioral variability in the application of force: We focused our analysis on the peak force rate (PFR) application because it is known to be influenced by planning-related mechanisms (Johansson and Westling, 1988; Gordon et al., 1993a). In presence of visual feedback, as in this study, peak force rate is also be influenced by online adjustments of grip force. We analyzed magnitude and time to peak force rate ($Time_{PFR}$) to assess behavioral variability, as previously reported by (Flanagan and Beltzner, 2000; Poston et al., 2008). To compute the rate of grip force application, we first smoothed the grip force signal through a zero-phase lag, 4^{th} order, low-pass

Butterworth filter (cutoff frequency: 14Hz) followed by calculating its first derivative with respect to the trial time (Flanagan and Beltzner, 2000). Separate analyses were then conducted for peak force rate (PFR) and $Time_{PFR}$. Intertrial variability in these measures were assessed by calculating their standard deviation (SD) around the mean value for each TMS delivery time point and force level. We performed repeated measures analysis of variance (rmANOVA) with within-subject factors such as TMS (0.5, 0.75, 1, 1.1, 1.2, and 1.3 s) and FORCE (5% and 30% of force).

Intertrial variability in corticospinal excitability (CSE): MEPs elicited using single TMS pulses were recorded to estimate the CSE (Parikh and Santello, 2017) during both sessions (Klein-Flugge et al., 2013; Parikh et al., 2014; Parikh and Santello, 2017). MEPs were also identified with pre-stimulus EMG contamination if the signal within 100 ms before TMS contained a peak-to-peak amplitude ≥0.1 mV (Klein-Flugge et al., 2013) and were removed from subsequent analysis (~2% of trials per subject). For *experiment* 1, The data were divided into 9 bins (10 trials for each stimulus intensity) per subject representing MEPs at a given intensity (Klein-Flugge et al., 2013). Bins with more than 5 trials were included if the average MEP exceeded 0.1 mv (Klein-Flugge et al., 2013). Bins with average MEPs exceeding the average MEP amplitude from all the bins by three standard deviations were identified and excluded from further analysis (Klein-Flugge et al., 2013). For *experiment 2*, MEPs with pre-EMG contamination (peak-to-peak signal ≥0.1 mV within 100 ms before TMS pulse; ~2% trials per subject) and MEP measuring <0.1 mV were discarded from the subsequent analysis (~8% trials per subject), thus matching the criteria used for *experiment 1*. Removal of trials with background EMG assured that the TMS pulse delivered at

different time points reflected planning rather than execution related activity. Overall, ~10% of trials were excluded during data processing across FDI, APB, and ADM muscles and time points. The coefficient of variation (CV = SD/mean) of MEP was used to quantify the intertrial variability in MEP (Klein-Flugge et al., 2013). MEP variability depends on the proportion of neurons in the motoneuron pool which are not consistently recruited by the stimulus (Kiers et al., 1993). At lower TMS intensities, a smaller proportion of neurons are consistently recruited, thus resulting in higher MEP variability. Conversely, at higher TMS intensities a larger proportion of neurons are consistently recruited leading to lower MEP variability. Consistent with this argument, several studies have found an inverse relationship between the coefficient of variation (CV) of MEP responses and MEP amplitude (Kiers et al., 1993; Devanne et al., 1997; Capaday et al., 1999; Darling et al., 2006; Klein-Flugge et al., 2013).

From *experiment 1*, we modelled a relation between MEP amplitude and its variability at rest using individual data points from all subjects (Darling et al., 2006; Klein-Flugge et al., 2013). The function characterizing this relationship was identified as the logarithmic curve of the form:

$$CV = a \times \log(\text{amplitude}) + b$$

The parameters a (slope) and b (intercept) were identified using the *modelfun* function in MATLAB (Mathworks, Natick, MA). These parameters were identified separately for three muscles (FDI, APB and ADM). We also assessed the residuals for the logarithmic fits for each muscle.

From *experiment 2*, Intertrial variability in MEPs (observed CV or CV_{OBS}) was assessed by calculating the CV of MEPs (Klein-Flugge et al., 2013) for every TMS

time point separately for each force level. The logarithmic model obtained from *experiment 1* was used to predict the CV of MEP (CV_{PRED}) that was primarily due to intrinsic changes in MEP amplitude while preparing to perform the task. Such a model has been found to robustly estimate CV_{PRED} for any intercept parameter and for the slope parameter within the range of -0.5 to infinity (Klein-Flugge et al., 2013). This predicted variability was then subtracted from the observed variability in CSE from *experiment 2* (CV_{DIFF} of MEP = $CV_{OBS} - CV_{PRED}$). The variability observed during task preparation is a combination of intrinsic variability and planning-related variability ((Fox et al., 2007; Klein-Flugge et al., 2013)). The resultant MEP variability (CV_{DIFF}) or its modulation during task preparation represents planning-related mechanisms (Klein-Flugge et al., 2013). For CV_{PRED} and CV_{DIFF} of MEP, we performed separate rmANOVA ($\alpha = 0.05$) with within-subject factors such as FORCE (2 levels: 5% and 30% of force) and TMS (6 levels: 0.5, 0.75, 1, 1.1, 1.2, and 1.3 s) for 3 muscles (FDI, APB, ADM).

To assess the repeatability of our findings, we performed this analysis on a dataset from 9 additional subjects. These subjects performed the force production task at either 10% of force or 1 N force under similar experimental paradigm (Parikh et al., 2014). As *experiment 1* was not conducted in the earlier study, we used the logarithmic model obtained using data points from all subjects in the current study. This logarithmic model resulted in the same results in *experiment 2*. These findings were presented earlier at the annual meeting of the Society for Neuroscience (Rao and Parikh, 2017) and are summarized in the Results section.

To assess the robustness of the analytical approach, we analysed data without using a lower bound cut-off criterion for MEP amplitude and without using a bin-based cut-off criterion. Furthermore, the results may be sensitive to parameters obtained by fitting a logarithmic model on data points from all subjects (i.e., a group-level model; *experiment 1* description above) versus fitting a separate model on data points from each subject (i.e., subject-level models). For each subject, a subject-level logarithmic model was used to calculate CV_{PRED} and the resulting CV_{DIFF} showed similar findings in *experiment 2* (see Results).

To investigate whether MEP variability during planning explained inter-individual differences in behavioural variability, we performed separate Pearson product-moment correlation analysis between the CV_{DIFF} of MEP and the behavioural measures i.e., SD of PFR and $Time_{PFR}$ and CoP ellipse area. We also performed the correlation analysis using standard deviation as a parameter to confirm that the findings are not sensitive to the measure of MEP variability (CV versus SD). First, we computed predicted value of SD from CV_{PRED} (SD_{PRED} = CV_{PRED} × mean MEP amplitude). Next, we computed inter-trial SD from the force task (experiment 2) to obtain SD_{OBS}. Finally, we obtained SD_{DIFF} by subtracting SD_{PRED} from SD_{OBS} (SD_{DIFF} = SD_{OBS} - SD_{PRED}).

EMG Analysis: We quantified the modulation in FDI and APB muscles involved in the production of grip force when subjects applied 30% and 5% of force on the object. For this purpose, we calculated the root mean square (RMS) value of the EMG signal for a 1.5s segment during steady force production at 5% and 30% of force separately for FDI and APB (Zhang et al., 2017; Hu et al., 2018). For data from each muscle, we performed paired t-test to compare the EMG activity measured at each force level.

Intertrial variability in digit placement: Although our experiment was designed to rule out differences in planning of digit position on each trial, it was important to confirm whether our design resulted in no difference in variability in digit contact points between 30% and 5% of force and between various TMS time points. To quantitatively evaluate this condition, we calculated the centre of pressure (CoP) for the thumb and index finger defined as the vertical and horizontal coordinates of the point of resultant force exerted by each digit on graspable surfaces of the grip device (Parikh and Cole, 2012).

$$CoP_{vertical} = \frac{M_x - (F_y \times w)}{F_n}; \qquad \text{equation 2}$$

$$CoP_{horizontal} = \frac{M_y - (F_x \times w)}{F_n}; \qquad \text{equation 3}$$

M_x and M_y are the moment about the x-axis and y-axis, respectively. F_x and F_y are the forces exerted on the grasp surface along the x-axis and y-axis, respectively. w is the distance between the surfaces of the F/T transducer and the grasp surface. F_n is the force component perpendicular to the grasp surface. To assess trial-to-trial variability in thumb and index finger CoPs, we computed area of an ellipse fitted to CoP (vertical and horizontal components calculated using equations 2 and 3). First, for each subject, we calculated an ellipse that contained CoP points within 95% confidence interval in each force level and at each TMS time point, separately for thumb and index finger. Surface area of these ellipses gave us a measure of intertrial variability in CoP across trials at a given TMS time point and at a given force level, as established in previous studies (Duarte and Zatsiorsky, 2002; Davare et al., 2007; Friendly et al., 2013). We performed separate rmANOVA with within-subject factors such as FORCE (2 levels:

30% and 5%) and TMS (6 levels: 0.5, 0.75, 1, 1.1, 1.2, and 1.3 s) for the thumb and index finger.

For all statistical analyses involving rmANOVA ($\alpha = 0.05$), we used Mauchly's test to assess the assumption of sphericity and applied Greenhouse-Geisser correction when needed. Post-hoc paired t-test comparisons were performed between adjacent TMS time points using Dunn-Sidak corrections. As stated earlier, we hypothesized that the modulation in CV of MEP and its relation with behavioural variability would be dependent on the magnitude of force (Dettmers et al., 1996; Ehrsson et al., 2001; Hendrix et al., 2009; Perez and Cohen, 2009; Parikh et al., 2014). Therefore, at each force level, we studied the modulation in CV of MEP using additional paired t-tests with appropriate Dunn-Sidak corrections and performed separate correlation analysis. The statistical analyses were performed using SPSS (version 25, SPSS Inc., Chicago, IL).

2.6.4. Results

Intertrial variability in behavioral variables

Variability in time to peak force rate ($Time_{PFR}$): SD in $Time_{PFR}$ from trial-to-trial was greater at 30% than 5% of force (main effect of FORCE: $F_{1,11} = 31.160$, $p < 0.001$, $\eta_p^2 = 0.739$; Figure 11). We observed no modulation in variability in $Time_{PFR}$ across different TMS delivery time points for TMS pulses (neither a main effect of TMS: $F_{5,55} = 1.370$, $p = 0.250$, $\eta_p^2 = 0.111$, nor FORCE × TMS interaction: $F_{5,55} = 0.469$, $p = 0.660$, $\eta_p^2 = 0.041$).

Variability in magnitude of peak force rate (PFR): The standard deviation (SD) of PFR was greater at 30% than 5% of force (main effect of FORCE: $F_{1,11} = 26.732$, $p < 0.001$, $\eta_p^2 = 0.708$; Figure 11). The delivery of TMS pulses at different time points of planning did not influence the variability in PFR (neither a main effect of TMS: $F_{5,55} = 0.244$, $p = 0.787$, $\eta_p^2 = 0.022$, nor FORCE × TMS interaction: $F_{5,55} = 2.456$, $p = 0.089$, $\eta_p^2 = 0.183$).

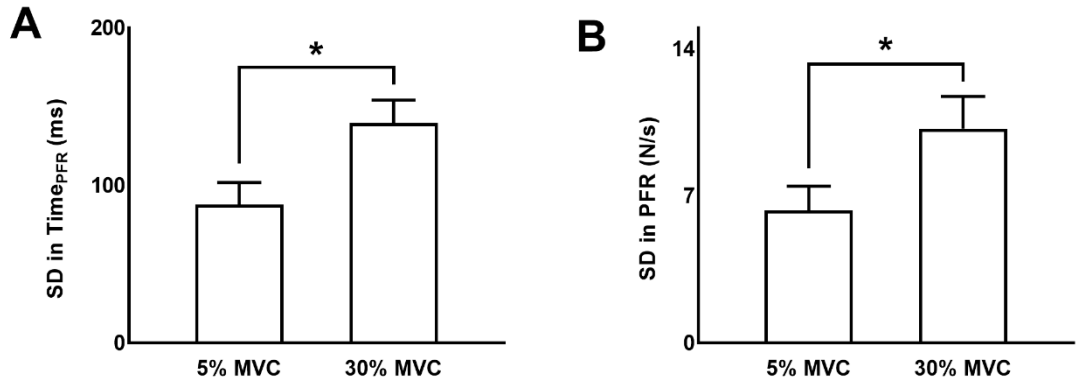

Figure 11: Behavioral variability. A and B: Standard deviation (SD) in time to peak force rate and peak force rate, respectively, at 5% and 30% of force. Data are averages across all subjects (vertical bars denote SE). Asterisks indicate $p < 0.05$.

Variability in digit contact points (CoP): Variability in CoP was assessed by calculating the area of 95% confidence interval ellipse containing the digit contact points (Duarte and Zatsiorsky, 2002; Davare et al., 2007; Friendly et al., 2013). For the index finger contact point, we did not find difference in ellipse area between 30% and 5% of force across TMS time points (no main effect of FORCE: $F_{1,11} = 0.38$, $p = 0.55$, $\eta_p^2 = 0.034$; no main effect of TMS: $F_{5,55} = 0.562$, $p = 0.728$, $\eta_p^2 = 0.049$; no FORCE ×

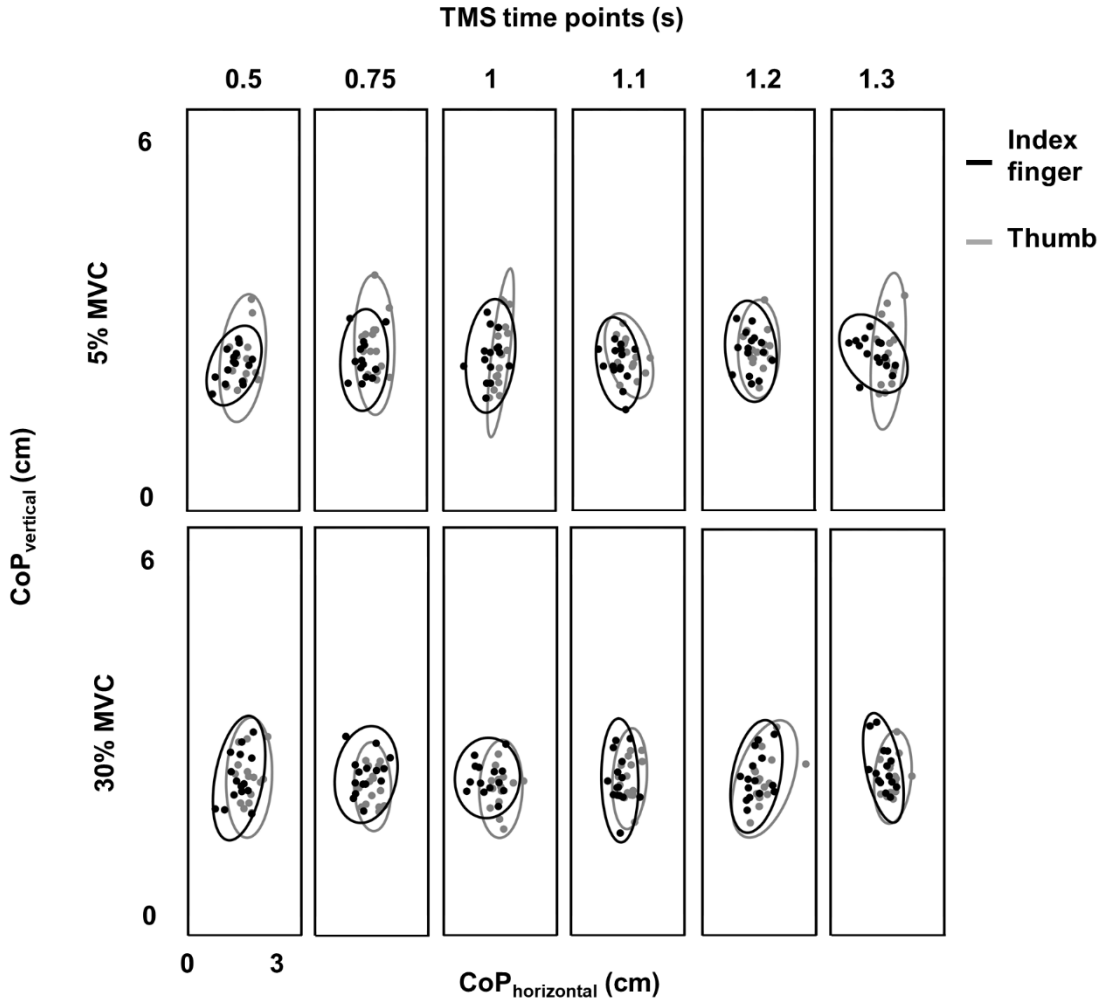

Figure 12: Variability in digit placement. Center of pressure (CoP) for thumb (gray) and index finger (black) for each TMS time point at 30% and 5% of force from a representative subject. Vertical and horizontal components of thumb and index finger CoP are shown on the same plot. Ellipse contained CoP points within 95% confidence interval in each task and at each TMS time point.

TMS interaction: $F_{5,55} = 0.606$; $p = 0.695$, $\eta_p^2 = 0.052$; mean ± SE at 30% = 2.75 ± 0.19 cm^2 and 5% = 2.71 ± 0.23 cm^2; Figure 12). Similarly, for the thumb contact point, we did not find difference in ellipse area between 30% and 5% trials across TMS time points (30% = 3.67 ± 0.41 cm^2 and 5% = 3.75 ± 0.40 cm^2 - no FORCE × TMS interaction: $F_{5,55} = 0.58$; $p = 0.71$, $\eta_p^2 = 0.05$; no main effect of FORCE: $F_{1,11} = 0.11$, $p = 0.75$, $\eta_p^2 = 0.01$; no main effect of TMS time points: $F_{5,55} = 0.976$, $p = 0.44$, $\eta_p^2 = 0.08$). These results suggest that the intertrial variability in digit contact points was

similar across force levels and TMS time points.

Relation between MEP CV with MEP amplitude at rest

We modelled a relation between CV of MEP and amplitude of MEP separately for each muscle (FDI, APB and ADM). The logarithmic relationship, as described in equation 1, for FDI was as below:

$$CV = [(-0.1078) \times \log (amplitude)] + 0.5258 \qquad \text{equation 4}$$

The values of the coefficients (a, b) from equation 1 for APB were (-0.0899, 0.4764) and for ADM were (-0.0773, 0.3116). The logarithmic fit and the residuals for FDI are shown in Figure 13.

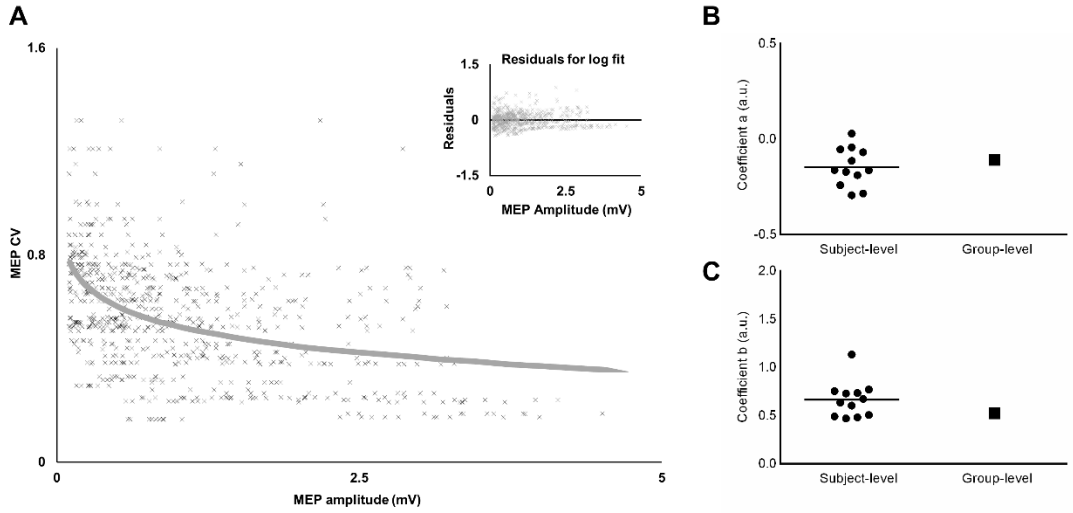

Figure 13: Relationship between variability (CV) and amplitude of MEP. A. The decrease in MEP CV with increase in MEP amplitude was characterized by a logarithmic fit. Inset plot shows trend in residuals for the logarithmic fit. B. Comparison of the slope-coefficient for subject-level versus group-level models. C. Comparing intercept-coefficient for subject-level versus group-level models. Each dot for the subject-level model represents coefficient from an individual subject.

Variability in MEP due to changes in MEP amplitude (CV_{PRED}) during task planning

We predicted MEP variability (CV_{PRED}) while planning to exert isometric grip force for individual subjects using the logarithmic model separately for each muscle.

For FDI, we found that CV_{PRED} of MEP was different across TMS time points (main effect of TMS: $F_{5,55} = 3.695$, $p = 0.006$, $\eta_P^2 = 0.251$; Figure 14). However, this time-dependent modulation of CV_{PRED} of MEP was not different across force conditions (No FORCE × TMS interaction: $F_{5,55} = 0.506$, $p = 0.770$, $\eta_P^2 = 0.044$; no main effect of FORCE: $F_{1,11} = 0.701$, $p = 0.420$, $\eta_P^2 = 0.060$). Post hoc comparisons found a significant increase in CV_{PRED} of MEP from 1.2s to 1.3s ($t_{11} = 3.2$, $p = 0.009$, Cohen's $d_Z = 0.92$). No difference in CV_{PRED} of MEP was found between other adjacent TMS time points (all p values > 0.05). Within each force level, we found significant increase in CV_{PRED} of MEP from 0.5s to 0.75s at 30% ($t_{11} = 2.9$, $p = 0.015$, Cohen's $d_Z = 0.84$; Figure 14), but not at 5% of force ($t_{11} = 2.1$, $p = 0.06$, Cohen's $d_Z = 0.61$). The change in CV_{PRED} of MEP at 30% of force was related to the change in MEP amplitude. Specifically, we found a decrease in MEP amplitude for FDI from 0.5s to 0.75s at 30% ($t_{11} = 2.9$, $p = 0.014$, Cohen's $d_Z = 0.84$), but not at 5% ($t_{11} = 1.4$, $p = 0.2$, Cohen's $d_Z = 0.40$) of force (Figure 14).

For APB, we did not observe modulation in CV_{PRED} of MEP across force conditions and TMS time points (no FORCE × TMS interaction: $F_{5,45} = 0.588$, $p = 0.709$, $\eta_P^2 = 0.061$; no main effect of FORCE: $F_{1,9} = 2.313$, $p = 0.163$, $\eta_P^2 = 0.204$; and no main effect of TMS: $F_{5,45} = 0.988$, $p = 0.436$, $\eta_P^2 = 0.099$). Similarly, for ADM, there was no modulation in predicted CV of MEP for across tasks and TMS time points (no FORCE × TMS: $F_{5,35} = 0.724$, $p = 0.610$, $\eta_P^2 = 0.094$; no main effect of FORCE: $F_{1,7} = 0.841$, $p = 0.390$, $\eta_P^2 = 0.107$; and no main effect of TMS: $F_{5,35} = 0.090$, $p = 0.993$, $\eta_P^2 = 0.013$).

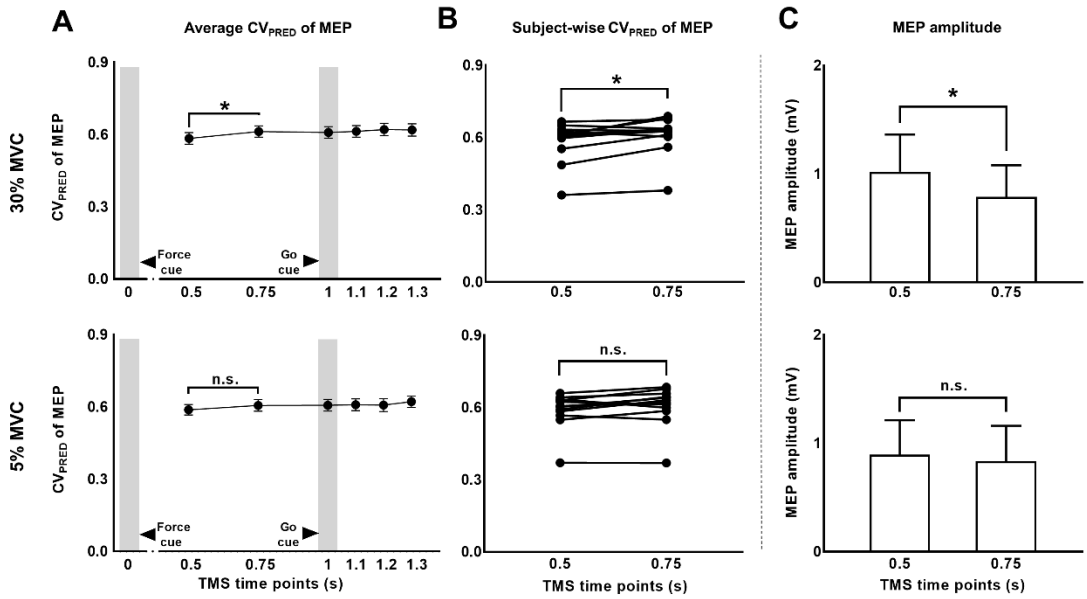

Figure 14: MEP CV due to changes in MEP amplitude during task preparation. A. Time-course of predicted CV of MEP at 30% compared to 5% of force. B. Subject-wise predicted CV of MEP data indicates a consistent rise across subjects from 0.5s and 0.75s at 30%, but not at 5% of force. C. A significant reduction in MEP amplitude from 0.5s to 0.75s explained the rise in predicted CV of MEP at 30% of force. Data in A and C are averages of all subjects (vertical bars denote SE). Asterisks indicate $p<0.016$ and n.s. indicates $p > 0.05$

MEP variability above and beyond predicted CV of MEP during task planning (CV_{DIFF})

To investigate whether MEP variability modulated beyond CV_{PRED} of MEP while planning for the force task, we subtracted CV_{PRED} of MEP from CV_{OBS} of MEP to obtain CV_{DIFF} of MEP. For FDI, we found modulation in CV_{DIFF} of MEP across TMS time points (main effect of TMS: $F_{5,55} = 4.730$, $p = 0.001$, $\eta_P^2 = 0.301$). However, CV_{DIFF} of MEP was similar across force conditions (no FORCE × TMS interaction: $F_{5,55} = 0.436$, $p = 0.821$, $\eta_p^2 = 0.038$ and no main effect of FORCE: $F_{1,11} = 0.065$, $p = 0.803$, $\eta_p^2 = 0.006$). Post hoc comparisons found a significant increase in CV_{DIFF} of MEP from 1.2s to 1.3s ($t_{11} = 3.1$, $p = 0.01$, Cohen's $d_Z = 0.89$). No difference in CV_{DIFF} of MEP was found between other adjacent TMS time points (all p values > 0.13).

Within each force level, we found significant increase in CV_{DIFF} of MEP from 1.2s to 1.3s at 30% ($t_{11} = 2.9$, $p = 0.015$, Cohen's $d_Z = 0.84$; Figure 15) but not at 5% ($t_{11} = 1.6$, $p = 0.14$, Cohen's $d_Z = 0.46$) of force. Most subjects showed a systematic increase in CV_{DIFF} of MEP from 1.2s compared with 1.3s at 30% of force (9 of 12 subjects; Figure 15). However, at 5% of force, the change in CV_{DIFF} of MEP from 1.2s to 1.3s was not consistent across subjects. Although the variability related to MEP amplitude were removed to obtain CV_{DIFF} of MEP, we confirmed that there was no change in MEP amplitude from 1.2s to 1.3s (30%: $t_{11} = 0.76$, $p = 0.47$, Cohen's $d_Z = 0.22$; 5%: $t_{11} = 1.04$, $p = 0.32$, Cohen's $d_Z = 0.30$; Figure 15).

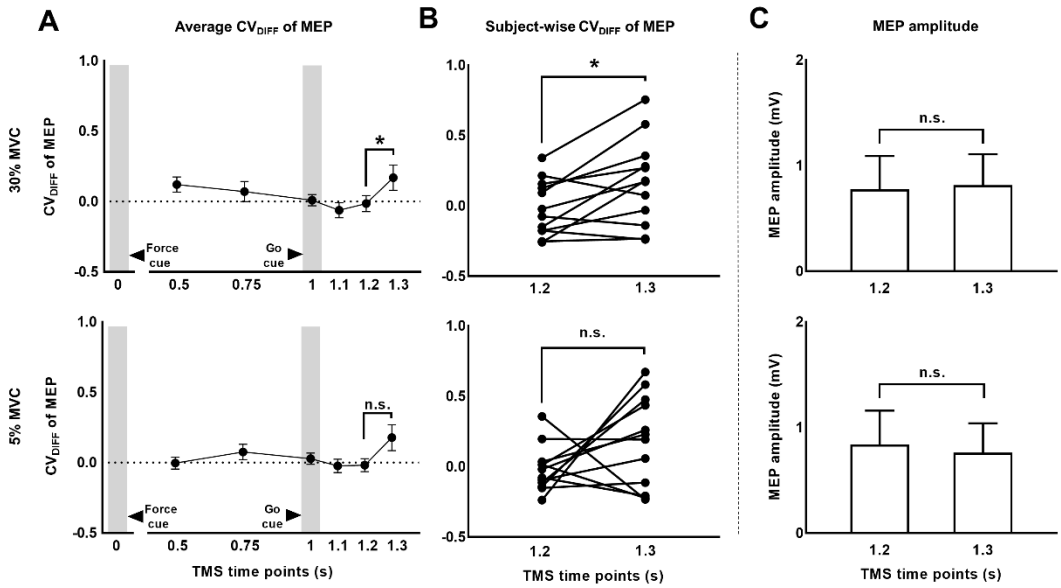

Figure 15: MEP CV rose above and beyond changes in MEP amplitude. A. Time-course of CV_{DIFF} (= observed – predicted CV) of MEP at 30% and 5% of force. B. Subject-wise CV of MEP data indicates a consistent rise across subjects from 1.2s and 1.3s at 30%, but not at 5% of force. (C) MEP amplitude analysis showed no modulation from 1.2s to 1.3s. Data in A and C are averages of all subjects (vertical bars denote SE). Asterisks indicate $p < 0.016$ and n.s. indicates $p>0.1$.

For APB, CV_{DIFF} of MEP was not different across force conditions and TMS time points (no FORCE × TMS time points interaction: $F_{5,45} = 0.302$, $p = 0.909$, $\eta_p^2 =$

0.032; no main effect of TMS: $F_{5,45} = 1.953$, $p = 0.104$, $\eta_P^2 = 0.178$, and no main effect of Force: $F_{1,9} = 0.290$, $p = 0.603$, $\eta_P^2 = 0.031$). Similarly, for ADM, CV_{DIFF} of MEP was not different across force conditions and TMS time points (no FORCE × TMS interaction: $F_{5,35} = 0.746$, $p = 0.532$, $\eta_P^2 = 0.096$; no main effect of TMS: $F_{5,35} = 2.880$, $p = 0.073$, $\eta_P^2 = 0.118$, and no main effect of FORCE: $F_{1,7} = 0.938$, $p = 0.365$, $\eta_P^2 = 0.118$).

To understand muscle-specific modulation in CV_{PRED} and CV_{DIFF} of MEP, we investigated modulation in FDI and APB EMG activity at 30% and 5% of force. We found that the EMG activity was greater for 30% versus 5% of force for FDI ($t_{11} = 2.7$, $p = 0.019$, Cohen's $d_Z = 0.78$), but not for APB ($t_{11} = 1.4$, $p = 0.18$, Cohen's $d_Z = 0.40$; Figure 16), thus suggesting asymmetrical contribution of FDI and APB in the application of grip force, in agreement with previous reports (Li et al., 2013, 2015; Nataraj et al., 2015).

Correlation between the rise in CV of MEP during planning and behavioral variability

We investigated whether the increase in task-related MEP variability (i.e., CV_{DIFF} of MEP) from 1.2s to 1.3s explained the inter-individual differences in trial-to-trial behavioral variability. We found that the increase in CV_{DIFF} of MEP from 1.2s to 1.3s explained 64% of inter-individual differences in $Time_{PFR}$ SD (Pearson's $r = 0.80$, $p = 0.0017$; Figure 17) at 30% of force. However, similar association between CV_{DIFF} of MEP and SD in $Time_{PFR}$ was not observed for 5% of force ($r = -0.25$, $p = 0.42$). Similar to the findings related to CV_{DIFF}, there was a significant association between SD_{DIFF} in MEP and SD in $Time_{PFR}$ for 30% force (Pearson's $r = 0.62$; $p = 0.03$), but not

5% force (Pearson's r = -0.20; p = 0.53).We also found no correlation between CV_{DIFF} of MEP and SD of PFR or CoP variability (all r-values < 0.26, all p values > 0.42).

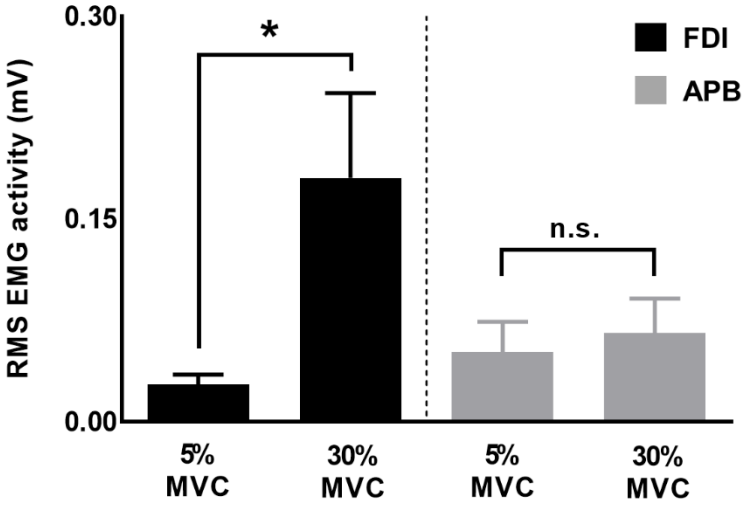

Figure 16: EMG activity for FDI and APB muscles. Force magnitude-dependent modulation in EMG activity was significant for FDI but not for APB muscles. Data are averages of all subjects (vertical bars denote SE), asterisk indicates p = 0.019 and n.s. indicates p>0.1.

Robustness and Repeatability of our findings

To test the robustness of the findings with respect to MEP pre-processing, we analyzed our data using no lower bound cut-off for MEP amplitude and no bin-based cut-off criteria (see *Methods*). Furthermore, we fitted a logarithmic model for each individual subject's data to understand if the findings were sensitive to the group-level model (see *Methods*). The results were similar to that reported above. Across individual logarithmic models, the intercept ranged from 0.47 to 1.13 and the slope ranged from -0.29 to 0.029 Figure 13). The logarithmic model obtained from *experiment 1* was used

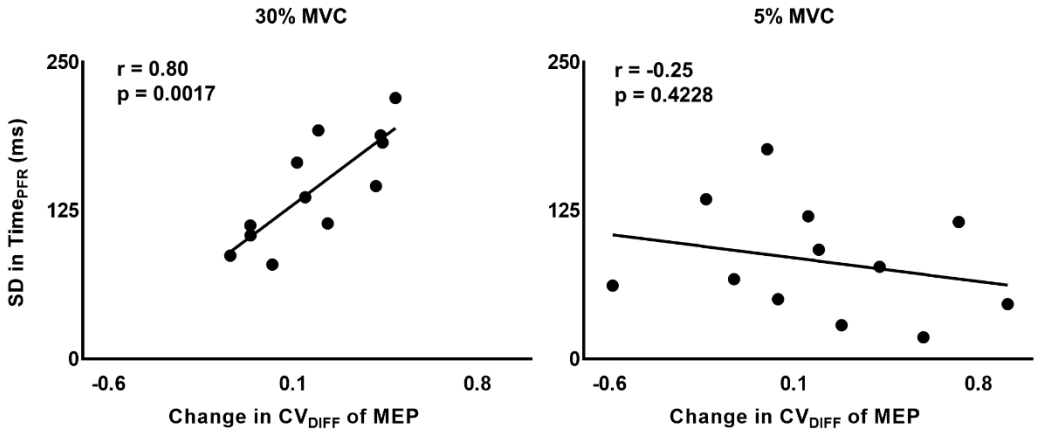

Figure 17: Correlation between intertrial task-specific variability in MEP and time to peak force rate. Modulation in intertrial MEP variability (CV_{DIFF} of MEP) for FDI muscle explained inter-individual differences in the trial-to-trial fluctuations in time to peak force rate, selectively at 30% (r = 0.80, p = 0.0017), but not at 5% (r = -0.25, p = 0.4228) of force.

to obtain CV_{PRED} for each subject. As done earlier, we subtracted CV_{PRED} of MEP from CV_{OBS} of MEP to obtain CV_{DIFF} of MEP. We found modulation in CV_{DIFF} of MEP in FDI across TMS time points (main effect of TMS: $F_{5,55} = 7.64$, $p < 0.001$, $\eta_p^2 = 0.41$). CV_{DIFF} of MEP was similar across force conditions (no FORCE × TMS interaction: $F_{5,55} = 0.55$, $p = 0.73$, $\eta_p^2 = 0.048$ and no main effect of FORCE: $F_{1,11} = 0.021$, $p = 0.88$, $\eta_p^2 = 0.002$). Post hoc comparisons found a significant increase in CV_{DIFF} of MEP from 1.2s to 1.3s ($t_{11} = 3.92$, $p = 0.002$, Cohen's $d_Z = 1.13$). No difference in CV_{DIFF} of MEP was found between other adjacent TMS time points (all p values > 0.10). Within each force level, we found significant increase in CV_{DIFF} of MEP from 1.2s to 1.3s at 30% ($t_{11} = 2.9$, $p = 0.015$, Cohen's $d_Z = 0.84$) but not at 5% ($t_{11} = 1.9$, $p = 0.08$, Cohen's $d_Z = 0.55$) of force. Importantly, the relationship between the modulation in CV_{DIFF} of MEP and intertrial behavioral variability was preserved. That is, the increase in CV_{DIFF} of MEP from 1.2s to 1.3s explained 61% of inter-individual differences in $Time_{PFR}$ SD (Pearson's $r = 0.77$, $p = 0.0029$) at 30% of force.

To test the repeatability of the MEP findings, we separately analyzed data from 9 additional subjects who had performed a similar task (low force = 1N grasp force and high force = 10% of force) as described in (Parikh et al., 2014). We found modulation in CV_{DIFF} of MEP in FDI across TMS time points (main effect of TMS: $F_{5,40} = 3.63$, $p = 0.0081$, $\eta_p^2 = 0.31$). CV_{DIFF} of MEP was similar across force conditions (no FORCE × TMS interaction: $F_{5,40} = 0.41$, $p = 0.84$, $\eta_p^2 = 0.048$ and no main effect of FORCE: $F_{1,8} = 0.029$, $p = 0.86$, $\eta_p^2 = 0.004$). Post hoc comparisons found an increase in CV_{DIFF} of MEP from 1.2s to 1.3s ($t_8 = 2.61$, $p = 0.03$, Cohen's $dz = 0.87$), however it failed to reach the corrected significance level likely due to lower sample size than the main study. No difference in CV_{DIFF} of MEP was found between other adjacent TMS time points (all p values > 0.15). Within each force level, we found an increase (although non-significant potentially due to low sample size) in CV_{DIFF} of MEP from 1.2s to 1.3s for the high force condition (10% of force; $t_8 = 2.16$, $p = 0.06$, Cohen's $d_Z = 0.72$) but not for the low force condition (1N grasp force; $t_8 = 1.8$, $p = 0.09$, Cohen's $d_Z = 0.60$). We found that the increase in CV_{DIFF} of MEP from 1.2s to 1.3s explained 40% of inter-individual differences in the SD of TimePFR for the high force condition (Pearson's $r = 0.63$, $p = 0.09$). Similarly, the increase in SD_{DIFF} of MEP from 1.2s to 1.3s explained 32% of inter-individual differences in the SD of TimePFR for the high force condition (Pearson's $r = 0.56$; $p = 0.1$). The findings were not significant likely due to lower sample size in the repeatability dataset. For the low force condition, the detection of the time to peak force rate was not reliable because, as instructed, subjects exerted minimal force (<1 N) perpendicular to its gripping surfaces (Parikh et al., 2014).

2.6.5. Discussion

We found that CSE variability increased beyond changes observed in CSE magnitude (i.e., CV_{DIFF} of MEP) while preparing to exert digit forces in a self-paced reach-to-grasp paradigm. The increase in CSE variability occurred after the 'go' cue presentation and this effect was temporally dissociated from the decrease in CSE magnitude that occurred before the 'go' cue presentation. The time-dependent modulation in CSE variability and CSE amplitude was evident at 30%, but not at 5% of force. Importantly, at 30% of force, individuals with larger increase in CSE variability also exhibited larger intertrial variability in time to peak force rate. These results were found to be repeatable across studies and robust to different data-analysis methods. We discuss our findings in relation to potential sources underlying the increase in CSE variability and its contribution to the application of grip force.

Modulation in CSE variability during task planning

Using a logarithmic model relating CSE magnitude and variability, we predicted the component of variability in CSE during task preparation that can be attributed to changes in CSE magnitude. We found a significant increase in predicted CV of MEP at 30%, but not at 5% of force. As predicted CV is primarily influenced by CSE magnitude, we found a corresponding reduction in CSE magnitude from 0.5s to 0.75s following the 'force' cue presentation at 30%, but not at 5% of force. This finding is consistent with our previous report demonstrating modulation in CSE magnitude at a higher force (Parikh et al., 2014). In contrast, other studies have reported an increase in MEP amplitude prior to movement onset (Starr et al., 1988; Chen et al., 1998; Chen and Hallett, 1999). However, this discrepancy might be due to differences in the task requirements. For instance, Chen and colleagues (1998) used a self-paced task and in

the current study we used an externally-cued task consisting of a multi-joint precision grip characterized by contact forces. We further show that the intertrial variability in CSE rose beyond predicted variability in CSE at 30%, but not at 5% of force. Interestingly, the decrease in CSE magnitude and the increase in task-specific variability in CSE were temporally dissociated because the later occurred from 1.2s to 1.3s following the presentation of 'force' cue during task preparation. This finding suggests distinct neural sources underlying the modulation in CSE magnitude and the component of CSE variability not related to changes in its magnitude. A consistent change in these variables across individuals at 30% of force (Figs. 5B and 6B) might represent important characteristics of individuals and thus the modulation in neural underpinnings during task planning (Kanai and Rees, 2011). Functional magnetic resonance imaging work has shown stronger activation in sensory- and motor-related fronto-parietal brain areas during application of lower but not higher precision grip force (Ehrsson et al., 2001). These findings suggest that precision grasping using smaller forces is a function of activation within a wider brain network. It is plausible that similar force-dependent activation is also present during task preparation (Hendrix et al, 2009). Large between-subject differences in the planning-related activation patterns within this wider network might have contributed to inconsistent modulation of MEP variability during planning at 5% of force. Lower and focal planning-related brain activation for 30% of force would have led to more consistent modulation of MEP variability.

Potential mechanisms that increased CSE variability during task planning

Our experimental design ruled out any difference in planning of digit position from trial-to-trial between force levels and across time points. These findings suggest that the modulation in CSE variability was specific to grasp force planning during the reach-to-grasp task and provides information about fluctuations in planning-related corticospinal activity.

CSE arises from activation of intracortical circuitry within M1, cortico-cortical inputs to M1, and subcortical and spinal structures (Bestmann and Krakauer, 2015). The modulation in neuronal activity within primate M1 and premotor cortices has been found to depend on the magnitude of grasp force (Hendrix et al., 2009). Parietal, occipital, cerebellum, dorsolateral prefrontal cortex, and basal ganglia are also known to contribute to the planning of grip force (Dettmers et al., 1996; Ehrsson et al., 2000b, 2001; Chouinard et al., 2005; Berner et al., 2007; Davare et al., 2007; Dafotakis et al., 2008). Virtual lesion studies using TMS have demonstrated contribution of human somatosensory, premotor dorsal, and supplementary motor regions in regulating the timing of digit force application (Davare et al., 2006; Schabrun et al., 2008; White et al., 2013). Evidence also exists in humans about the functional role of reticulospinal tracts in the control of coordinated hand movements such as those performed in our study (Honeycutt et al., 2013). It is less likely that changes in spinal motor neuron pool directly contributed to the increase in CSE variability during motor planning because variability in spinal motor neuronal excitability (as assessed by modulation in H-reflex) has been suggested to arise from changes in descending drive from supraspinal structures to spinal cord during motor planning (Collins et al., 1993; Misiaszek, 2003). Taken together, the increase in CSE variability observed during task preparation in our

study is potentially sourced within supraspinal structures. Modulation in activation of these potential sources might have contributed to intertrial fluctuations in presynaptic inputs to M1 neurons (Lemon, 2008), thus resulting in modulation in CSE variability. As noted above, the inputs to M1 that influence CSE magnitude (Parikh et al., 2014) might be distinct from the inputs to M1 that influence CSE variability.

Rise in CSE variability explains inter-individual differences in behavioral variability

In monkeys, neuronal firing rate variability within M1 and premotor regions during movement preparation has been suggested to explain ~50% of variability in reach speed from trial-to-trial (Churchland et al., 2006b, 2006a). Consistent with this primate work, we found that the intertrial variability in CSE specific to task-planning explained ~64% of inter-individual differences in behavioral, viz. $Time_{PFR}$, variability in humans. The rise in CSE variability was associated with $Time_{PFR}$ variability but not with variability in magnitude of peak force rate, although both factors are known to be important for accurate force application (Poston et al., 2008). It is plausible that the intertrial variability in CSE during force planning may encode the variability in timing of force application as a control variable. Disruption of human premotor dorsal area using single pulse TMS while preparing to grasp an object was found to affect the timing, but not the magnitude, of grip force application (Davare et al., 2006). The observed relationship between CSE and $Time_{PFR}$ variability, therefore, may suggest the contribution of premotor dorsal area to the modulation in CSE variability. Interestingly, single pulse TMS over M1 as used in the current study did not impair subjects' ability to control digit placement and apply grip force. Further studies using repetitive TMS, a more robust way to perturb neural activity (Paus, 2005), might provide better insight

into the central mechanisms underlying behavioral variability. Other task attributes such as attention and arousal levels may also contribute to behavioral and neural variability (Cohen et al., 1997; Fontanini and Katz, 2008; Masquelier, 2013; Dinstein et al., 2015). Our findings provide evidence for the contribution of variability in planning-related neural mechanisms to motor output variability and corroborate earlier behavioral work in humans (van Beers, 2009). Fluctuations in neural activity during task execution may explain the remaining inter-individual differences in timing variability. A recent neuroimaging study found that the variability in BOLD-activity within intraparietal cortex recorded concurrently with task performance (i.e., during movement execution) accounts for ~25% of inter-individual differences in movement extent variability (Haar et al., 2017). In our study, the neural activity engaged during force planning may also be present during force execution and thus potentially contributing to the inter-individual differences in behavioral variability.

Overall, our study provides a novel insight into the contribution of planning related mechanisms to behavioral variability by assessing variability in human CSE in a self-paced reach-to-grasp paradigm. Our findings suggest that individuals with a greater increase in the neural variability during planning exhibit a greater behavioral variability.

Contribution to the field

Traditionally, motor variability has been construed as noise in the peripheral system arising due to complex demands of the task or ever-changing surrounding conditions. Challenging this notion, recent research in primates showed that components of behavioral variability arise due to variable neuronal activity during

motor preparation. Our study extends the scope of this knowledge by showing for the first time that variability in human corticospinal excitability modulates while planning the grasp force and is associated with behavioral variability. Further, we show that the variability in corticospinal excitability is temporally dissociated from the amplitude-based modulation of the corticospinal tract and is likely to originate from supraspinal neural activity. Findings from this study could guide future research investigating the role of neural variability in shaping human behavior in healthy as well as clinical populations.

2.6.6. Acknowledgements

We thank Drs. Sheng Li, Stacey Gorniak, Marco Santello, and Joseph Francis for their comments on an earlier version of this manuscript.

Funding: This work was supported by the University of Houston Division of Research High Priority Area Research Seed Grant to PJP.

2.7 Motor variability and moment-to-moment force control

Controlling forces from moment-to-moment enables a plethora of interactions with the surrounding (Enoka et al., 2003; Dideriksen et al., 2012; Wu et al., 2014; Hadjiosif and Smith, 2015; Dhawale et al., 2017; Feeney et al., 2018). One may encounter moment-to-moment force control while performing routine tasks such as holding a coffee mug, or while driving a car, or simply while standing upright for elongated duration. Holding a coffee mug is especially difficult when the mug is filled to the brim, so is driving a car on an extremely narrow lane or standing upright for long without any movement. Even for healthy young individuals with intact physiological processes, the inherent motor variability limits their control in such tasks

at varying levels. Deficits in this ability is evident among patients with movement disorders such as stroke, Parkinson's disease, cerebral palsy, and focal hand dystonia(Fellows and Noth, 2003; Chu and Sanger, 2009; Lodha et al., 2013) (a few of these illustrations depicted in Figure 2). Although the average force exerted might be comparable to the respective control data, the aberrations in the force traces are markedly evident among patients from control subjects. Given the vital role these fluctuations (or variability) play in our routine activities, do we already know why such variations occur, or what factors underlie such variability? How biological processes such as aging or specific ailments affect these fluctuations, and what is the nature of this variability? Understandably, scientific inquiry to answer these questions has been an ongoing effort, despite decades of research. Although it would be paramount to address these questions through unifying investigations, the proposed dissertation aims to briefly cover previous developments in the motor control literature, identify critical research gaps that currently limit our understanding about moment-to-moment force control and motor variability, and adopt a scientific approach to test the hypotheses addressing the identified research gaps. While motor control and variability could, in principle, be studied through several behavioral paradigms such as walking, grasping, or learning to sing (Churchland et al., 2006a; Kwon et al., 2011; Dideriksen et al., 2012; Dhawale et al., 2017), we build upon the conceptual framework of variability in digit forces, as established within the digit force control literature (Slifkin and Newell, 1999; Enoka et al., 2003; Sosnoff et al., 2006; Feeney et al., 2018).

Seemingly small fluctuations in digit force while grasping a coffee mug, or while holding a spoon often go unnoticed as mere 'noise'. Yet, numerous studies employ this ubiquitous 'noise' to understand the factors affecting motor variability (Newell et al., 1984; Harris and

Wolpert, 1998; Slifkin and Newell, 1999; Enoka et al., 2003). In isometric force production tasks, digit force variability is known to modulate with force magnitude exerted on the object (Slifkin and Newell, 1999). Studies quantifying linear variations in digit forces around its average value (i.e., using standard deviation, SD) have reported an increment in digit force variability with that in force magnitude (Galganski et al., 1993; Slifkin and Newell, 1999). Investigating the signal-dependent nature of the force variability, earlier reports showed that SD of grip force increased in a non-linear fashion with digit force magnitude as shown in Figure 18 (Slifkin and Newell, 1999). Interestingly other measures of variability including entropy which quantifies the structure of force output (Slifkin and Newell, 1999)), and signal-to-noise ratio (quantifying the noise with respect to the signal magnitude), further showed non-linear relationships of force variability with force magnitude (Slifkin and Newell, 1999). However, the distinct nature of these relationships based on the measure of variability prompted further studies on identifying systemic origins to this variability. The study also established that motor variations in the force are parametrically associated with increase in signal (isometric force) magnitude. Importantly, these findings challenged the earlier notion which neglected variability as a signal-dependent noise. Yet, the notion that force variability was a systemic property as opposed to an unwanted component called for further investigation.

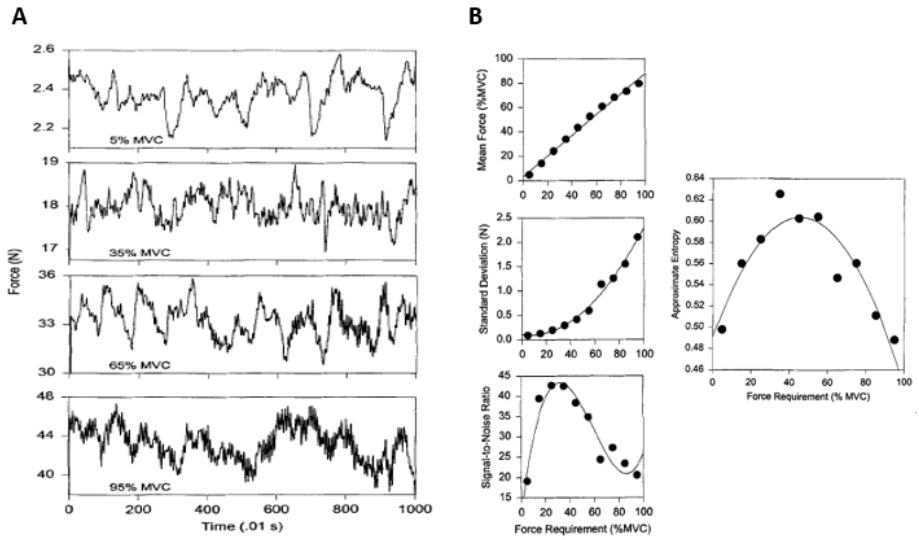

Figure 18: (A) Changes in digit force variability with force magnitude in terms of % of maximum voluntary contraction (MVC). Note the change in y-axis scale for each force level. (B) Non-linear nature of changes in SD of force as well as signal to noise ratio (=mean/SD) with increase in force magnitude (figure adopted from Slifkin and Newell 1996)

Within the peripheral systems, a direct pre-cursor to force production is the muscle contraction that depends on concurrent recruitment of the motor units and their discharge rates to enable efficient force control (De Luca et al., 1996; Enoka et al., 2003; Duchateau and Enoka, 2011; Enoka and Duchateau, 2017; Miller et al., 2017; Feeney et al., 2018). One of the studies involving healthy individuals to perform 12 s long force contraction task at 50% of their maximum voluntary contraction (MVC) capacity found that the individuals with greater changes in firing rates showed higher twitch force potentiation (Miller et al., 2017). Thus, influence of recruitment threshold on motor unit firing rate further affected the characteristics of force steadiness (Miller et al., 2017). These findings proposed the systematic influence of muscle properties on force control. As muscle dynamics is known to alter with aging, evidence further supporting the proposed notion was that from older individuals among whom force variability was indeed affected as shown in Figure 19 (Galganski et al., 1993; Vaillancourt and Newell, 2003; Miller et al., 2017). These studies attributed the reduced ability among older

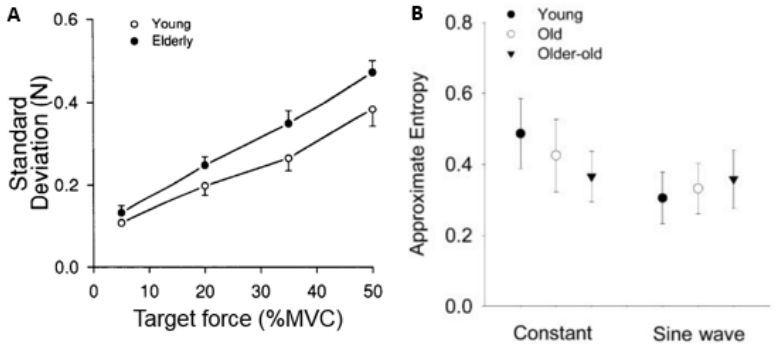

Figure 19: (A) Reduced standard deviation in digit forces with aging (figure adopted from Galganski et al 1993). (B) Reduced regularity with aging during the constant force task but directionally reversed trend for a sinusoidal force matching task. Young, old, and older-old correspond to the age groups 20-24 years, 64-69 years and 75-90 years respectively (figure adopted from Vaillancourt et al 2003).

individuals to sustain steady force contraction to the peripheral reorganization of motor units with aging (Galganski et al., 1993). Besides the SD of force signal, the regularity in force variability (as assessed by entropy) also revealed altered variability post aging such that older adults aged 64-69 years showed lower entropy than the younger adults (aged 20-24 years), but higher entropy than the relatively older adults (aged 75-90 years) during a constant force production task (Vaillancourt and Newell, 2003). This trend was reversed when the participants performed a sinusoidal force matching task, i.e., the older adults showed a higher entropy in force variability than younger adults but lower entropy than that in 'older-old' adults (Vaillancourt and Newell, 2003). These results highlighted the complementary information quantified by standard deviation (SD, group-level, sequence-independent variations) and entropy (structural, sequence-dependent variations). Importantly though, the notion that muscle dynamics could account for observed force fluctuations was systematically tested by two studies. One of these studies (Nagamori et al., 2021) modeled muscle dynamics first based on Fuglevand model which accounted for the experimental observation of signal-dependent variability however, failed to account for the physiological properties of motoneuron-motor

unit rate coding as well as tendon elasticity. The authors further incorporated these properties and identified that the new, physiologically accurate muscle dynamics fail to explain the

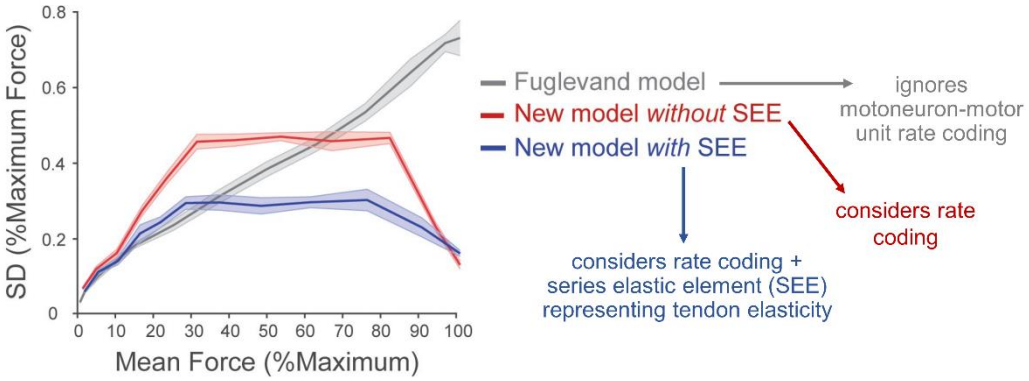

Figure 20: Incorporating the physiological dynamics such as motoneuron-motor unit rate coding as well as tendon elasticity failed to explain the observed increase in SD vs. magnitude of force shown in **Figure 18** (current figure adopted from Nagamori et al 2021; explanation of models added for quick reference)

majority of grip force variability observed experimentally as shown in **Figure** 20 (Nagamori et al., 2021). Corroborating this evidence, a study by (Feeney et al., 2018) found that muscle property such as motor unit firing rate variability failed to account for grip force variability. Interestingly however, (Feeney et al., 2018) identified that corticospinal inputs leading to common synaptic input variability significantly explained the variations in grip forces, indicating that grip force variability received systemic contributions from the corticospinal inputs rather than arise as a peripheral bi-product of muscle dynamics. These findings rather strengthened the notion that central, but not peripheral, processes underlie the modulation in within-trial grip force fluctuations (Kilner et al., 2003; Feeney et al., 2018; Nagamori et al., 2021).

The central correlates of grip force variability have also been of interest based on the studies assessing force variability among clinical populations. For instance, several studies have shown changes in force variability with neurological disorders including stroke,

Parkinson's disease (PD), and cerebral palsy (Fellows and Noth, 2003; Chu and Sanger, 2009; Lodha et al., 2013). Among patients with focal hand dystonia (also known as *writer's cramp*- a physiological condition affecting the sensorimotor system), it was observed that force variability was reduced compared to that in healthy control subjects. As these neurological ailments also entailed deficits in the sensorimotor systems (e.g. muscle spasticity post stroke, tremors in PD, hyperreflexia in cerebral palsy - CP), besides the neurological dysfunction, there has been an interest in characterizing the influence of sensory information such as availability of visual feedback, on force variability (Prodoehl et al., 2006).

2.8 Visual information and central processing during force control

Availability of visual information typically conveys the need as well as the degree of correction essential during the ongoing force production task (Prodoehl et al., 2006; Baweja et al., 2009). Removal of this information poses a need to direct the force production based on other available information (mainly via proprioception and touch-based mechanoreceptors) in the task (Prodoehl et al., 2006; Baweja et al., 2009). Such disruption and the re-weighting of other sensory modalities is often manifested as a drift in the force exerted without visual information (Baweja et al., 2010). Does the influence of visual information on force variability also depend on the force magnitude? Multiple studies have typically modulated the gain of the visual feedback to alter the extent of visual information available during force control (Baweja et al., 2009, 2010; Christou, 2011).

Based on previous reports, mean force magnitude has been shown to be unperturbed with changes in visual gain. For instance, a study failed to observe significant difference between mean force exerted at 2% MVC with a lower visual gain (0.5-16 pixels/N) versus that at higher

visual gain (32-1424 pixels/N), as was the case for mean force magnitude at 10% MVC (Baweja et al., 2010). Interestingly however, force variability (as assessed by SD of digit force) showed a reduction with increase in visual gain as shown in Figure 21 (Baweja et al., 2010). The study also showed a reduction in the spectral power of the force signal, especially in the lower frequency range of 0-1 Hz and 3-7 Hz. The reduction in 0-1 Hz explained 50% and that in 3-7 Hz explained 20% of reduction in SD of digit force. Besides the relevance of visual inputs and low frequency components in the force signal, the findings suggested critical mechanistic contribution of sensorimotor processes to force variability beyond the previously characterized influence of peripheral muscle properties.

Consistent with previous findings, multiple studies later showed critical contribution of low frequency oscillations to force variability (Baweja et al., 2010; Dideriksen et al., 2012; Lodha et al., 2013; Moon et al., 2014; Lodha and Christou, 2017; Feeney et al., 2018). In fact, one of the studies showed that oscillations with frequency <0.5 Hz predicted ~94% of changes in force variability (Lodha and Christou, 2017). Furthermore, the <0.5 Hz oscillations were prominent in tasks involving force control with multiple variations, including finger abduction, precision grip, power grip, as well as ankle dorsiflexion as shown in Figure 22 (Kwon et al., 2011; Lodha et al., 2013; Moon et al., 2014; Lodha and Christou, 2017). These findings established that the contribution of <0.5 Hz oscillations to force variability is neither dependent on the number of digits used to exert the force, nor the effector used in the force control task, but is rather representative of the oscillations from the spinal motor neuron pool influenced by the voluntary drive from the cortical regions (Neto et al., 2010; Lodha et al., 2013; Moon et al., 2014; Lodha and Christou, 2017). The notion is consistent with reports depicting a decrease in force precision while exerting 5% MVC (with lower voluntary drive) versus 30% MVC with

increased voluntary drive (Schmidt and et al, 1979; Slifkin and Newell, 1999; Slifkin et al., 2000; Lodha and Christou, 2017). Collectively, these findings support the involvement of task-relevant sensory information (i.e., visual feedback) and properties of the corticospinal tract (via spectral characteristics) in moment-to-moment force control.

The influence of visual information on the behavioral force variability and its relationship with the low frequency components in the force signal has been accompanied by an increasing interest in understanding the role of central processes underlying force variability. Primarily,

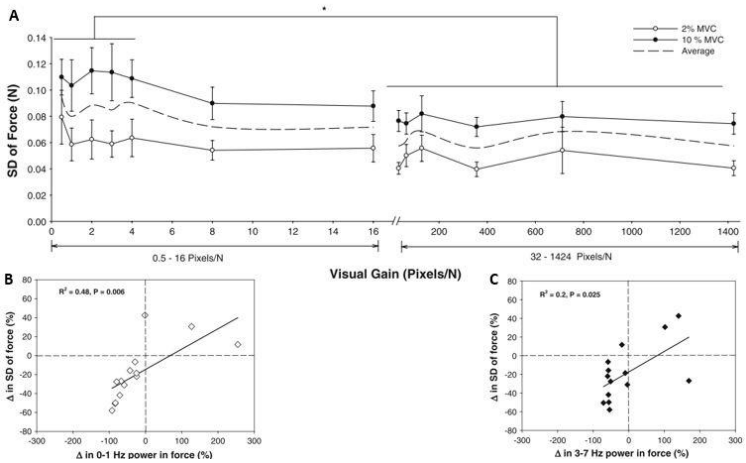

Figure 21: (A) SD in force reduces when force feedback is presented with higher versus lower visual gains. (B)Changes in 0-1 Hz power in force signal explained ~48% of variability in changes in SD of force, and (C) Changes in 3-7 Hz power in force signal accounted for ~20% of variability in changes in SD of force (plots adopted from Baweja et al 2009)

the dependence of isometric force variability on visual information implied a reliance of the former also on the associated visuomotor processing, mainly known to occur at the cortical and subcortical levels (Vaillancourt et al., 2003b; Grafton, 2010; Lodha et al., 2013; Moon et al., 2014; Lodha and Christou, 2017). Secondly, the low frequency components in the force signal indicated the influence of neural commands on muscle activity via the descending tracts from the central origins as shown in Figure 22 (Vaillancourt et al., 2003b; Neto et al., 2010; Moon et al., 2014).

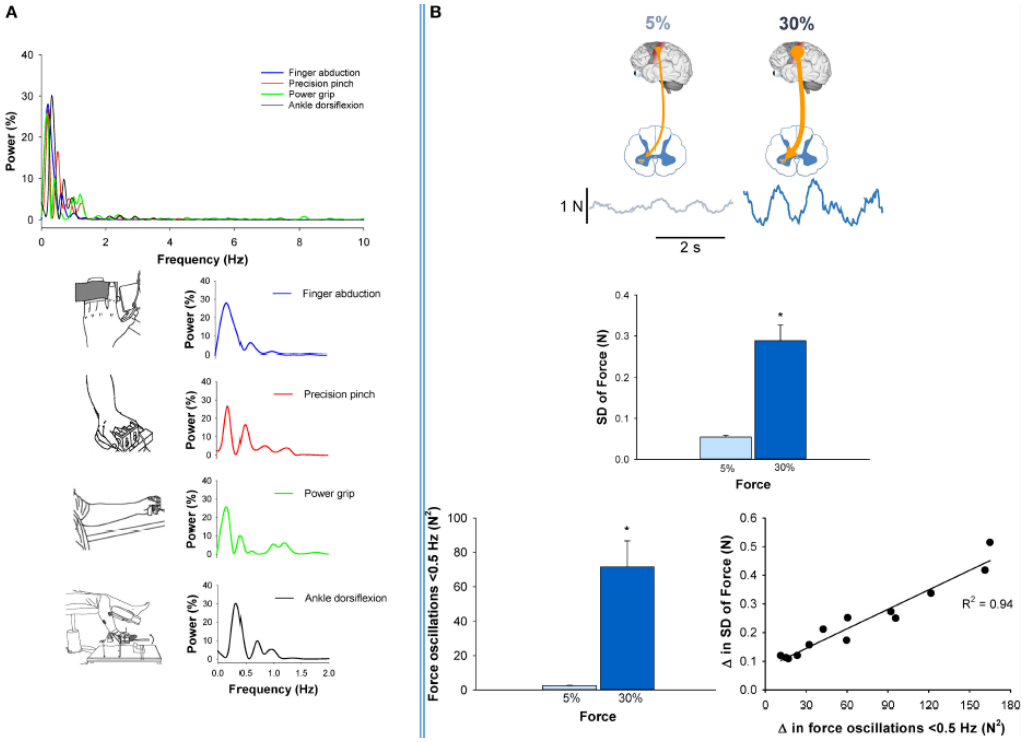

Figure 22: (A) Power spectrum showing increased low frequency components during multiple force exertion tasks. (B) Voluntary drive spanning the cortical centers to muscles via the spinal motor neuron pool is lesser while exerting 5% MVC than that in 30% MVC (top panel), changes in force variability and associated low frequency (<0.5 Hz) components (figure adopted from Lodha and Christou 2017)

Processing task-relevant visual inputs and directing the subsequent action accordingly has been known to involve multiple cortical regions (Vaillancourt et al., 2003b; Grafton, 2010; Poon et al., 2013; van Polanen and Davare, 2015). A study involving 10 participants to exert a precision pinch force at 15% MVC recorded their blood oxygen level dependent (BOLD) activity using functional magnetic resonance imaging (fMRI) during four different conditions: (1) at rest, (2) while exerting force with visual feedback, (3) exerting force with no visual

feedback, and (4) having visual feedback of automated cursor movements but with no force exerted(Vaillancourt et al., 2003b). Comparing BOLD activity in the second and the fourth conditions helped the experimenters observe brain regions specifically involved in visuomotor processing related to the digit force task, beyond those processing visual inputs alone. Notably, combination of cortical and subcortical regions including the parietal, premotor, anterior prefrontal cortices, ventral thalamus, lateral and intermediate cerebellum, putamen, and dentate nucleus were found to be associated with the visuomotor processing in the task (Vaillancourt et al., 2003b). These findings served as evidence supporting the role of localized frontal and parietal brain regions in visuomotor transformations essential for digit force control.

Within the fronto-parietal brain regions, studies have suggested critical role of the primary motor cortex (M1) in integrating visuomotor inputs pertaining to the digit force application depicted in Figure 23 (Davare et al., 2007, 2008, 2009, 2011; Grafton, 2010; Rao and Parikh, 2019; Parikh et al., 2020). For instance, M1 activity in conjunction with the ventral premotor (PMv) and anterior intraparietal sulcus (aIPS) has been shown to process visuomotor commands related to object properties (e.g. object shape, size)(Grafton, 2010; Davare et al., 2011). Temporary disruption to M1 activity was further shown to affect participants' ability to process this information during a grasping task (Davare et al., 2010, 2011; van Polanen and Davare, 2015). Besides processing the visuomotor inputs, M1 activity averaged across multiple trials is also known to modulate with the magnitude of digit force to be exerted (Ehrsson et al., 2000a, 2001; Hendrix et al., 2009; Perez and Cohen, 2009; Davare et al., 2010, 2011). In 18 healthy young adults, corticospinal excitability of the finger muscles assessed over M1 decreased prior to exerting a higher (10% MVC) versus lower grip force (<1 N) during an object grasping task(Parikh et al., 2014). Furthermore, the trial-to-trial variations in

corticospinal excitability (also assessed over M1) explained ~40% of intertrial variations in digit force application across 12 individuals (Rao and Parikh, 2019) with the remaining variability speculated to arise from cortical network activity associated with M1, sub-cortical and cerebellar activity sensitive to the grip force applications, and likely the ascending and descending spinal tracts (Osborne et al., 2005; Churchland et al., 2006a; Honeycutt et al., 2013; Haar et al., 2017; Lei et al., 2018; Rao and Parikh, 2019). The results were robust to the analytical modelling and consistent across datasets from different individuals in variants of the experiment, suggesting the role of M1 in modulating corticospinal variability during digit force applications (Parikh et al., 2014; Rao and Parikh, 2019).

2.9 Visuomotor integration post M1 inhibition

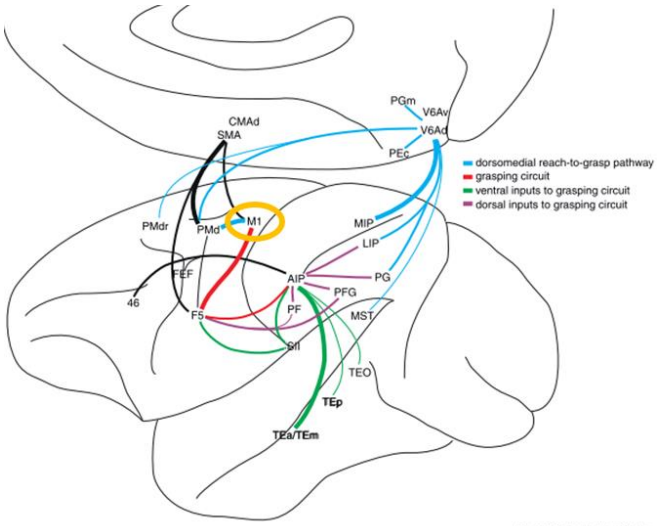

Figure 23: Cortical areas involved in grasping (adopted and modified from Davare et al 2011, Grafton 2010). Colored connections depict functional association of each cortical region within the grasping circuit. M1 is indicated as one of the critical nodes processing the grasp information. Note the primate brain depicted in the illustration.

One of the studies aimed at understanding the involvement of M1 in grip force production after removal of visual feedback instructed 12 participants to repeatedly exert brief pinch force synchronized with a 2 Hz metronome (Therrien et al., 2011). The experimenters conducted baseline, cTBS, or sham sessions over M1 prior to the task and observed that the

overproduction of force, immediately after the removal of visual feedback, was reduced post cTBS but not sham and baseline sessions as shown in Figure 24 (Therrien et al., 2011). The finding is consistent with the notion of attenuating predictable sensory information to increase the salience of external stimuli (Voss et al., 2007; Therrien et al., 2011). Such sensory attenuation is known to weaken the sensation of self-exerted forces (Voss et al., 2007; Therrien et al., 2011, 2013). This, in turn, leads to an overproduction of the grip force upon removal of visual feedback. The process of sensory attenuation has been previously discussed to rely on forward models using the efference copy of motor commands from M1 (Voss et al., 2007; Therrien et al., 2011, 2013). Consequently, application of cTBS over M1 could have diminished the sensory attenuation resulting into reduced force overproduction (Therrien et al., 2011, 2013). These observations suggest critical role of M1 in directing the voluntary drive essential for moment-to-moment digit force control (Chouinard et al., 2005; Parikh et al., 2014; Rao and Parikh, 2019). Bridging across the previously discussed literature, the findings underscore the role of M1 in processing visuomotor information as well as digit force magnitude during grasping. Interestingly however, the causal involvement of M1 in modulating the amount and structure of digit force variability during sustained force production **remains unknown**.

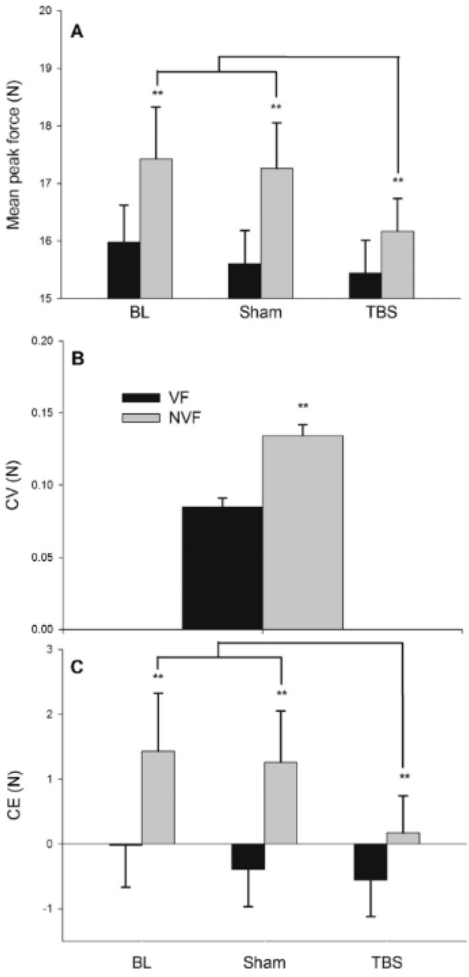

Figure 24: (A) Modulation in mean peak force with baseline (BL), sham, and TBS; (B) changes in CV of force with availability of visual feedback (VF: visual feedback, NVF: no visual feedback); (C) Constant error (CE, a measure of task accuracy) during NVF during BL, post sham and TBS with or without visual feedback (figure adopted from Therrien et al 2011).

2.10 Fronto-parietal cortical network processes underlying force control

Beyond M1, and as noted above, the cortical network processing digit force and sensory inputs during grasping spans from frontal to parietal and a few occipital regions (Ehrsson et al., 2000a, 2003; Vaillancourt et al., 2003b; Grafton, 2010; Davare et al., 2011). Neuroimaging studies have shown that activity in these cortical regions is selectively observed for specific phases as well as processing required for digit force applications (Ehrsson et al., 2000a, 2003;

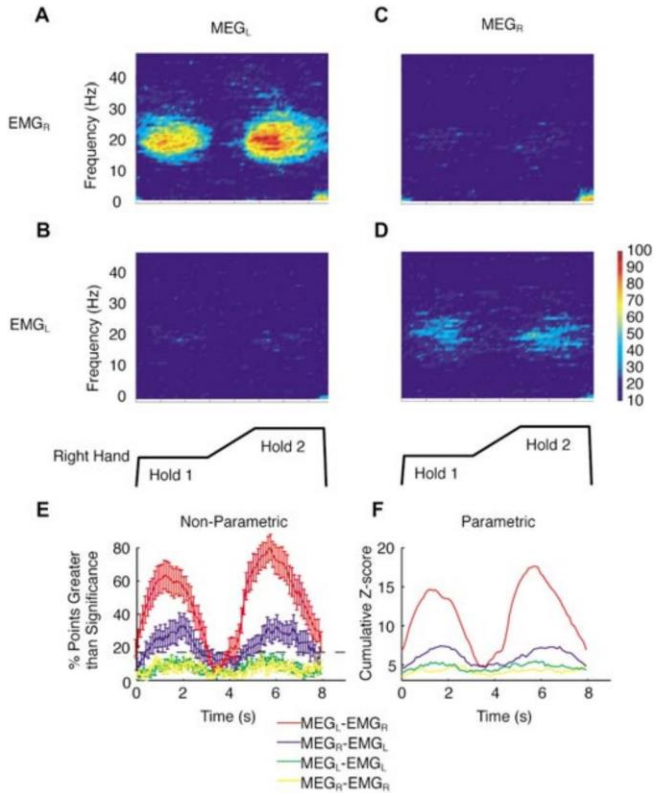

Figure 25: Modulation in MEG-EMG coherence during grip force control. The MEG was recorded over left and right sensorimotor cortices and the EMG from left and right first dorsal interosseus (FDI) muscle. The coherence pattern observed in the beta range was as shown in (A) left MEG (MEG_L) and right EMG (EMG_R), (B) MEG_L and left EMG (EMG_L), (C) right MEG (MEG_R) and EMG_R, and (D) MEG_R and EMG_L. (E) and (F) show the changes in coherence over time during the hold1, ramp, and hold2 phases assessed using non-parametric and parametric tests respectively. Note that ipsilateral hand always maintained a stable grip force regardless of the ramp phase for contralateral hand.

Kilner et al., 2003; Vaillancourt et al., 2003b; Grafton, 2010; Davare et al., 2011; Poon et al., 2013). An fMRI-based study previously showed that tasks involving force production using a precision grip involves extensive activation within the cortical regions including premotor, parietal and prefrontal areas (Ehrsson et al., 2000a). A study investigating changes in magnetoencephalography (MEG) showed task-dependent modulation in MEG-EMG coherence in beta band (15-30 Hz) during the stable hold phase versus ramp phase while exerting grip force (Kilner et al., 2003). Interestingly, this modulation was stronger for contralateral but not ipsilateral hand as shown in Figure 25 (Kilner et al., 2003).

Another fMRI-based study investigating the role of visuomotor processes in grip force control further showed cortical, subcortical, and cerebellar involvement during the visuomotor transformation in the task (Vaillancourt et al., 2003b). Importantly, this involvement was observed after accounting for visual and motor processes separately. These findings, along with later investigations, indicated changes in brain activity specifically pertaining to visuomotor transformation and grip force generation processes (Ehrsson et al., 2001, 2003; Vaillancourt et al., 2003b; Marneweck et al., 2018; Parikh et al., 2019, 2020; Marneweck and Grafton, 2020).

Despite earlier reports of changes in brain activity and the role of multiple brain regions during digit force applications, the findings based on temporal brain signals (mostly via electroencephalography, EEG) have been divergent. For instance, EEG activity in time-domain over fronto-parietal regions was reported to modulate based on visual feedback gain during the ramp phase, whereas that in frequency domain in the alpha band (7.5-13 Hz) modulated during the stable hold phase in a grip force task (Rearick et al., 2001). Another study assessing average power in neural activity via EEG reported marginal changes in the gamma band (30.5-45 Hz)

when exerting 75% versus 25% MVC force (Cao et al., 2015). This change was observed for selected electrodes spanning the central, parietal and frontal activity (C3, C4, Cz, Pz, Fz) (Cao et al., 2015). However, similar changes in power were observed only in one electrode activity (C3) for beta band (13.5-30 Hz), with no modulation in any other frequency bands, nor sensor activity with grip force level or associated fatigue (Cao et al., 2015). Similarly, no modulation in EEG activity was detected in response to changes in digit force magnitude during a grip force task (Siswandari et al., 2019). Importantly however in this study, the authors reported statistically significant and observable modulation in EEG signals related to the task after incorporating neural dynamics-based multi-variate approach. Our previous work assessing the reconstruction of grip force trajectories from EEG signals incorporated the multiple regression framework and identified that low frequency oscillations in the delta band (< 1 Hz) over the frontal regions were positively correlated with grip force whereas that in parietal regions correlated negatively with grip forces. These findings indicated that albeit controversial previous reports, it is possible to extract the task-relevant information with due consideration to neural dynamics that are critical to force control.

2.11 Variability in electrocortical activity during force control

Conventionally, the role of cortical activity during force control has been typically discussed by assessing the average neural signals (or changes in mean value) thereby, ignoring the signal variability (Aguirre et al., 1998; Birn, 2012; Grady and Garrett, 2018). Averaging the neural activity filters out the moment-to-moment fluctuations within the neural activity which, in turn, neglects the contribution of *neural variability* to a given task. In fact, multiple recent studies have confirmed critical role of neural variability across behavioral paradigms, including perceptual matching, attentional cueing, face recognition, and delayed match-to-

sample tasks (Garrett et al., 2010, 2011a, 2013a, 2013b, 2014). A study involving 18 healthy young adults to perform a face comparison task showed that moment-to-moment variability in the brain signal decreased with incremental changes in task difficulty (Garrett et al., 2014). Importantly, the reduction in neural variability depicted a pattern distinct from that revealed by average activity in the brain signal (Garrett et al., 2014). **Furthermore, a direct assessment of the neural average and neural variability showed no consistent relationship between the two measures, which reinforced the notion that brain signal variability is dissociable from the average neural activity and may provide complementary information** (Garrett et al., 2013a, 2014)**.**

Previous reports investigating changes in neural variability with aging showed that young adults with faster reaction time (RT) performance exhibited higher neural variability than that among older adults with slower RT performance depicted in Figure 26 (Garrett et al., 2011a). Similar modulation in brain signal variability (including the quantification of regularity) have been reported among children while performing face recognition tasks(McIntosh et al., 2010). These findings collectively suggest that neural variability could convey orthogonal and spatially differentiated information from that conveyed by neural means (McIntosh et al., 2010; Garrett et al., 2011a, 2014). Importantly, researchers argue that brain signal variability could be suggestive of three important underlying processes: 1) the dynamic range of outputs to assess dynamic versus static stimuli, 2) uncertainty in the stimulus, and 3) cognitive state transition in which greater variability could facilitate brain's transition from one cognitive state to another for processing the ongoing task demands (McIntosh et al., 2010; Garrett et al., 2011a, 2014; Grady and Garrett, 2018). Despite the applicability and significance of moment-

to-moment brain signal variability to several behavioral tasks, the mechanistic involvement of neural variability during moment-to-moment grip force control **remains poorly understood**.

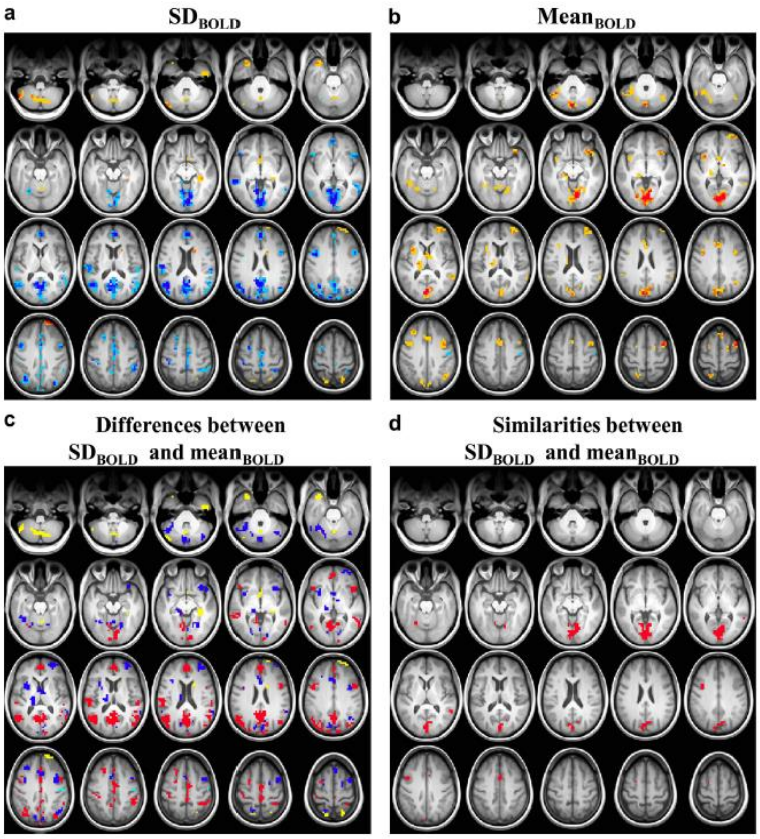

Figure 26: Neural variability (standard deviation - SD in BOLD activity) and neural means with age and reaction time (RT) performance (adopted from Garrett et al. 2011). (a) Blue represents greater and red/yellow depict lower neural variability with younger age and faster, more consistent RT performance. (b) Blue represents greater and red/yellow depict lower neural mean with younger age and faster, more consistent RT performance. (c) Overlay plot with differences in spatial patterns between neural variability and neural means with following color scheme: red for greater neural variability with younger age and better RT performance but no changes in neural mean, yellow for lower neural variability with younger age and better RT performance but no changes in neural mean, cyan for greater neural means with younger age and better RT performance but no changes in neural variability, blue for lower neural means with younger age and better RT performance but no changes in neural means. (d) Overlapping information conveyed by neural variability and means, red indicating greater neural variability and lower means with younger age and better RT performance.

Taken together, these findings convey two critical knowledge gaps in the literature: 1) while knowing that M1 is an important node for processing digit force magnitude and

visuomotor information during grasping, the causal involvement of M1 in moment-to-moment digit force control in presence (or absence) of visual feedback remains unknown. 2) Despite knowing the involvement of multiple cortical regions to facilitate grasping and accumulating recent evidence underscoring the involvement of neural variability in several behavioral paradigms, the mechanistic role of neural variability during digit force application remains unclear. We plan to bridge these research gaps by determining the causal involvement of M1 in processing digit force variability and identifying the mechanistic role of neural variability during digit force application (Figure 27).

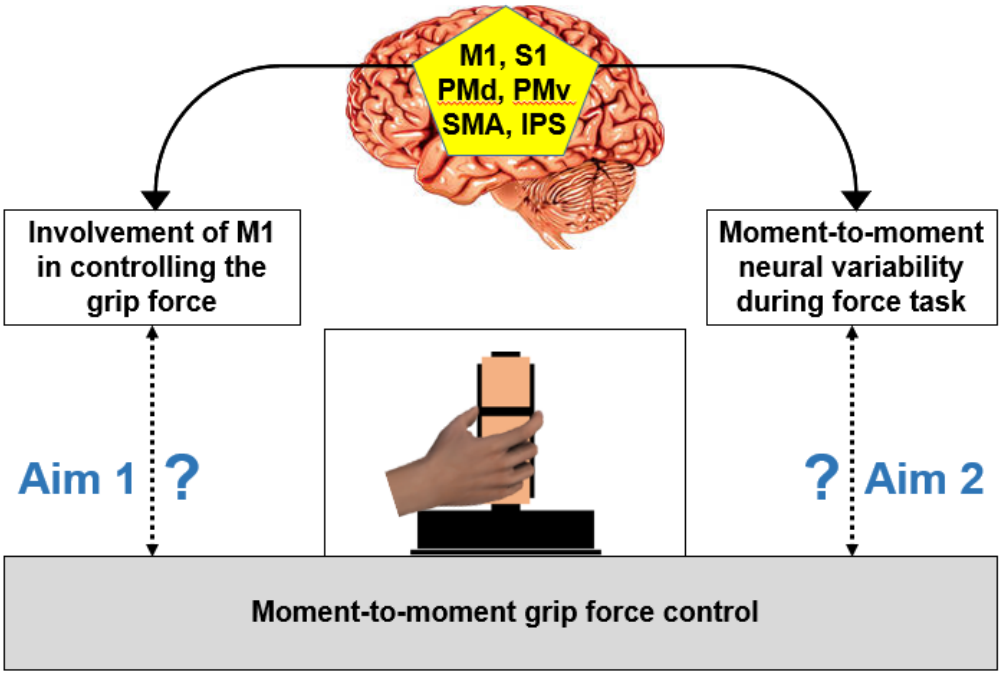

Figure 27: Conceptual framework of the identified research studies (picture of brain adopted from fotosearch.com)

Chapter 3. (Manuscript 1) Integrity of M1 is critical for maintaining temporal structure of digit force variability in the presence of visual feedback

3.1. Introduction

Variability in motor responses influences the ability to perform everyday motor tasks and learn new skills (Schmidt et al., 1979; Harris and Wolpert, 1998; Slifkin and Newell, 1999; Wu et al., 2014). An increase in variability is commonly observed due to aging or pathological changes (Bilodeau et al., 2000; Vaillancourt et al., 2002; Vaillancourt and Newell, 2003; Enoka et al., 2003; Blennerhassett et al., 2006; Chu and Sanger, 2009; Christou, 2011; Parikh and Cole, 2012; Lindberg et al., 2012; Lodha et al., 2013; Gorniak et al., 2014; Kang and Cauraugh, 2014; Ko et al., 2015; Lodha and Christou, 2017). While the behavioral and pathological factors influencing variability have been extensively documented, the knowledge on physiological processes contributing to variability in human behavior remains limited.

Variability has been suggested to arise from the peripheral neuromuscular, subcortical, and cortical systems (Eisen et al., 1996; Bilodeau et al., 2000; Jones et al., 2002; Enoka et al., 2003; Vaillancourt et al., 2003a; Churchland et al., 2006a; Christou, 2011; Ko et al., 2015). Traditionally, variability has been believed to arise primarily from motor noise whose amplitude increases with magnitude of the force exerted. A recent modelling work has found marginal contribution of motor unit properties to force variability (Nagamori et

al., 2021). For instance, modelling the population activity in motor units by incorporating motor unit discharge rate coupling, fusion of motor unit twitches, aponeurosis and tendon elasticity failed to account for majority of the force variability (Nagamori et al., 2021). Similarly, the association between inter-spike interval variability in motor units and force fluctuations was found to be weak (Feeney et al., 2018). Our recent work found an association between the variability in the excitability of corticospinal tract to the variability in time to peak grip force rate during a similar isometric grip force production task (Rao and Parikh, 2019). Overall, these studies point out the contribution of variability in common synaptic inputs to motor neurons to force fluctuations, indicating significant contribution of descending inputs to motoneuronal pool in modulating force variability (Feeney et al., 2018; Nagamori et al., 2021).

Importantly, the cortical activity within frontal and parietal regions may contribute to the variability in kinematic or kinetic features of motor output (Osborne et al., 2005; Churchland et al., 2006a; Fox et al., 2007; Hohl et al., 2013; Chaisanguanthum et al., 2014; Lisberger and Medina, 2015; Mizuguchi et al., 2016; Haar et al., 2017). Mainly, firing rates of neurons within primate primary motor (M1) explained variability in their peak reach velocity (Churchland et al., 2006a). In humans, changes within source localized activation patterns within M1 correlated with increase in grip force variability (viz. variability around the mean) when increasing the sensitivity of the sensorimotor system to errors during isometric force contraction (Poon et al., 2013). The cortical activity within the M1 and fronto-parietal regions showed temporal selectivity shortly after the increasing the gain of visual feedback of the grip force, implicating potential involvement of M1 in processing visuomotor information to direct the force output (Vaillancourt et al., 2003b; Prodoehl et

al., 2006; Baweja et al., 2009; Poon et al., 2013). However, the causal role of M1 in visuomotor integration critical to regulate force variability remains unclear.

To this end, we used transcranial magnetic stimulation (TMS) over M1 in healthy young adults to determine the causal role of M1 in modulation of grip force variability subject to the availability of visual feedback. We considered SD and the coefficient of variation (CV = SD/mean) as critical measures to assess within-trial grip force variability (Lodha et al., 2013; Poon et al., 2013; Moon et al., 2014; Lodha and Christou, 2017). Additionally, we investigated the degree of regularity in the signal using sample entropy such that higher entropy indicated lesser regularity (and increased complexity) whereas lower entropy indicated higher regularity (lesser complexity). Entropy measures have been previously shown to characterize developmental maturation as well as pathological disruption in sensorimotor processes (Mcintosh et al., 2008; Garrett et al., 2011a; Stergiou and Decker, 2011; Lodha and Christou, 2017; Shah-Basak et al., 2020). Assessment of sample entropy at multiple timescales is indicative of systematic interactions across the frequency spectra such that finer (or lower) timescales encompass interactions from a broader band of frequencies (low and high frequencies, short latency, local processing) whereas coarser (or higher) timescales encompassing narrower band of frequency-interactions (low frequencies, long-range temporal correlations – LRTCs, long-range processing) (Costa et al., 2005; Stergiou and Decker, 2011; Kosciessa et al., 2020; Shah-Basak et al., 2020). Consequently, we characterized spectral interactions in grip force variability by assessing sample entropy in the grip force signal over multiple timescales viz. multiscale sample entropy (Costa et al., 2005; Stergiou and Decker, 2011). Considering more complex temporal regulation of grip force with lower force magnitude in conjunction

with the evidence supporting involvement of M1 in temporal processing of visuomotor inputs and directing motor commands for digit force control (Baweja et al., 2010; Stergiou and Decker, 2011; Poon et al., 2013; Vieluf et al., 2015), we hypothesized that disrupting the M1 activity would alter the sequential structure of grip force variability when visual feedback of the grip force is available. We used continuous, intermittent, or sham theta burst stimulation (types of repetitive TMS) to induce temporary (lasting for ~25-30 minutes) inhibitory, excitatory, or placebo stimulation respectively over M1 in a cross-over counterbalanced design (Huang et al., 2005, 2007; Parikh et al., 2020; Rao et al., 2020). Participants performed isometric grip force matching task during which visual feedback of the exerted grip force was made available for the first 8s (visually guided condition) followed by subsequent 8s of exerting grip force with no visual feedback of the force (memory-guided condition). Building on a set of robust findings, we argue that integrity of M1 activity is critical to incorporate visuomotor information for regulating grip force variability.

3.2. Methods

3.2.1. Participants

Thirteen healthy, young adults provided written informed consent to participate in this study. The study required each participant to participate in three sessions separated at least 4 days apart. Three participants could not complete all three of their visits due to scheduling conflicts. Consequently, we report the data collected from ten individuals (five females, five males; age (mean ± SD): 22.50 ± 4.45 years) who completed all three visits for the study. Participants were right-hand dominant

(Oldfield, 1971) with normal or corrected-to-normal vision, no upper limb injury, no musculoskeletal or neuromuscular disorders. They were screened for their eligibility and potential adverse reactions to TMS using the TMS Adult Safety Screen Questionnaire (Keel et al., 2001; Rossi et al., 2009a). For each session, subjects were compensated by a $10 gift card and parking validation as a token of appreciation for their time. The study procedures were approved by Institute Review Board of the University of Houston.

3.2.2. Experimental procedures

Grip force characterization: We used a customized object equipped (Figure 28) with force sensors to record the grip force and affixed to the table during the isometric force production task (Parikh et al., 2014, 2020; Rao and Parikh, 2019). The object was equipped with two six-dimensional force/torque transducers (Figure 28; Nano-25, ATI Industrial Automation, Garner, NC) attached on each of the graspable surfaces, with a separation of 6.5 cm (Goel et al., 2019; Rao and Parikh, 2019; Rao et al., 2020). A 12-bit analog-to-digital converter board (sampling frequency 1 kHz, model PCI-6225, National Instruments, Austin, TX, United States) was used to acquire force data.

3.2.3. Electromyography

We recorded electromyographic (EMG) activity of right first dorsal interosseous (FDI) and right abductor policis brevis (APB) using differential surface electrodes (Delsys Bagnoli EMG System, Boston, MA, US). The reference electrode was placed on the dorsum of the right wrist. The skin was prepared using isopropyl alcohol pads prior to electrode placement. The experimenter verified that the electrodes remained in place throughout the experiment. CED data acquisition board (Micro1401, Cambridge, England; sampling frequency 5 kHz; band-pass filter with a cut-off frequency range of 20–450 Hz) was used for EMG data acquisition.

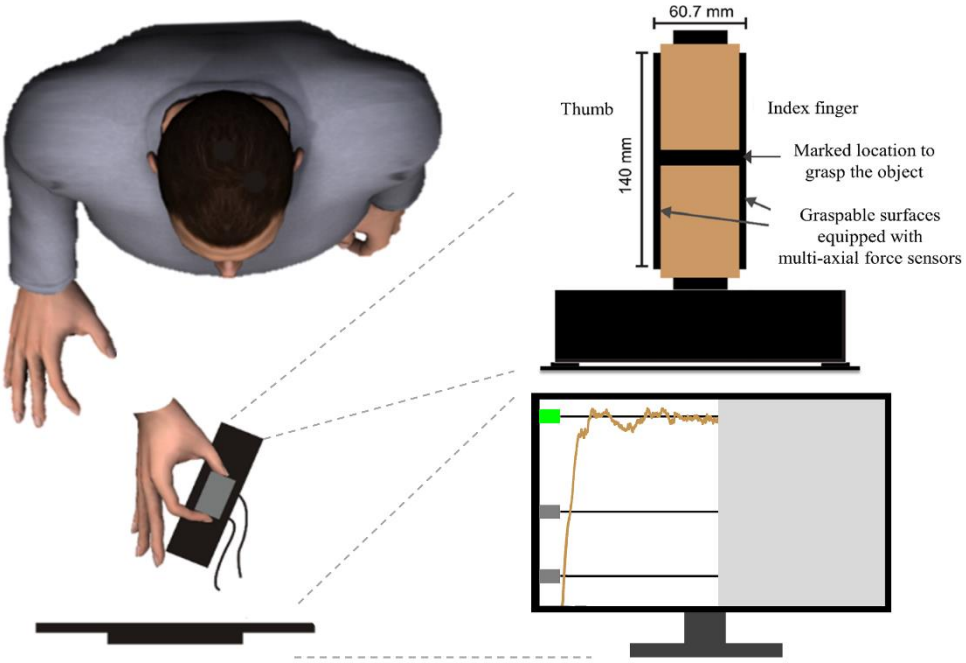

Figure 28: Experimental task setup depicting the customized grip device (top right) and the task succession with visual feedback of grip force shown for first 8s followed by no visual feedback of the grip force for the next 8s.

3.2.4. Transcranial magnetic stimulation

TMS and the use of theta burst stimulation (TBS) has been previously characterized to assess cortical contribution to grasping and digit force application (Huang et al., 2005; Davare et al., 2008; Di Lazzaro et al., 2008a; Parikh and Santello, 2017; Parikh et al., 2020). Using TBS, TMS can temporarily inhibit (cTBS) or excite (iTBS) cortical activity within the M1 region for ~25 minutes (Huang et al., 2005; Davare et al., 2019; Goel et al., 2019; Parikh et al., 2020; Rao et al., 2020). In the present study, TMS was used to: 1) assess changes in the corticospinal activity (CSE) over M1 via the single-pulse protocol, 2) assess the intra-cortical activity via the paired-pulse protocol, and 3) disrupt M1 activity via the theta burst stimulation (TBS) protocol. Single-pulse, paired-pulse, and TBS involve one, two, and a repetitive train of TMS pulses respectively. Following is the description of each of these procedures.

Single-pulse protocol (Figure 29): We first estimated the resting motor threshold (rMT) by delivering suprathreshold single monophasic TMS pulses over left primary motor cortex (M1) using a 70-mm figure-of-eight coil (Magstim 200, Whitland, UK) held tangential to the scalp and perpendicular to the presumed direction of the central sulcus, 45° from the midsagittal line, with the handle pointing backward, inducing current in the posteroanterior direction. The coil position was adjusted to optimize the motor-evoked potential (MEP) recorded via the EMG electrodes in the first dorsal interosseus (FDI) and abductor policis brevis muscles (APB). Following the optimal adjustment of coil that elicited MEPs over FDI and APB, the rMT was estimated as the minimum TMS-intensity to elicit MEP with an amplitude of ~50 μV (peak-to-peak of EMG signal) for at least 5 of the 10 consecutive trials in the FDI muscle as shown in **Figure 29** (Perez

and Cohen, 2009; Davare et al., 2011; Klein-Flugge et al., 2013; Parikh et al., 2014; Rossini et al., 2015; Parikh and Santello, 2017). The TMS coil was stabilized using a coil holder mounted on the TMS chair (Rogue Research, Montreal, QC, Canada). The TMS coil position on the subject's scalp was recorded using neuronavigation system (Brainsight software, Rogue Research). Average rMT across sessions for all subjects was 37 ± 8% of the maximum stimulator intensity output. The coil location was regularly checked to ensure continued proper placement during a session.

Paired-pulse protocol (Figure 29): Previous studies from our group as well as others have shown that delivering a TMS pulse over M1 (conditioning pulse) followed by a test pulse separated at specific interstimulus interval (ISI) can inhibit or facilitate the muscle response initiated by the first pulse (Olivier et al., 2007; Parikh et al., 2014). The cortical inhibition/facilitation depends upon the intensity (subthreshold for conditioning, suprathreshold for test pulse) as well as the ISI between the two pulses i.e., 1-5 ms for short intracortical inhibition – SICI, whereas ISI of 6-50 ms for short intracortical facilitation – ICF (Kujirai et al., 1993; Cohen, 2000; Parikh et al., 2014). Notably, the magnitude of SICI and ICF convey the inhibitory and facilitatory properties of cortical connections within the surrounding M1 region (Kujirai et al., 1993; Parikh et al., 2014). We first validated the paired pulse protocol in five healthy young individuals by delivering the conditioning and test TMS pulse at 80% and 120% of their rMT with 7 different ISI (1, 2, 4, 8, 10, 12, 15 ms). Additionally, we also delivered single test pulse to record the subjects' MEP. Fifteen trials for each ISI and test pulse were delivered in pseudo-randomized sequence. Quantification of inhibitory and excitatory response was conducted by normalizing the SICI and ICF responses with the test pulse (Parikh et al.,

2014). Consistent with previous reports, we observed inhibition of the test pulse for ISI of 1, 2, and 4 ms, and a facilitation of the test pulse at ISI of 8, 10, 12, and 15 ms (Figure 29). Consequently, we selected ISI of 2 ms and 10 ms to assess the SICI and ICF respectively for the grip force task (Figure 30).

Theta burst stimulation (Figure 29): We estimated active motor threshold (aMT) to set the stimulation intensity of continuous, intermittent, and sham theta burst stimulation (cTBS, iTBS, SHAM respectively). For estimating aMT, we instructed subjects to exert 20% of their maximum voluntary contraction (MVC) on the grip device. The object was to be grasped with the tips of index finger and thumb only. A computer screen displayed visual feedback of the grip force exerted on the object. The aMT was determined as the TMS intensity that induced ~200 μV peak-to-peak MEPs in 5 of 10 trials in the FDI muscle during force production at 20% of MVC (Rossini et al., 1994).

For administering continuous theta burst stimulation (cTBS), we delivered repetitive, biphasic TMS pulses over left M1 using a figure-of-eight coil at 80% of aMT. Delivery of the TMS pulses was conducted in the form of bursts of three pulses at 50 Hz at a rate of 5 Hz for 40s (i.e., 200-ms inter-burst interval; Figure 29). This protocol involves delivering a total of 600 pulses and is reported to temporarily inhibit the M1 activity at rest (~25 minutes) thereby, generating a "virtual lesion" (Di Lazzaro et al., 2005; Huang et al., 2005; Parikh and Santello, 2017; Rao et al., 2020). The average theta burst stimulation intensity across sessions for all subjects was 34 ± 7% of the maximum stimulator intensity output. Throughout the TBS delivery, the position of the coil was registered via the neuronavigation software and was monitored visually, similar to that mentioned before.

The intermittent TBS (iTBS; Figure 29) involved estimation of aMT as described before, but a slightly different approach of delivering TMS pulses from that in cTBS. The iTBS protocol was administered by delivering TMS pulses in the form of bursts of three pulses at 50 Hz at a rate of 5 Hz for ~190 s. However, the burst of TMS pulses were intermittently delivered for 2s in every 10s interval thereby, constituting a total of 600 pulses over the ~190s duration. This protocol is reported to temporarily (~25 minutes) excite the M1 activity at rest (Huang et al., 2005). The exact positioning of the coil was registered and monitored as previously described.

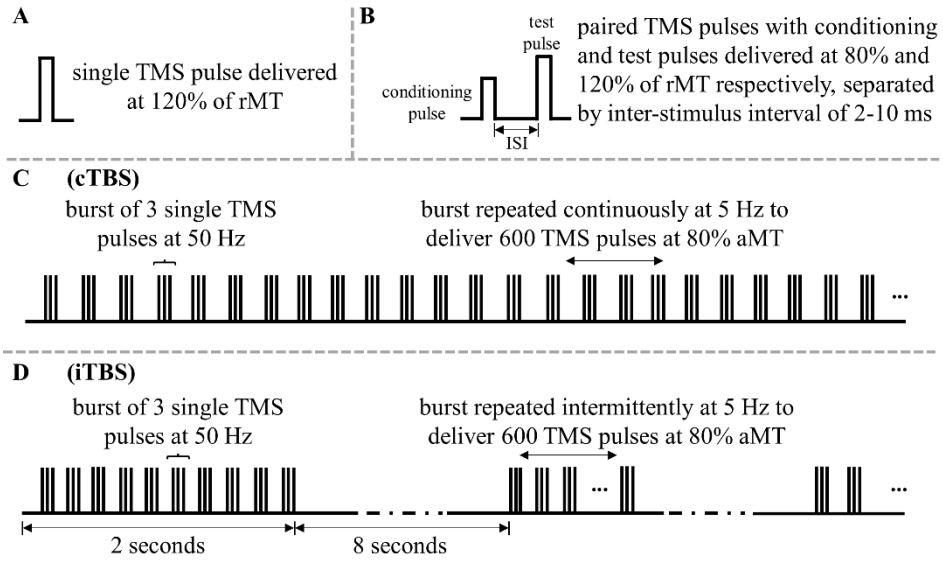

Figure 29: TMS protocols for (A) single pulse to assess corticospinal excitability; (B) dual or paired pulse to assess short interval intracortical inhibition and facilitation; (C) continuous theta burst stimulation (cTBS); and (D) intermittent theta burst stimulation (iTBS). rMT: resting motor threshold, aMT: active motor threshold, ISI: inter-stimulus interval.

The sham stimulation (Sham) mimicked a placebo condition in which the TMS pulses are delivered in almost the same manner as the cTBS protocol, but with the coil pointing perpendicular to the scalp. As a result, no TMS pulses are delivered to the cortical tissue yet, the participant is unaware of the change due to similar task setup. Sham protocol in a similar fashion has been administered by previous studies (Davare

et al., 2006; Goel et al., 2019). Based on the experimental design and in accordance with TMS guidelines, only one of cTBS, iTBS or Sham was delivered to a participant during each session. Hence, each subject participated in three sessions with the stimulation protocols assigned in a randomized sequence. To avoid any influence of administering one protocol on another, each session was conducted at least 4 days apart (Parikh and Santello, 2017; Goel et al., 2019; Parikh et al., 2019).

3.2.5. Experimental design

The experimental design is shown in (Figure 30)**.** We instructed the participants to perform an isometric force production task at three force levels (5%, 15%, and 30% of their MVC). In this within-subject, crossover design, each session (cTBS/iTBS/sham) was conducted at least 4 days apart and the sequence of these sessions was counterbalanced across subjects. During each session, participants were first seated comfortably on a chair equipped to position the TMS coil (Rao and Parikh, 2019). After obtaining informed written consent, the experimenters recorded maximum voluntary contraction (MVC) for each subject. During this procedure, the subjects were

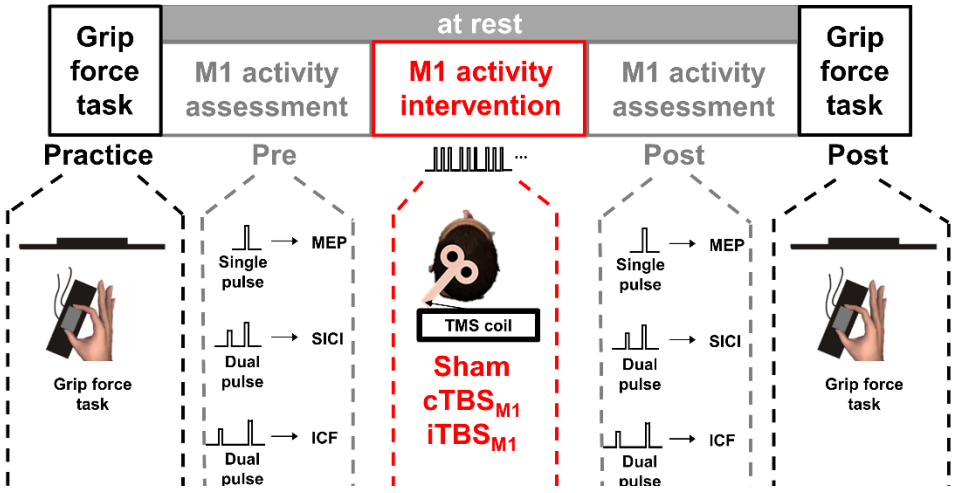

Figure 30: Within-subject counterbalanced experimental design with subjects participating in cTBS/iTBS/sham sessions each at least 5 days apart

instructed to grip using their index finger and thumb the customized object placed on the table ~30cm away from the chair with their maximal effort. Three such repetitions were assessed for consistent estimate of MVC. They were instructed to grasp the customized object at the marked location and exert 5, 15 or 30% of their MVC. For each trial, subjects were instructed to maintain the force for 16s during which visual feedback of their grip force and the target force was available for the first 8s, following which the visual feedback was removed for the subsequent 8s. Each trial started with a verbal as well as visual cue to exert the grip force level. Both the practice and the post blocks consisted of 15 trials, with 5 trials for each force level presented in a pseudo-randomized order.

3.2.6. Data analysis

Grip force data was subjected to zero phase lag, fifteenth order low pass Butterworth filter with 14 Hz cut-off frequency for removal of the high frequency noise (Flanagan and Beltzner, 2000; de Freitas and Lima, 2013; Rao and Parikh, 2019). The first three seconds after object-contact has been shown to comprise of the initial ramp phase (de Freitas and Lima, 2013). Consequently, we considered grip force data in the 4.8s epoch (data segment) following the initial 3s after object contact for subsequent analysis. For the segment when no visual feedback of the grip force was available to the participants, we considered 4.8s segment starting 500ms after the removal of visual feedback to ensure consistent segment length with the visual feedback condition. To test the hypothesis that temporarily disrupting M1 activity would modulate the moment-to-moment digit force control, we quantified the control of digit force via grip

force variability (using SD and sE-based measures) among the same individuals post cTBS/iTBS/sham sessions. The equation for SD is described below:

$$SD = \sqrt{\frac{\sum_{i=1}^{n}(\mathrm{GF(i)} - GFmean)^2}{n}}$$

where SD represents standard deviation, i represents i^{th} sample, n is total number of samples within a trial, GF(i) for grip force at i^{th} instance, and GFmean for average value of GF in that trial. It has been previously shown that SD scales positively with the magnitude of grip force due to which multiple studies have considered mean-normalized variability by computing coefficient of variation (CV) as follows:

$$CV = \frac{SD\ in\ grip\ force}{Mean\ grip\ force}$$

where CV represents coefficient of variation, SD the standard deviation, and mean represent average of grip force within a trial. As noted above, the SD and CV quantify linear variations around the average value, independent from the sequence of data in the grip force signal. However, while SD is known to scale with the amplitude of the grip force exerted, CV was used to assess the amplitude normalized component of grip force variability.

To quantify the temporal regularity in the signal, we performed sample entropy-based analysis using the following equation:

$$sE(r,m) = -\ln\left(\frac{A}{B}\right)$$

where sE stands for sample entropy, *ln* is the natural logarithm (with base *e*), and the quantity $\frac{\mathrm{A}}{\mathrm{B}}$ represents "*conditional probability that two sequences within a tolerance of r for m points remain within r of each other at the next point*" (Moorman, 2019). In other words, the sample entropy assesses the regularity in a data-stream by quantifying the probability of how a sequence of data repeats itself within the data-stream. Consequently, a signal with perfect repetition (e.g. a horizontal line or a sinusoidal wave where one segment repeats itself over ad infinitum) would have the ratio $\frac{\mathrm{A}}{\mathrm{B}}$ close to 1, and an sE nearing 0. On the other hand, a signal with no repetitions could have a high enough value indicating a highly unpredictable signal. Typically, sE for physiological tasks including grip force (or balance control for instance) is known to be within the range of 0.2 to 2.2 (Lodha et al., 2013; Vieluf et al., 2015). For the current study, the parameters *r* and *m* were selected based on the behavioral application, typically set to 0.2 and 2 respectively (Vieluf et al., 2015; Zhang et al., 2017) which were considered for subsequent analysis. Furthermore, isometric force generation has been known to underlie interactions among the constituent frequency spectra leading to complexity in grip force structure across multiple timescales (Garrett et al., 2011b; Kosciessa et al., 2020; Shah-Basak et al., 2020). We considered understanding the effects of disrupting M1 activity on spectral interactions across the timescales using the multi-scale sample entropy (MSE) analysis (McIntosh et al., 2010; Vieluf et al., 2015; Shah-Basak et al., 2020). MSE has been previously studied in the context of grip force fluctuations, maturation and age-dependent changes in human physiology (McIntosh et al., 2010;

Vieluf et al., 2015; Shah-Basak et al., 2020). MSE first involves constructing a signal at specified time-series, by taking samples from the grip force trial data at fixed intervals, i.e., downsampling. Following this, it computes sE over the downsampled time-series. This process is further repeated for coarser scales to understand the regularity at each scale such that finer (or lower) timescales represent interactions from a broader band of frequencies (low and high frequencies, short latency, local processing) whereas coarser (or higher) timescales representing narrower band of spectral interactions (low

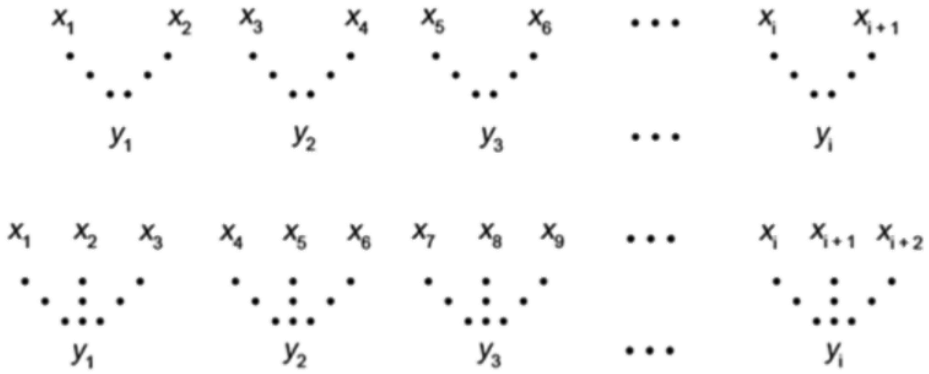

Figure 31: Developing coarse time scales (TS) in a time-series data x(i) by averaging every two consecutive points (TS=2), three consecutive points (TS=3), and so on. Note that keeping the time series in its initial form is by default TS=1 (figure adopted from Busa and van Emmerik, 2016)

frequencies, LRTCs, long-range processing) (Costa et al., 2005; Stergiou and Decker, 2011; Kosciessa et al., 2020; Shah-Basak et al., 2020). Figure 31 adopted from (Busa and Emmerik, 2016). We also assessed changes in cortical neurophysiological measures (MEP, SICI, ICF) pre- and post-TBS to quantify the effects of TBS on corticospinal excitability.

Statistical analysis: For SD, CV, MSE, and mean grip force, we employed the repeated measures analysis of variance (rm-ANOVA, α=0.05) to assess effects of Stimulation (3 levels: cTBS, iTBS, sham), Grip force (3 levels: 5, 15, 30% MVC), Visual feedback (2 levels: visual feedback, no visual feedback), and Timescale (6 levels: timescales 1 to 6

– MSE only). The force magnitude-dependent effects on grip force variability have already been reported previously and we considered the rm-ANOVA for each force level. Post-hoc comparisons were assessed through Dunnett's paired t-tests that allowed comparison between a control group (sham) with experimental groups (cTBS and iTBS) using appropriate correction for multiple comparisons. Assessment of intracortical excitability (MEP test pulse, SICI, ICF) was conducted using rm-ANOVA (α=0.05) with interstimulus interval (ISI: 2 and 10ms), Time (pre, post), and Stimulation (sham, cTBS, iTBS) as within-subjects factors. In case of violation of the sphericity assumption, Huynh-Feldt correction was used. Statistical analyses were performed using SPSS software version 25.0 (IBM, USA) and GraphPad Prism software version 7.0 (GraphPad Software Inc., USA).

3.3. Results

3.3.1. Multiscale entropy in grip force modulated following cTBS, but not iTBS or sham stimulation over M1

First, we report findings on the effects of theta-burst stimulation over M1 on the temporal structure of grip force signal measured using Multiscale Entropy (MSE). MSE of grip force measures sample entropy of the force signal at successively down-sampled time series (see Methods). MSE of grip force at a time scale of 1 represents sample entropy of the originally recorded grip force time series while a time scale of t represents sample entropy for a force time series created by averaging t adjacent points (Mcintosh et al., 2008).

Each subject received cTBS, iTBS, or sham stimulation on separate sessions. We found that the effect of stimulation (sham, cTBS, and iTBS) on sample entropy depended on the timescale (Stimulation × Timescale interaction: $F_{(1.806,16.255)}$=5.991, p=0.013, η_p^2=0.400; main effect of Stimulation: $F_{(2,18)}$=7.399, p=0.005, η_p^2=0.451; main effect of Timescale: $F_{(1.021,9.190)}$=166.907, p<0.001, η_p^2=0.949; Figure 32). Importantly, MSE in grip force modulated based on the availability of the visual feedback as well as the magnitude of grip force, and both these effects varied across timescales (Vision × Timescale interaction: $F_{(1.036,9.326)}$=76.248, p<0.001, η_p^2=0.894; Force × Timescale interaction: $F_{(1.045,9.407)}$=15.006, p=0.003, η_p^2=0.625; main effect of vision: $F_{(1,9)}$=57.722, p<0.001, η_p^2=0.865; main effect of Force: $F_{(1.037,9.329)}$=15.761, p<0.001, η_p^2=0.637; Figure 32). Follow-up comparison for 5% MVC trials with visual feedback found statistically significant increase in sample entropy of grip force at each timescale following cTBS over M1 compared to sham stimulation (Dunnett's post-hoc test for sham vs. cTBS: Timescale 1: adjusted p=0.036; Timescale 2: adjusted p=0.033; Timescale 3: adjusted p=0.034; Timescale 4: adjusted p=0.030; Timescale 5: adjusted p=0.029; Timescale 6: adjusted p=0.032). There was no difference between iTBS and sham stimulation (Dunnett's post hoc test for sham vs. iTBS: all adjusted p-values >0.970).

For 15% MVC trials with visual feedback, a similar effect of cTBS was observed (Dunnett's post-hoc test for sham vs. cTBS: Timescale 1: adjusted p=0.017; Timescale 2: adjusted p=0.018; Timescale 3: adjusted p=0.017; Timescale 4: adjusted p=0.018, d=1.026; Timescale 5: adjusted p=0.020; Timescale 6: adjusted p=0.023). No

difference in MSE was found between iTBS and sham stimulation (Dunnett's test: for sham vs. iTBS: all adjusted p-values >0.480).

For 30% MVC trials with visual feedback, cTBS over M1 was not accompanied by a modulation in multiscale entropy (Dunnett's post hoc test for sham vs. cTBS: all adjusted p-values >0.890). Also, we found no difference in MSE between iTBS and sham stimulation (Dunnett's test: sham vs. iTBS: all adjusted p-values >0.480).

For the no visual feedback condition, we failed to observe any effect of stimulation on MSE of grip force at 5% MVC (all adjusted p-values >0.170; Figure 33), 15% MVC (all adjusted p-values >0.340), and 30% MVC (all adjusted p-values >0.109). No other two-way or three-way interactions were found to be significant (all F-values < 2.250; all p-values >0.120)

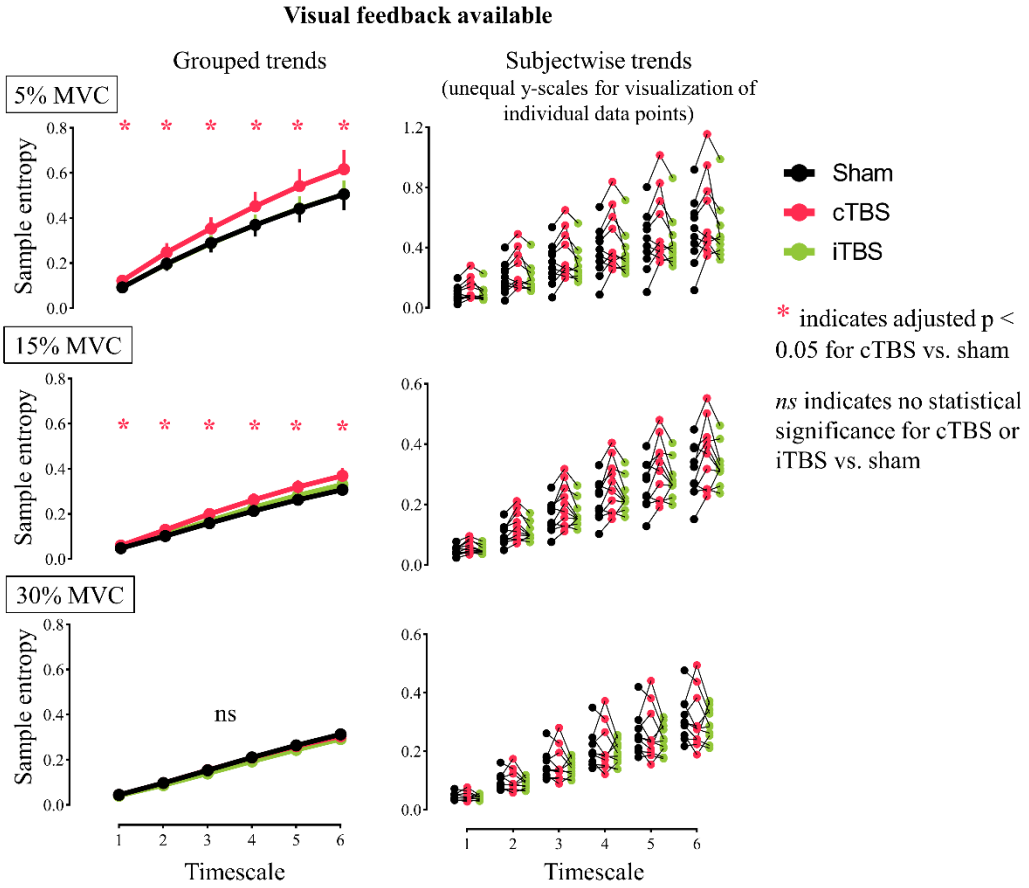

Figure 32: Modulation in MSE with availability of visual feedback and force level post stimulation over M1; dot and error bars denote mean and standard error respectively; note the difference in y-scale to facilitate visualization of subjectwise trends

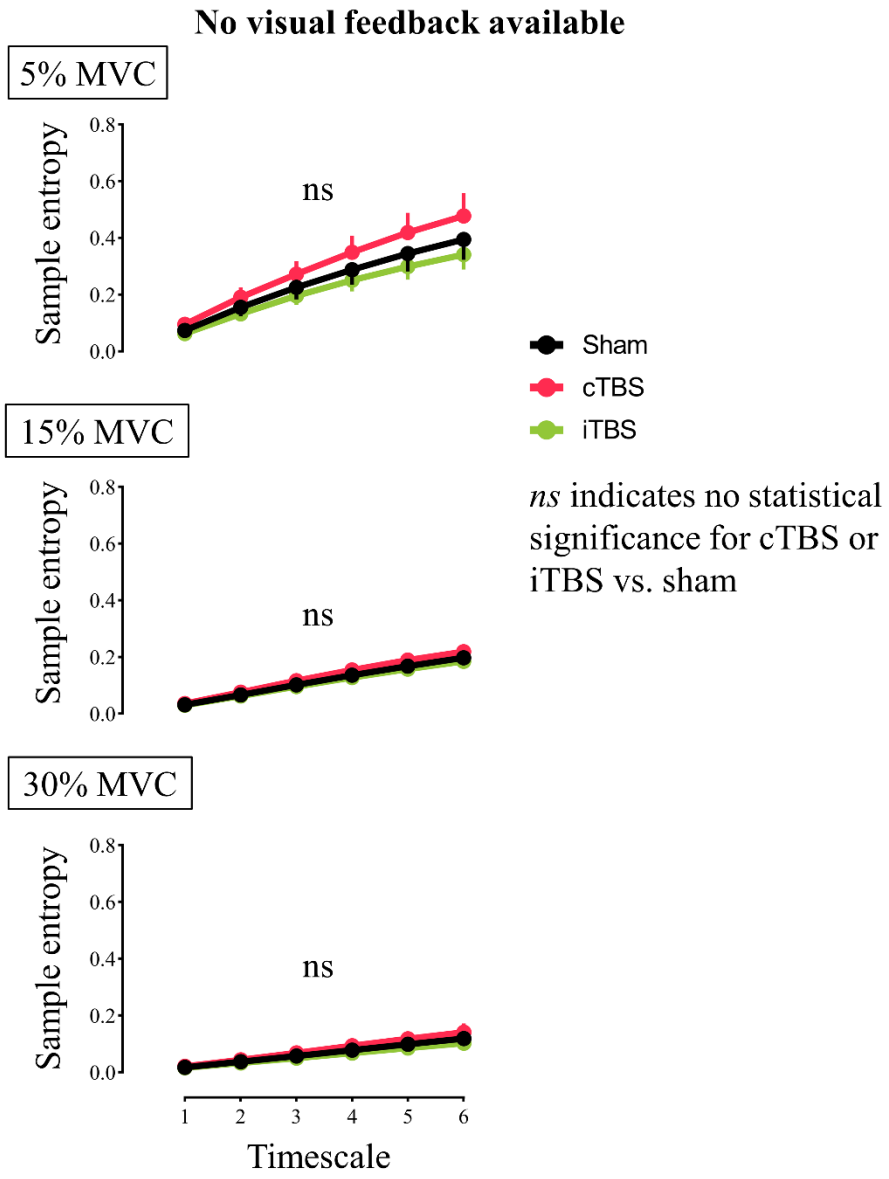

Figure 33: No modulation in MSE post cTBS/iTBS vs. sham stimulation for any of the three force levels when visual feedback of the exerted grip force was removed

3.3.2. Stimulation over M1 did not alter the subjects' ability to exert required grip force

After delivering the cTBS/iTBS/sham stimulation over M1, we observed no modulation in grip force magnitude exerted on the object with stimulation conditions (no main effect of Stimulation: $F_{(2,18)}=0.756$, $p=0.484$, $\eta_p^2=0.077$; no Vision ×

Stimulation interaction: $F_{(1.367,12.300)}$=2.400, p=0.142, η_p^2=0.211; no Force × Stimulation interaction: $F_{(2.242,20.178)}$=0.710, p=0.519, η_p^2=0.073; no Vision × Force × Stimulation interaction: $F_{(2.449,22.044)}$=2.069, p=0.142, η_p^2=0.187). The grip force exerted on the object changed only depending upon the availability of the visual feedback and force level required for the task (main effect of Vision: $F_{(1,9)}$=25.186, p=0.001, η_p^2=0.737; main effect of Force: $F_{(1.001,9.011)}$=69.860, p<0.001, η_p^2=0.886; Vision × Force interaction: $F_{(1.377,12.395)}$=53.546, p<0.001, η_p^2=0.856; Figure 34). The exerted grip force was higher when the visual feedback of the same was available compared to that when visual feedback was not available ($t_{(9)}$=5.034, p=0.001, d=1.592). Expectedly, the exerted grip force increased with the required force level (5 vs 15% MVC: $t_{(9)}$=-8.656, p<0.001, d=2.737; 5 vs 30% MVC: $t_{(9)}$=-8.378, p<0.001, d=2.649; 15 vs 30% MVC: $t_{(9)}$=-8.184, p<0.001, d=2.588; further comparisons in Table 2). Moreover, subjects showed no fatigue with progression of the session, nor with the type of stimulation (no Time × Stimulation interaction: $F_{(2,18)}$=0.646, p=0.536, η_p^2=0.067; no main effect of Time: $F_{(1,9)}$=4.666, p=0.059, η_p^2=0.341; no main effect of stimulation: $F_{(2,18)}$=1.414, p=0.269, η_p^2=0.136). Similarly, there was no change in tactile sensitivity assessed using the Semmes-Weinstein monofilament test following stimulation. That is, subjects could sense the buckling force equivalent to that exerted by 0.008mg via the SWME (filament evaluator size of 1.65mm) pre- and post-stimulation, and for stimulation types (sham, cTBS, iTBS).

3.3.3. SD and CV in grip force showed no change following the stimulation over M1

As expected, the SD in grip force scaled in proportion to the magnitude of grip force, (main effect of Force: $F_{(1.179,10.608)}=64.615$, $p<0.001$; $\eta_p^2=0.878$; Table 2). This scaling relied on the presence (or absence) of visual feedback (Vision × Force interaction: $F_{(2,18)}=37.715$, $p<0.001$, $\eta_p^2=0.807$; main effect of Vision: $F_{(1,9)}=48.371$, $p<0.001$, $\eta_p^2=0.843$; Figure 34), but not stimulation (no Force × Stimulation interaction: $F_{(1.808,16.273)}=0.530$, $p=0.581$, $\eta_p^2=0.056$; no Vision × Stimulation interaction: $F_{(1.342,12.074)}=1.645$, $p=0.230$, $\eta_p^2=0.155$; no main effect of Stimulation: $F_{(2,18)}=2.218$, $p=0.138$, $\eta_p^2=0.198$; no Vision × Force × Stimulation interaction: $F_{(2.791,25.119)}=0.344$, $p=0.780$, $\eta_p^2=0.037$).

CV of grip force scaled inversely to the magnitude of applied grip force (main effect of Force: $F_{(2,18)}=4.678$, $p=0.023$, $\eta_p^2=0.342$; Table 2). Furthermore, this scaling of CV in grip force was dependent on the presence (or absence) of vision (Vision × Force interaction: $F_{(2,18)}=7.958$, $p=0.003$, $\eta_p^2=0.469$; main effect of Vision: $F_{(1,9)}=44.920$, $p<0.001$, $\eta_p^2=0.833$; Figure 34). Similar to SD findings, we failed to observe changes in CV in grip force based on the stimulation condition (no Vision × Stimulation interaction: $F_{(2,18)}=2.714$, $p=0.093$, $\eta_p^2=0.232$; no Force × Stimulation interaction: $F_{(4,36)}=1.028$, $p=0.406$, $\eta_p^2=0.103$; no main effect of Stimulation: $F_{(2,18)}=1.332$, $p=0.289$, $\eta_p^2=0.129$; no Vision × Force × Stimulation interaction: $F_{(4,36)}=0.683$, $p=0.608$, $\eta_p^2=0.071$).

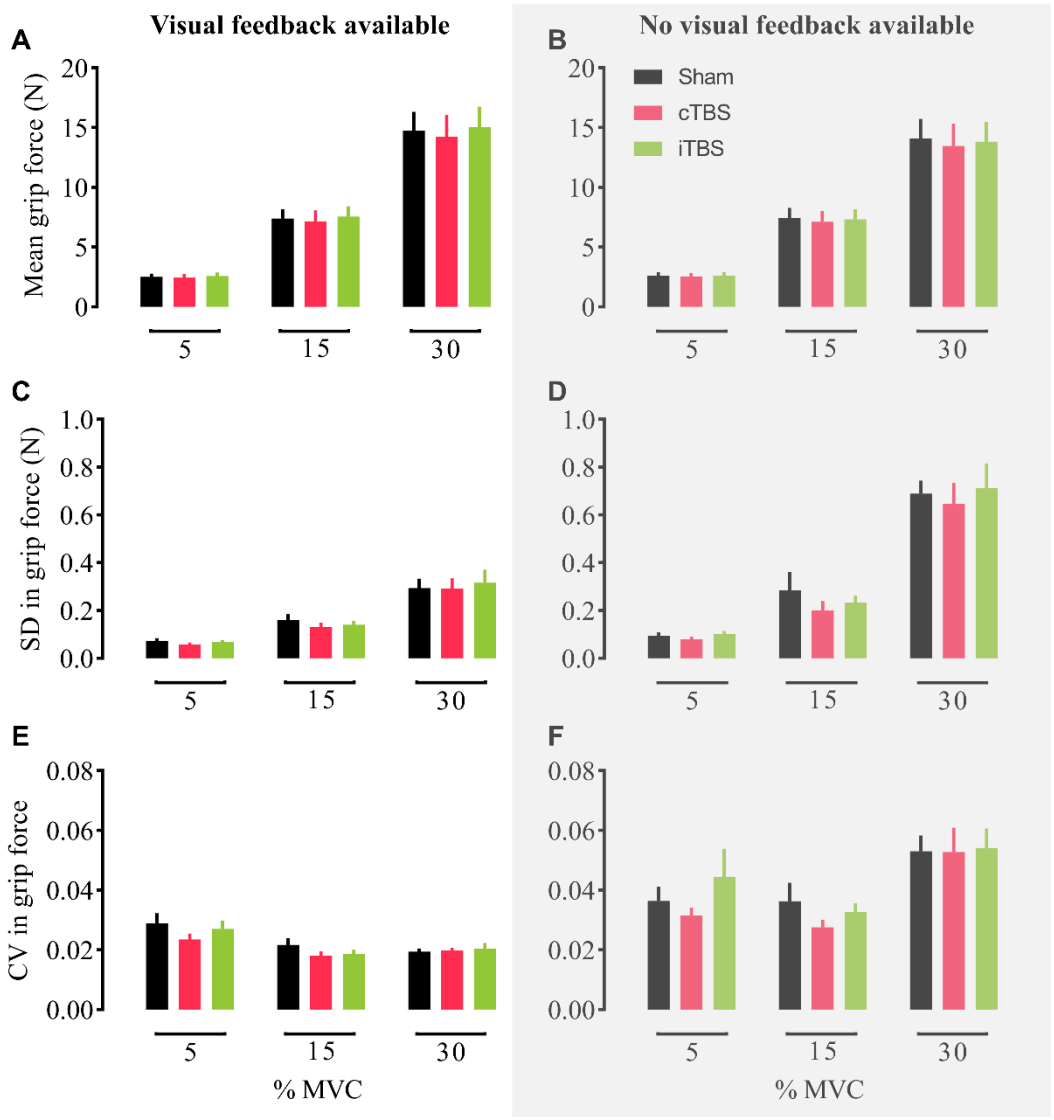

Figure 34: Modulation in mean, SD, and CV with force levels in presence of visual feedback (A, C, E), and absence of visual feedback (B, D, F); bars and error bars represent mean and standard error respectively.

Table 2: Comparisons for mean, SD, and CV in grip force post stimulation with force levels (5/15/30) and availability of visual feedback (v/nv); SD, CV, df, p, d indicate standard deviation, coefficient of variation, degrees of freedom, p-value, and effect size

for dependent 2-tailed t-test respectively; a value of 0.000 under the *p* column indicates p<0.001.

Measure	Pairs	Mean	SD	t (df = 9)	P	d
Mean (Post)	v5 - v15	-4.858	1.739	-8.837	0.000	2.794
	v15 - v30	-7.299	2.665	-8.661	0.000	2.739
	v5 - v30	-12.157	4.403	-8.731	0.000	2.761
	nv5 - nv15	-4.717	1.762	-8.465	0.000	2.677
	nv15 - nv30	-6.500	2.683	-7.660	0.000	2.422
	nv5 - nv30	-11.216	4.429	-8.008	0.000	2.532
	v5 - nv5	-0.063	0.076	-2.649	0.027	0.838
	v15 - nv15	0.078	0.196	1.265	0.238	-
	v30 - nv30	0.877	0.397	6.994	0.000	2.212
SD (Post)	v5 - v15	-0.077	0.033	-7.290	0.000	2.305
	v15 - v30	-0.157	0.082	-6.049	0.000	1.913
	v5 - v30	-0.234	0.114	-6.498	0.000	2.055
	nv5 - nv15	-0.148	0.137	-3.424	0.008	1.083
	nv15 - nv30	-0.442	0.138	-10.148	0.000	3.209
	nv5 - nv30	-0.590	0.233	-8.028	0.000	2.539
	v5 - nv5	-0.025	0.020	-4.060	0.003	1.284
	v15 - nv15	-0.096	0.104	-2.911	0.017	0.921
	v30 - nv30	-0.382	0.158	-7.632	0.000	2.413
CV (Post)	v5 - v15	0.007	0.004	5.420	0.000	1.714
	v15 - v30	0.000	0.002	-0.552	0.594	-
	v5 - v30	0.007	0.006	3.736	0.005	1.181
	nv5 - nv15	0.005	0.017	0.974	0.355	-
	nv15 - nv30	-0.021	0.018	-3.723	0.005	1.177
	nv5 - nv30	-0.016	0.026	-1.938	0.085	-
	v5 - nv5	-0.011	0.012	-2.896	0.018	0.916
	v15 - nv15	-0.013	0.009	-4.333	0.002	1.370
	v30 - nv30	-0.033	0.020	-5.259	0.001	1.663

3.3.4. No difference in MSE, SD, and CV of grip force during practice trials across stimulation sessions

As noted above, each subject practiced the isometric force production task prior to receiving the stimulation during each session. We investigated whether the behavioral measures based on practice trials were different across stimulation sessions.

We found that MSE of grip force during practice trials was not different across sessions (no Vision × Session interaction: $F_{(2,18)}$=0.136, p=0.874, η_p^2=0.015; no Force × Session interaction: $F_{(3.016,27.141)}$=1.745, p=0.181, η_p^2=0.162; no Session × Timescale interaction: $F_{(1.707,15.367)}$=1.659, p=0.223, η_p^2=0.156; no main effect of Session: $F_{(2,18)}$=1.947, p=0.172, η_p^2=0.178; no Vision × Force × Stimulation interaction: $F_{(4,36)}$=0.939, p=0.453, η_p^2=0.094; no Vision × Stimulation × Timescale interaction: $F_{(1.799,\ 16.189)}$=0.109, p=0.879, η_p^2=0.012; no Force × Stimulation × Timescale interaction: $F_{(3.518,\ 31.663)}$=1.680, p=0.185, η_p^2=0.157; no Vision × Force × Stimulation × Timescale interaction: $F_{(2.750,\ 24.749)}$=1.026, p=0.393, η_p^2=0.102).

As expected, MSE in grip force varied with the availability of visual feedback, grip force magnitude, and timescale (main effect of Vision: $F_{(1,9)}$=76.142, p<0.001, η_p^2=0.894; main effect of Force: $F_{(1.073,9.658)}$=21.147, p=0.001, η_p^2=0.701; main effect of Timescale: $F_{(1.024,9.215)}$=196.568, p<0.001, η_p^2=0.956; no Vision × Force interaction: $F_{(2.000,18.000)}$=2.383, p=0.121, η_p^2=0.209; Vision × Timescale interaction: $F_{(1.025,9.226)}$=102.048, p<0.001, η_p^2=0.919; Force × Timescale interaction: $F_{(1.095,9.854)}$=22.196, p=0.001, η_p^2=0.711; Vision × Force × Timescale interaction: $F_{(2.126,19.131)}$=5.189, p=0.015, η_p^2=0.366; Table **3**). Multiscale entropy was greater when

the visual feedback of grip force was available versus that when no visual feedback was available ($t_{(9)}$=9, p<0.001, d=2.846), greater for 5% versus 15% ($t_{(9)}$=4.724, p=0.003, d=1.494) and 30% MVC ($t_{(9)}$=4.432, p=0.004, d=1.402), and greater for 15% versus 30% MVC ($t_{(9)}$=3.333, p=0.025, d=1.054). The entropy in grip force was the least for timescale 1 and sequentially increased for higher timescales (1 vs. 2: $t_{(9)}$=-11.200, p<0.001, d=3.542; 1 vs 3: $t_{(9)}$=-12.222, p<0.001, d=3.865; 1 vs 4: $t_{(9)}$=-13.333, p<0.001, d=4.216; 1 vs 5: $t_{(9)}$=-13.733, p<0.001, d=4.343; 1 vs 6: $t_{(9)}$=-13.722, p<0.001, d=4.339).

Table 3: Changes in multiscale entropy at timescales (t1 vs t2 to t6, dependent 2-tailed t-tests) at force levels (5/15/30) and in presence/absence of visual feedback (v/nv respectively) during practice trials.

Pairs		Mean	SD	t (df = 9)	p	d
v5	t1 - t2	-0.104	0.104	-3.190	0.011	1.009
	t1 - t3	-0.196	0.127	-4.899	0.001	1.549
	t1 - t4	-0.279	0.151	-5.857	0.000	1.852
	t1 - t5	-0.355	0.177	-6.336	0.000	2.004
	t1 - t6	-0.419	0.198	-6.679	0.000	2.112
v15	t1 - t2	-0.059	0.035	-5.253	0.001	1.661
	t1 - t3	-0.119	0.050	-7.509	0.000	2.375
	t1 - t4	-0.175	0.061	-9.161	0.000	2.897
	t1 - t5	-0.226	0.068	-10.472	0.000	3.312
	t1 - t6	-0.273	0.075	-11.504	0.000	3.638
v30	t1 - t2	-0.047	0.027	-5.442	0.000	1.721
	t1 - t3	-0.097	0.043	-7.247	0.000	2.292
	t1 - t4	-0.149	0.056	-8.342	0.000	2.638
	t1 - t5	-0.198	0.067	-9.373	0.000	2.964
	t1 - t6	-0.242	0.073	-10.434	0.000	3.300
nv5	t1 - t2	-0.081	0.080	-3.178	0.011	1.005
	t1 - t3	-0.152	0.101	-4.770	0.001	1.508
	t1 - t4	-0.217	0.123	-5.592	0.000	1.768
	t1 - t5	-0.274	0.144	-5.999	0.000	1.897
	t1 - t6	-0.323	0.163	-6.255	0.000	1.978
nv15	t1 - t2	-0.031	0.018	-5.425	0.000	1.715
	t1 - t3	-0.063	0.026	-7.505	0.000	2.373
	t1 - t4	-0.092	0.034	-8.725	0.000	2.759
	t1 - t5	-0.120	0.040	-9.541	0.000	3.017
	t1 - t6	-0.145	0.045	-10.117	0.000	3.199
nv30	t1 - t2	-0.016	0.015	-3.405	0.008	1.077
	t1 - t3	-0.032	0.022	-4.559	0.001	1.442
	t1 - t4	-0.048	0.030	-5.053	0.001	1.598
	t1 - t5	-0.063	0.038	-5.323	0.000	1.683
	t1 - t6	-0.079	0.045	-5.521	0.000	1.746

As expected, the magnitude of grip force exerted on the object during practice trials altered only with the availability of visual feedback and with force level (main effect of vision: $F_{(1,9)}=27.314$, $p=0.001$, $\eta_p^2=0.752$; main effect of force: $F_{(1.001,9.006)}=68.983$, $p<0.001$, $\eta_p^2=0.885$; vision × force interaction: $F_{(1.074,9.669)}=41.520$, $p<0.001$, $\eta_p^2=0.822$). Grip force exerted on the object was greater when visual feedback

of the force was available versus that when visual feedback was not available ($t_{(9)}$=5.250, p=0.001, d=1.660) and greater with increased requirement to exert force (5 vs 15% MVC: $t_{(9)}$=-8.590, p<0.001, d=2.716; 5 vs 30% MVC: $t_{(9)}$=-8.322, p<0.001, d=2.632; 15 vs 30% MVC: $t_{(9)}$=-8.138, p<0.001, d=2.573; further comparison in Table 4). However, there was no change in the magnitude of exerted force with stimulation condition (no main effect of stimulation: $F_{(2,18)}$=0.529, p=0.598, η_p^2=0.056; no vision × stimulation interaction: $F_{(2,18)}$=3.106, p=0.069, η_p^2=0.257; no force × stimulation interaction: $F_{(2.103,18.929)}$=0.794, p=0.537, η_p^2=0.081; no vision × force × stimulation interaction: $F_{(2.340,21.057)}$=1.610, p=0.222, η_p^2=0.152).

Similarly during practice trials, we observed modulation in SD in grip force only with force magnitude and availability of the visual feedback (main effect of vision: $F_{(1,9)}$=63.567, p<0.001, η_p^2=0.876; main effect of force: $F_{(1.078,9.704)}$=56.135, p<0.001, η_p^2=0.862; vision × force interaction: $F_{(1.238,11.145)}$=52.390, p<0.001, η_p^2=0.853but not with stimulation session (no main effect of stimulation: $F_{(2,18)}$=1.375, p=0.278, η_p^2=0.133; no vision × stimulation interaction: $F_{(2,18)}$=0.884, p=0.430, η_p^2=0.089; no force × stimulation interaction: $F_{(4,36)}$=0.422, p=0.791, η_p^2=0.045; no vision × force × stimulation interaction: $F_{(2.264,20.376)}$=0.296, p=0.773, η_p^2=0.032). SD of grip force pre-stimulation was greater for higher force magnitude and altered with visual feedback (Table 4).

The CV in grip force for practice trials showed modulation with the availability of visual feedback and force magnitude (main effect of vision: $F_{(1,9)}$=27.320, p=0.001, η_p^2=0.752; main effect of force: $F_{(1.282,11.542)}$=4.860, p=0.042, η_p^2=0.351; vision × force interaction: $F_{(1.169,10.518)}$=11.598, p=0.005, η_p^2=0.563; post-hoc comparisons in Table

4), but not with stimulation session (no main effect of stimulation: $F_{(2,18)}$=1.332, p=0.289, η_p^2=0.129; no vision × stimulation interaction: $F_{(2,18)}$=0.845, p=0.446, η_p^2=0.086; no force × stimulation interaction: $F_{(4,36)}$=0.824, p=0.519, η_p^2=0.084; no vision × force × stimulation interaction: $F_{(4,36)}$=0.580, p=0.679, η_p^2=0.061).

Table 4: Posthoc comparisons (dependent 2-tailed t-test) for mean, SD, and CV in grip force with force levels (5/15/30) and availability of visual feedback (v/nv) during practice trials.

Measure	Pairs	Mean	SD	t (df = 9)	p	d
Mean (Pre)	v5 - v15	-4.870	1.756	-8.768	0.000	2.773
	v15 - v30	-7.275	2.659	-8.651	0.000	2.736
	v5 - v30	-12.145	4.415	-8.699	0.000	2.751
	nv5 - nv15	-4.596	1.731	-8.394	0.000	2.654
	nv15 - nv30	-6.528	2.716	-7.602	0.000	2.404
	nv5 - nv30	-11.123	4.441	-7.920	0.000	2.504
	v5 - nv5	-0.033	0.084	-1.226	0.251	-
	v15 - nv15	0.241	0.168	4.534	0.001	1.434
	v30 - nv30	0.989	0.524	5.971	0.000	1.888
SD (Pre)	v5 - v15	-0.074	0.038	-6.218	0.000	1.966
	v15 - v30	-0.173	0.119	-4.584	0.001	1.450
	v5 - v30	-0.247	0.148	-5.261	0.001	1.664
	nv5 - nv15	-0.159	0.077	-6.521	0.000	2.062
	nv15 - nv30	-0.460	0.178	-8.174	0.000	2.585
	nv5 - nv30	-0.618	0.232	-8.440	0.000	2.669
	v5 - nv5	-0.017	0.021	-2.591	0.029	0.819
	v15 - nv15	-0.101	0.061	-5.246	0.001	1.659
	v30 - nv30	-0.389	0.154	-7.967	0.000	2.519
CV (Pre)	v5 - v15	0.008	0.007	3.739	0.005	1.182
	v15 - v30	-0.002	0.005	-1.407	0.193	-
	v5 - v30	0.006	0.010	1.959	0.082	-
	nv5 - nv15	-0.001	0.009	-0.377	0.715	-
	nv15 - nv30	-0.022	0.023	-3.061	0.014	0.968
	nv5 - nv30	-0.023	0.028	-2.639	0.027	0.834
	v5 - nv5	-0.007	0.007	-3.038	0.014	0.961
	v15 - nv15	-0.016	0.008	-6.278	0.000	1.985
	v30 - nv30	-0.036	0.026	-4.326	0.002	1.368

3.3.5. No effect of stimulation on the intracortical and the corticospinal excitability

We observed changes in the intracortical excitability with interstimulus interval (main effect of ISI: $F_{(1,9)}$=25.716, p=0.001, η_p^2=0.741) such that we observed SICI at 2 ms and ICF at 10 ms. Intracortical excitability (both SICI and ICF) did not change following stimulation (no main effect of Time: $F_{(1,9)}$=0.083, p=0.780, η_p^2=0.009; no main effect of Stimulation: $F_{(2,18)}$=0.193, p=0.826, η_p^2=0.021; no interaction effects: all F<1.889, all p>0.170). Similarly, the MEP amplitude, a measure of corticospinal excitability, did not alter post-stimulation when compared to pre-stimulation (no main effect of Time: $F_{(1,9)}$=1.638, p=0.233, η_p^2=0.154; no main effect of Stimulation: $F_{(1.087,9.784)}$=0.565, p=0.484, η_p^2=0.059; no Time × Stimulation interaction: $F_{(1.108,9.974)}$=1.523, p=0.249, η_p^2=0.145). Although counterintuitive, similar findings regarding no change in MEP following cTBS application has been reported in our previous study, especially when cTBS accompanied subjects performing a sensorimotor task in the same session, indicating reduced sensitivity of MEP to cTBS-induced disruption in M1 due to limiting neuroplasticity mechanisms (Parikh et al., 2020).

3.4. Discussion

We characterized the role of M1 in processing visuomotor information critical for regulating digit force variability during an isometric force production task. Continuous theta burst stimulation (cTBS) over M1 in healthy young adults caused an increase in sample entropy of the grip force for all timescales compared to sham stimulation. This increase was specific

to the magnitude of the grip force, i.e., these effects were observed at 5% and 15% but not at 30% MVC. Furthermore, the disruptive effects were sensitive to the availability of the visual feedback of the exerted grip force and the target force. Importantly, we did not find any change in SD and CV following M1 cTBS when compared with sham stimulation. We further showed that subjects' ability to exert required grip force, their tactile sensitivity, and their MVC did not change post stimulation and across sessions. We failed to observe any change in sample entropy, SD, and CV following intermittent theta burst stimulation (iTBS) over M1 when compared with sham stimulation. These findings highlight the dissociation in the causal involvement of M1 in processing sequence-dependent temporal structure (i.e., MSE), but not in the sequence-independent component (i.e., SD, CV) of grip force variability.

3.4.1. Temporal structure of grip forces: force magnitude and visual feedback

The temporal structure in grip force, as quantified by MSE, is sensitive to the sequential force control over multiple timescales. The sequential control is mainly driven by interactions among broader band of frequencies at finer timescales and that among narrower band of frequencies (mainly lower) at coarser timescales. The increase in MSE in grip force with timescales is suggestive of long-range temporal correlations (LRTCs) with narrower frequency bands (Kosciessa et al., 2020; Shah-Basak et al., 2020). Importantly, we observed MSE reducing for both - the broader band frequency interactions and the LRTCs represented by finer and coarser timescales respectively with the removal of visual feedback. This observation is in lines with the notion that inclusion of a sensory modality (visual feedback in this case) that serves functional relevance for the task success (i.e., efficient grip force control) increases the temporal complexity

embedded in the grip force signal (Vaillancourt et al., 2003b; Baweja et al., 2010; Kosciessa et al., 2020). Moreover, the reduction in MSE with force magnitude is consistent with previous reports suggesting higher complexity with increased precision for lower forces (Stergiou and Decker, 2011; Vieluf et al., 2015).

3.4.2. Involvement of M1 in error monitoring, visuomotor integration for regulating digit forces

We found that cTBS over M1 altered the regularity of grip force when compared to sham stimulation during the isometric grip force production task. Mainly, the sample entropy of grip force increased at all six timescales following M1 cTBS versus sham. Similar findings were not observed following iTBS over M1. Increase in sample entropy following M1 cTBS at finer timescales might suggest altered interactions within broader band of frequencies likely resulting from alteration in interconnectivity among local neural populations (Mcintosh et al., 2008; Vakorin et al., 2011; Wang et al., 2018). On the other hand, increase in sample entropy at coarser (or higher) timescales following M1 cTBS might indicate alteration in long-range interactions across distributed neural populations (Costa et al., 2005; Stergiou and Decker, 2011; Kosciessa et al., 2020; Shah-Basak et al., 2020). TMS work in animals using similar burst frequencies has been previously shown to affect the temporal structure of neural activity by disrupting its phase-relationship (Allen et al., 2007). Similar disruption could have influenced the phase-relationship among neural activity within M1 and its long-range interactions thereby, resulting in the altered MSE in grip forces.

Importantly, the increase in multiscale entropy was observed at 5% and 15% MVC force condition but not at 30% force condition following M1 cTBS when compared with sham stimulation. It is known that the performance of two-finger precision grip in routine tasks involves grip force magnitudes below 15-20% MVC, beyond which a multi-finger grasp involving more than two fingers could provide greater precision than the two-finger counterpart. (Gordon et al., 1993b; Burstedt et al., 1999; Smith et al., 2018; Wolbrecht et al., 2018). In addition, the application of lower versus higher grip forces elicit activation within distinct cortical networks (Ehrsson et al., 2000a, 2001). It is likely that performance of the isometric force production task using a precision two-digit grip might have primarily engaged the cortical network involved in the production of lower forces (5% and 15%). Therefore, M1 cTBS mainly disrupted this network level processing for the regulation of grip force at 5% and 15% MVC levels but not at 30% MVC level. Overall, our findings depicting changes in the structure of grip force variability following cTBS vs. sham over M1 are in agreement with the theoretical as well as experimental evidence underscoring the role of common synaptic output in the moment-to-moment control of digit forces (Slifkin and Newell, 1999; Jones et al., 2002; Vaillancourt et al., 2003b; Harris & Wolpert, 2004; Osborne et al., 2005; Feeney et al., 2018; Nagamori et al., 2021).

The increase in MSE following M1 cTBS when compared with sham stimulation was observed during the performance of isometric force production task under visual feedback but not when this feedback was blocked. The isometric production of grip force relies on continuous monitoring of the error in motor output based on the available feedback, processing the feedback information to assess contextual relevance of the error

for task success, and integrating the processed information for directing the subsequent motor command (Vaillancourt et al., 2003b; Feeney et al., 2018; Siswandari et al., 2019). As visual feedback of the exerted grip force was available for the first 8s of each trial in the present study, the error in motor output during this phase would be primarily monitored via a combination of visual and somatosensory inputs (Poon et al., 2012). Studies assessing neural correlates of this process have shown increased activation in M1 and associated parietal cortical regions such that an increase in visual gain of the feedback led to temporal changes in M1 activity (Poon et al., 2012, 2013). Feedforward models involving correction of movement based on available sensory feedback implicate the role of M1 in processing sensory prediction errors which consider previous motor output to generate a sensory prediction about the upcoming motor output (Shadmehr et al., 2010; Herzfeld et al., 2014; Uehara et al., 2018).

Removal of visual feedback has been shown to lead to an increase in activation over the left ventral premotor and prefrontal cortex but only transient changes in M1 activity, suggesting the role of M1 primarily in the integration of processed visuomotor information with a likelihood of its involvement in visuomotor error monitoring and/or processing its contextual relevance (Vaillancourt et al., 2003b; Poon et al., 2012; Uehara et al., 2018; Atique and Francis, 2021) Consequently, sensitivity of M1 neural population to a combination of these processes could underlie the altered temporal structure of the grip forces following cTBS versus sham over M1. We are certain that the observed findings were not due to the spread of cTBS current to the primary somatosensory cortex (S1). This contention is supported by the fact that we failed to observed changes in tactile sensitivity among subjects following M1 cTBS. Such a change would be expected

following disruption over S1 (i.e., via cTBS), as shown in our previous work (Rao et al., 2020).

Notably, we did not observe stimulation-specific changes in either SD or CV in grip force. As modulation in SD in grip force is associated with that in low frequency content (< 5 Hz, which also consists of maximum power in a grip force signal), no change in SD with stimulation in our study is indicative of intact spectral content following stimulation over M1. When taken together with MSE findings, no change in SD or CV in grip force following stimulation highlights a dissociation in the role of M1 in processing sequential interactions in grip force (as assessed by MSE) but not in modulating the sequence-independent component (as assessed by SD, CV) of the grip force variability.

3.4.3. No modulation in cortical excitability following theta burst stimulation over M1

While we observed a characteristic effect of cTBS over M1 leading to changes in motor behavior, polarizing effect of iTBS was not evident in the data. Similar discrepancy pertaining to iTBS efficacy has been previous documented in the literature (Wischnewski and Schutter, 2015; Katagiri et al., 2020). iTBS effects are known to have high inter-individual variability especially when it is administered in conjunction with ongoing motor practice (Gentner et al., 2008; Katagiri et al., 2020). With ongoing motor task (similar to the current study), Katagiri and colleagues observed consistent effects in neurophysiological parameters across participants for cTBS but higher inter-individual variability following iTBS protocol (Katagiri et al., 2020). In fact, another study assessing the iTBS effects repeatedly for 5 days showed no changes in MEP or intracortical

measures on any day, nor a cumulative effect of iTBS versus sham (Perellón-Alfonso et al., 2018). Similarly, cTBS over M1 failed to modulate the corticospinal excitability and intracortical excitability. These findings may not seem surprising as the effect of cTBS over M1 on the corticospinal excitability are dependent on whether subjects perform a motor task prior to M1 cTBS. Our previous work has shown that if subjects perform a sensorimotor task prior to M1 cTBS, then the corticospinal excitability is not influenced by cTBS (Parikh et al., 2020). However, when subjects do not perform a motor task prior to M1 cTBS, a reduction in CSE following cTBS to M1 is noticed (Huang et al., 2005; Parikh et al., 2020). Therefore, the lack of CSE reduction following cTBS in our study, where subjects performed a motor task prior to cTBS, is consistent with previous reports from our group and others (Perellón-Alfonso et al., 2018). Although specific underlying mechanisms remain under debate, it is likely that the nature of the ongoing motor task could have engaged task-specific synaptic plasticity thereby, restricting the induction of long-term potentiation or depression (LTP or LTD respectively) like mechanisms via iTBS or cTBS, respectively (Di Lazzaro et al., 2008a; Huang et al., 2011; Guerra et al., 2016; Katagiri et al., 2020).

3.4.4. Conclusion

Our findings highlight the role of M1 in processing visuomotor information critical to regulate grip force variability at lower force levels. In the process, we observe a dissociation of the role of M1 in processing sequence-dependent, but not sequence-independent component of grip force variability. The current study adds causal evidence corroborating the theoretical framework underscoring central contribution to behavioral variability.

Chapter 4. (Manuscript 2) Lateralized neural variability characterizes the force used in a precision task.

4.1. Introduction

Efficient digit force control ensures we do not accidentally spill the coffee while drinking from a coffee mug filled to the brim. The seemingly simple task belies the underlying physiological complexity that is evident from the aberrant control of finger forces among patients with motor ailments e.g. stroke, Parkinson's disease, cerebral palsy, focal hand dystonia (Fellows and Noth, 2003; Olivier et al., 2007; Chu and Sanger, 2009; Grafton, 2010; Lodha et al., 2013). Despite the ubiquitous nature of the task, mechanisms underlying moment-to-moment force control remain poorly understood.

Neuroimaging studies have shown that the activity within frontal and parietal cortical regions is associated with the application of digit forces on a hand-held object (Ehrsson et al., 2000a, 2003; Kilner et al., 2003; Vaillancourt et al., 2003b; Grafton, 2010; Davare et al., 2011; Poon et al., 2013). While grasping an object, such fronto-parietal cortical activity might be lateralized to one hemisphere as a function of task phases and the processing requirements for digit force applications (Ehrsson et al., 2000a, 2003; Kilner et al., 2003; Vaillancourt et al., 2003b; Grafton, 2010; Davare et al., 2011; Poon et al., 2013). Importantly, the role of cortical activity during force control has been typically discussed by assessing the average neural signals (or changes in mean value). Notably, the cortical dynamics pertaining to a task could be characterized by assessing the moment-to-moment fluctuations in neural activity, an aspect which is analytically overlooked by averaging/pooling the neural activity over the trial duration, or across multiple trials

(Aguirre et al., 1998; Birn, 2012; Grady and Garrett, 2018). Recent evidence highlights critical role of neural variability across behavioral paradigms, including perceptual matching, attentional cueing, face recognition, and delayed match-to-sample tasks (Garrett et al., 2010, 2011a, 2013a, 2013b, 2014). A study by (Garrett et al., 2014) showed that moment-to-moment variability in the brain signal decreased with increase in task difficulty during a face-comparison task. Importantly, the reduction in neural variability depicted a pattern distinct from that revealed by average (or pooled) activity in the brain signal (Garrett et al., 2014). Further, modulation in BOLD-related cortical variability has been shown to characterize age-related changes in task performance (Garrett et al., 2013a). Similarly, variability in EEG signals quantified using sample entropy showed structured increase in complexity of the signal with developmental maturation (Mcintosh et al., 2008). Additionally, direct assessment of the association between neural average activity and neural variability showed no consistent relationship between the two measures in a dataset of two million samples encompassing multiple brain regions, conditions in the task, and subjects, reinforcing the notion that brain signal variability is dissociable from the average neural activity (Garrett et al., 2013a, 2014). These findings collectively suggest that neural variability could convey orthogonal and spatially differentiated information from that conveyed by neural means (McIntosh et al., 2010; Garrett et al., 2011a, 2014). Importantly, the brain signal variability could be suggestive of three underlying processes: 1) the identifying the range of motor outputs for dynamic versus static stimuli, 2) uncertainty in the stimulus, and 3) the cognitive state transition in which greater variability could facilitate the transition from one cognitive state to another for processing the ongoing task demands (McIntosh et al., 2010; Garrett et al., 2011a, 2014; Grady and Garrett, 2018).

Despite the potential applicability and significance of brain signal variability to sensorimotor behavior, its contribution to the control of grip force remains unknown. Considering the evidence that fronto-parietal cortical processing for digit force control applications is spatially lateralized, we hypothesized that variability in EEG activity recorded over the fronto-parietal region will be lateralized and systematically modulated with increase in grip force magnitude. We characterized neural variability using standard deviation (SD) and sample entropy (sE) in EEG activity. While SD quantifies deviation in neural activity around its mean, sE is known to quantify the degree of regularity in the signal such that higher entropy indicates lesser regularity and increased complexity whereas lower entropy indicates higher regularity and lesser complexity (Mcintosh et al., 2008; Lodha and Christou, 2017; Shah-Basak et al., 2020). Notably, the measure of SD is sensitive to the scaling of signal amplitude but invariant to its underlying sequence, whereas sE is sensitive to the sequential structure of the signal but invariant to the constant scaling of the signal amplitude – making these measures complementary for quantifying neural variability (Garrett et al., 2013b; Grady and Garrett, 2014; Shah-Basak et al., 2020).

4.2. Methods

4.2.1. Participants

The current study has been performed based on data collected at Arizona State University, and reported in our previous article (Paek et al., 2019). Eleven healthy young adults (three females, eight males; age range: 18-35 years) participated in the study. Subjects provided written informed consent in accordance with the protocol approved by the Institute Review Board at the Arizona State University. Three of the

subjects participated in pilot version of the study with slight variation in the task described subsequently. Two of the three subjects participated in one task whereas one subject participated in both the tasks of pilot study. Eight of the eleven subjects participated in both the tasks of the finalized study. To ensure consistency in the task setup, analysis reported for the current study has been conducted on data from eight subjects.

4.2.2. Grip device

A customized instrumented grip device was used for this study. Two force sensors (six-dimensional force/torque transducers; Nano-25, ATI Industrial Automation, Garner, NC) were instrumented on each graspable side of the grip device to independently record force exerted on each graspable surface (Figure 35). 12-bit analog

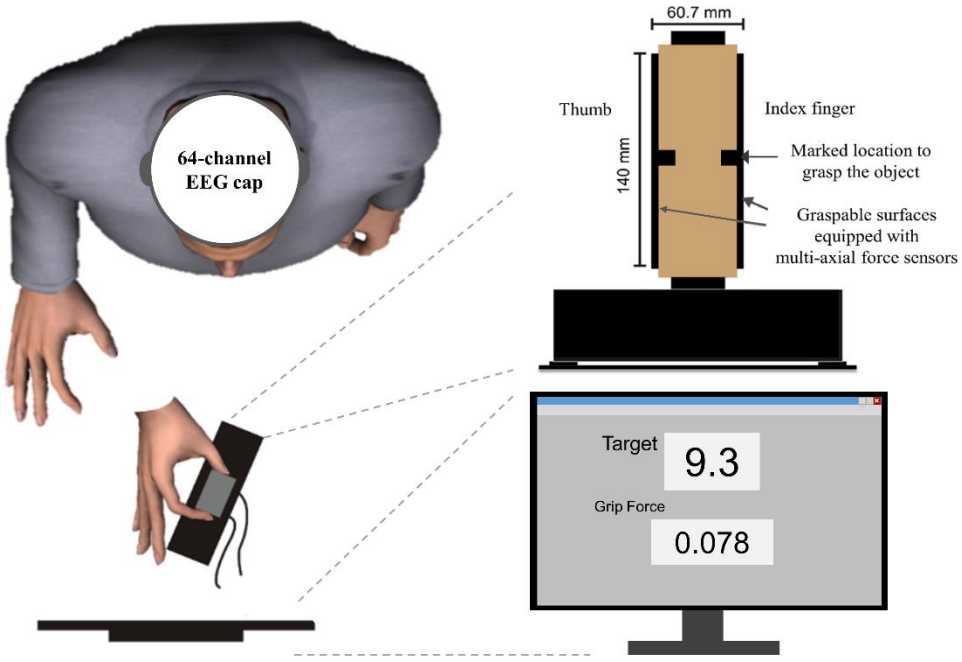

Figure 35: Experimental setup depicting the subject with EEG cap, grasping the grip device while the feedback of applied grip force is displayed on the screen

to digital converter board (sampling frequency 1 kHz, PCI-6225, National Instruments, Austin, TX, United States) was used to acquire the force data.

4.2.3. Electroencephalography

We used 64 channel standardized 10-20 EEG system (Luu et al., 2016; Goel et al., 2019) to assess the cortical activity of the participants as they performed the grip force task. The EEG system (BrainAmps DC amplifiers, Brain Products GLMB; sampling frequency 1 kHz for each electrode) consisted of one ground and one reference electrodes (placed on the subject's earlobes) and four of the 64 channels dedicated to the measurement of electrooculography (placed near eyes and the temple) to get an improved estimate of eye movements for subsequent artifact removal (Paek et al., 2019). To ensure proper contact of the electrode with the scalp skin, the electrodes were supplied with saline gel. EEG pre-processing and signal analysis used in this study are discussed later in the section.

4.2.4. Experimental task

During the experimental sessions, participants were seated comfortably and instructed to perform an isometric force production task using their right hand. The customized object to be grasped was placed on a table in front of the chair (~30cm away from the subject). Maximum voluntary contraction (MVC) for each participant was estimated as the maximal grip force exerted by the participant on the grip device when grasping only using their index finger and thumb (Lukos et al., 2013; Paek et al., 2019; Rao and Parikh, 2019). For every participant, the experimenters performed at least three such repetitions to determine a consistent MVC (Paek et al., 2019; Rao and

Parikh, 2019). Before each trial, the subject was asked to bring their hand near the graspable surfaces of the object and cued to exert 5%, 10%, or 15% of their maximum voluntary contraction (MVC). The participants were also instructed to maintain this force level for 8s following which they were cued to stop exerting the force. The target force to be exerted as well as the actual grip force exerted by the subjects was displayed for the entire duration of the trial visually (Figure 35). At least hundred trials were recorded for each subject during the session resulting into ~33 trials per force level. We recorded EEG activity (Figure 35) while subjects performed the trials.

4.2.5. EEG preprocessing

We preprocessed the EEG data using pre-processing pipeline formulated in Figure 36 (Delorme and Makeig, 2004; Paek et al., 2019). First, we re-referenced the sensor activity to that recorded from the mastoids (TP7, TP8; Figure 37) followed by removal of ocular artifacts using the H-infinity adaptive filter. The mastoid-based re-referencing primarily takes into the account any changes in sensors' activity due to temporary shifts in ground and/or reference electrodes. Undertaking this step before the removal of ocular artifacts is essential to prevent loss of relevant information as H-infinity is sensitive to sudden changes in signal amplitude. Next, the possibility of a scalar drift (usually ~0 Hz activity) in the signals was addressed by removal of any residual offset. This step was conducted by application of a high-pass filter at 0.1 Hz (zero-phase, 4^{th} order Butterworth filter). Notch filters were subsequently used to remove the power line noise and associated harmonics at 60, 120, and 180 Hz. Post line noise removal, it was important to detect changes in head movements and remove its influence from the neural signal using the artifact subspace reconstruction (ASR). Next, we applied

independent component analysis (ICA) to remove the artifacts associated with muscle activity. Detailed description about these procedural steps is provided below.

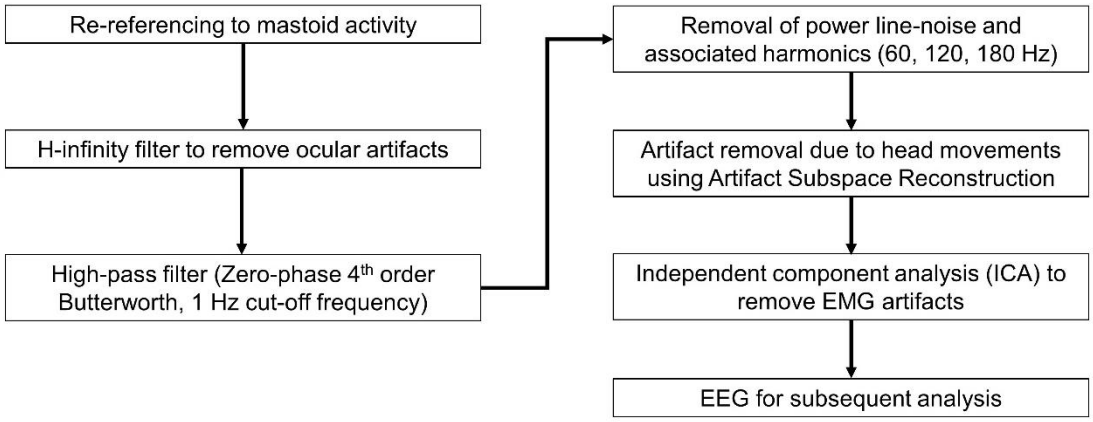

Figure 36: EEG preprocessing flowchart (sequence adopted from Dr. Paek's doctoral thesis)

H-infinity adaptive filtering: After re-referencing the sensor activity with that in mastoids, the H-infinity adaptive filter was applied to remove the ocular artifacts. The electrooculography (EOG activity) was recorded by placing two sensors below the subjects' right and the left eyes (IO1 and IO2 sensor) as well as near their temples (LO1 and LO2; Figure 37). Vertical EOG reference was computed by averaging the difference between EOG over IO1 and EEG over Fp1 (corresponding frontal activity), and that between EOG from IO2 and EEG over Fp2, as described below:

$$EOG_{vertical} = 0.5 * \left((EOG_{IO1} - EEG_{Fp1}) + (EOG_{IO2} - EEG_{Fp2})\right)$$

where $EOG_{vertical}$ is the vertical reference, EOG_{IO1} and EOG_{IO2} represent EOG below the left and right eyes respectively, whereas EEG_{Fp1} and EEG_{Fp2} represent EEG

corresponding to frontal activity from the left and the right side respectively according to 10-20 EEG system.

The horizontal EOG reference was computed by taking the difference between the EOG near the temples (LO1 and LO2) as described below:

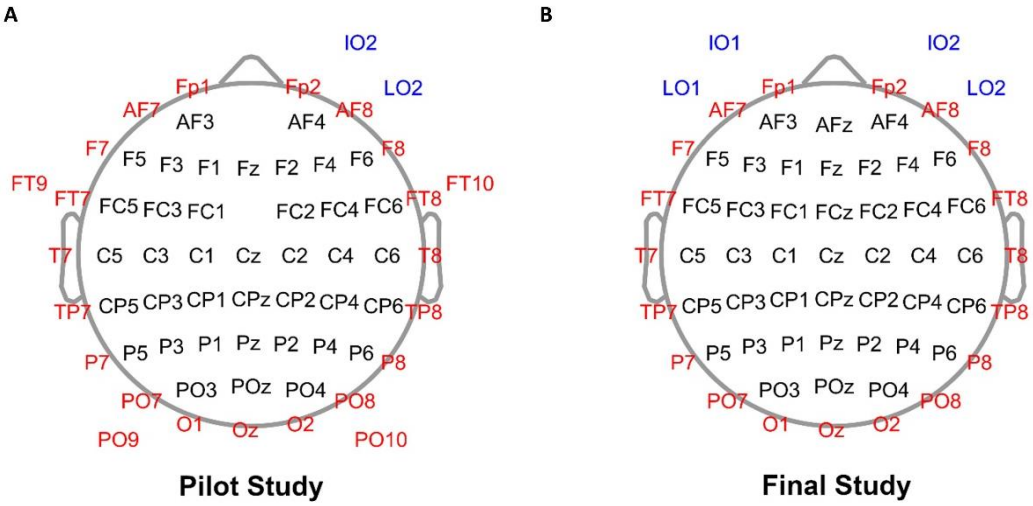

Figure 37: Scalp map for EEG sensor placement for (A) two subjects whose data was imported from the pilot study, and (B) rest of the subjects who participated in the final study. Sensors indicated with red and blue colors were respectively removed and considered for the EOG assessment. (figure adopted from Dr. Andrew Paek's doctoral dissertation)

$$EOG_{horizontal} = \left((EOG_{LO1} - EOG_{LO2})\right)$$

where $EOG_{horizontal}$ represents the horizontal reference for EOG, EOG_{LO1} and EOG_{LO2} represent EOG over the left and the right temples respectively. After this computation, the H-infinity filter estimates the ocular artifacts using vertical and horizontal EOG references. As designed by Kilicarslen and colleagues and previously reported (Paek et al., 2019), the H-infinity filter is sensitive to the parameters γ and q. Based on these parameters, the filter adaptively estimates the output measures and isolates the ocular artifacts from the rest of the EEG activity. The parameters γ and q were optimized to

1.5 and 10^{-20} (determined using trial-and-error (Paek et al., 2019)) to balance removal of the ocular artifact while preserving the integrity of EEG activity.

Artifact Subspace Reconstruction: The H-infinity filtering was followed by removal of low-frequency offset (high-pass filter at 0.1 Hz) and power-line noise for 60, 120, 180 Hz. The next step involved removal of brief head movements leading to aberrant EEG activity. This could be accomplished by the artifact subspace reconstruction (ASR) using *clean_asr* function in the MATLAB-based *EEGlab* toolbox. The ASR first identifies instances with unusual power spectrum (>10 standard deviations) in windows of 500 samples and step size of 250. This data is set to be reconstructed. Subsequently, the function generates epochs of 1-second-long data where no more than 3 EEG channels (and 2 for the pilot data) exceed power spectrum beyond -3.5 and 5.5 standard deviation compared to a robust EEG distribution. The ASR procedure estimates the robust distribution from each channel where the clean data is to be reconstructed based on truncated Gaussian distribution. Ultimately, the function reconstructs cleaner epochs for the instances identified as artifacts associated with sudden head movements, to be followed by removal of EMG artifacts using the ICA.

Independent component analysis (ICA): ICA was mainly applied to eliminate artifacts associated with muscle and forehead movements. First, a surrogate data stream (as shown in Figure 38) was high pass filtered at 2 Hz to obtain a clearer estimate of scalp projections. This stream of data was run through the ICA cleaning procedure which identified components contributing to observed variance. These components were individually identified and removed if they (a) contained spectral power concentrated in the low frequency range within the frontal regions (characteristics of

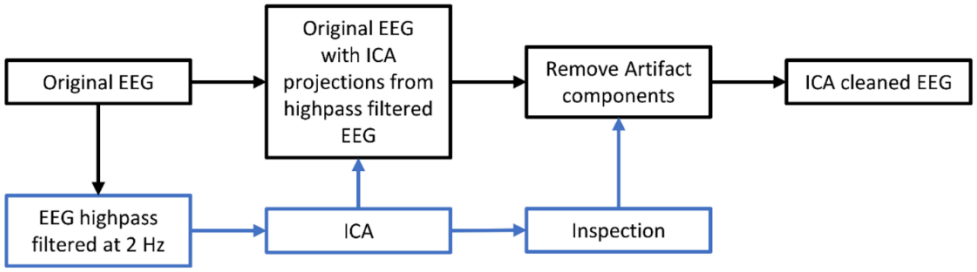

Figure 38: Flowchart for ICA preprocessing pipeline (figure adopted from Dr. Andrew Paek's doctoral dissertation)

forehead movement), or (b) 50% power within the frequency range of 30 to 200 Hz with components localized to the peripheral scalp regions (typical attributes of muscle artifacts). An average of ~35 components were identified and removed from the isometric force production task across subjects, and the resulting components representing cleaner EEG activity were utilized for subsequent analysis.

4.2.6. Data analysis

Based on our previous findings highlighting the role of frontal and parietal cortical activity during digit force control (Parikh and Santello, 2017; Paek et al., 2019; Rao and Parikh, 2019; Parikh et al., 2020), we defined our region of interest (ROI) within the contralateral (left) frontal and parietal electrodes (i.e., F1, F3, FC1, FC3, C1, C3, CP1, CP3, P1 and P3) and their ipsilateral counterparts (i.e., F2, F4, FC2, FC4, C2, C4, CP2, CP4, P2 and P4). To test our hypothesis whether neural variability within the frontal and parietal regions was lateralized and systematically modulated with digit force magnitude, we computed the standard deviation and sample entropy (SD and sE respectively) in neural activity over the fronto-parietal brain regions (i.e., ROI defined above) using sensor-based activation. We focused our analysis on the variability (SD and sE) in time-domain EEG activity using a 1.6 s long hold phase epoch. A computerized script as well as visual inspection were used to remove the initial ramp

phase (de Freitas and Lima, 2013; Feeney et al., 2018). Parameters for sE (m=2, r=0.2) were consistent with previous reports (Svendsen and Madeleine, 2010; Vieluf et al., 2015).

In some cases, activity registered via the EEG sensor-space could be enhanced with spatial resolution via the computation of bipoles (Rearick et al., 2001; Nunez and Srinivasan, 2005; Cao et al., 2015; Paek et al., 2019). The guidelines to compute bipoles suggest subtracting the EEG activity recorded over the one electrode (bipole reference) from that recorded over an electrode of interest (Nunez and Srinivasan, 2005; Cao et al., 2015; Paek et al., 2019). Processing via the bipoles involve optimal selection of bipole references for each electrode of interest such that the distance between the pair is less than 3cm (Nunez and Srinivasan, 2005; Cao et al., 2015; Paek et al., 2019). Based on our research question and the selected ROI, it was critical to retain frontal, central, and parietal electrode activity due to which bipole references were selected for each electrode of interest as shown in Figure 39.

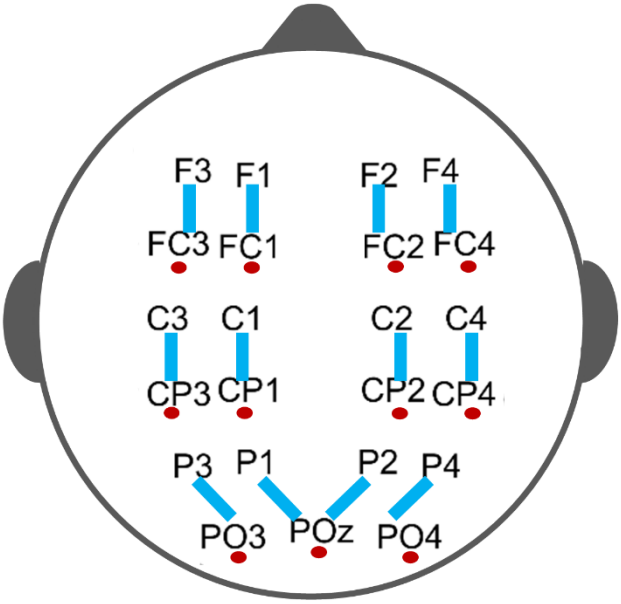

Figure 39: Bipole pairs with red dots indicating the reference for the electrode(s) of interest connected with the blue line

Grip force data was assessed by first applying the zero-phase lag, fourth order, low-pass Butterworth filter with cutoff frequency of 14 Hz (Flanagan and Beltzner, 2000; Rao and Parikh, 2019), followed by computing the mean, SD, sE, and coefficient of variation (CV = SD/mean) of grip force in the epoch defined earlier. Notably, SD and CV indicated amplitude-dependent and amplitude-normalized components of grip force variability. As SD and CV quantify sequence-independent variations, we also included sE to quantify the sequence-dependent component of grip force variability. We assessed changes in these variables with force magnitude using repeated measures analysis of variance (rmAnova, α=0.05) with Force (5, 10, and 15% MVC) as within-subjects factor. To assess the modulation in neural variability across both hemispheres and with different force levels, we performed rmANOVA (α=0.05) on sE as well as SD of EEG activity recorded over the ROI including within-subjects factors (Laterality: left, right hemispheres; Channels: 4 electrodes for each of the central, frontal, and

parietal topography in ROI; Force: 5, 10, 15% MVC). We applied Huynh-Feldt corrections when the sphericity assumption was violated. Post hoc comparisons were performed with Tukey's method. Similar analysis was performed for EEG activity assessed using bipole-configuration, as well as the SD in EEG activity. Statistical analyses were performed using SPSS software version 25.0 (IBM, USA) and GraphPad Prism software version 7.0 (GraphPad Software Inc., USA).

4.3. Results

We first provide findings related to the grip force execution during the epoch of interest, followed by changes in fronto-parietal EEG activity. The primary motive for this study was to characterize the modulation in neural variability with lateralized activation, channel topography, and the magnitude of grip force exerted on the object. We quantified the temporal structure of neural variability by computing the sample entropy of the EEG signal and assessed the sequence-independent changes by SD in the signal over the ROI.

4.3.1. Modulation of grip force variability with force magnitude

Consistent with expectation and previous reports, mean grip force exerted on the object increased based on the requirement to exert appropriate force magnitude during the task (main effect of Force: $F_{(1.003,7.024)}=145.955$, $p<0.001$, $\eta_p^2=0.954$; post hoc Tukey's test for 5 vs. 10, 10 vs 15, and 5 vs. 15% MVC: all adjusted $p<0.0001$; Figure 40). The exertion of higher grip force magnitude also accompanied an increase in standard deviation in the grip force (main effect of Force: $F_{(2,14)}=23.305$, $p<0.001$, $\eta_p^2=0.769$; post hoc Tukey's test for 5 vs. 10% MVC: adjusted $p=0.014$, 10 vs. 15% MVC: adjusted $p=0.025$, 5 vs. 15% MVC: adjusted $p=0.001$). On the other hand, CV

of grip force reduced with increase in magnitude of grip force (main effect of Force: $F_{(2,14)}$=10.434, p=0.002, η_p^2=0.598;) from 5 to 10% MVC (post hoc Tukey's test: adjusted p=0.012), and from 5 to 15% MVC (post hoc Tukey's test: adjusted p=0.009) but not from 10 to 15% MVC (post hoc Tukey's test: adjusted p=0.640). The sample entropy in grip force reduced with higher magnitude of grip force (main effect of Force: $F_{(2,14)}$=9.923, p=0.002, η_p^2=0.586) especially from 10 to 15% MVC (post hoc Tukey's test: adjusted p=0.018) and from 5 to 15% MVC (post hoc Tukey's test: adjusted p=0.019), but not from 5 to 10% MVC (post hoc Tukey's test: adjusted p=0.143).

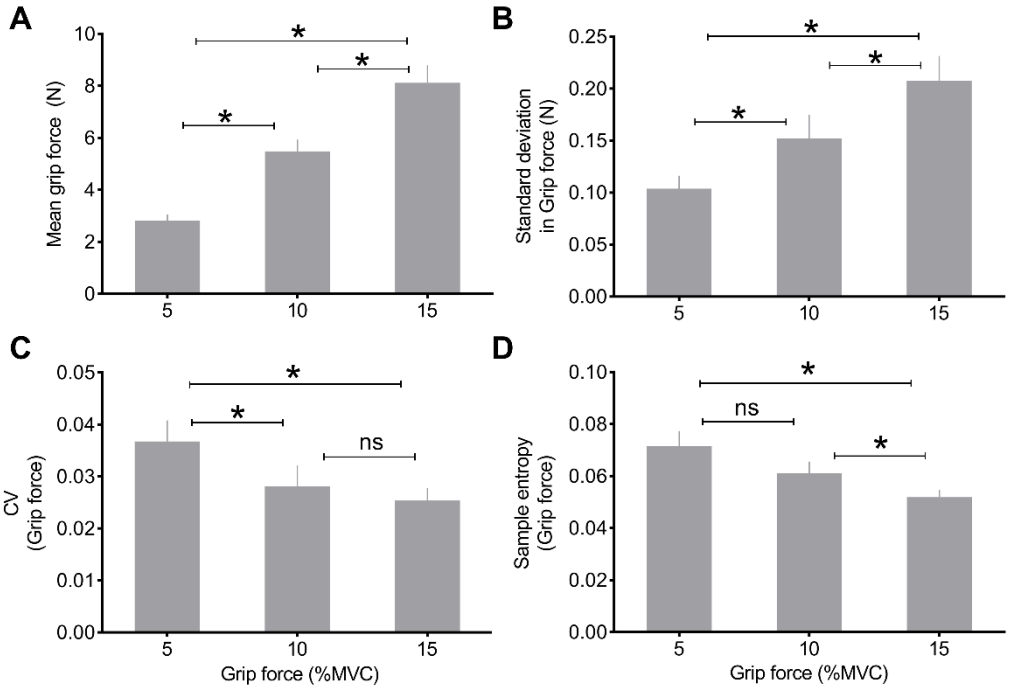

Figure 40: Changes in (A) mean, (B) SD, (C) CV, and (D) sE in grip force with force magnitude. Bars and error bars indicate mean and standard error respectively, asterisk indicates adjusted p<0.05 and *ns* indicates no statistical significance

4.3.2. Lateralized and force magnitude-dependent modulation in sE over central electrodes

Sample entropy (sE) in EEG signals recorded over the central electrodes modulated based on the laterality and force magnitude (Laterality × Force interaction: $F_{(2,14)}$=4.197, p=0.037, η_p^2=0.375; Figure 41). Post hoc comparisons showed statistically significant lateralized modulation when comparing C1 vs. C2 electrode activity from 10% to 15% MVC (post hoc Tukey's test: adjusted p=0.048) but not from 5 to 10% MVC (post hoc Tukey's test: adjusted p=0.687) nor from 5 to 15% MVC (post hoc Tukey's test: adjusted p=0.687). C3 vs. C4 electrode activity showed no modulation in EEG activity with force magnitude (post hoc Tukey's test: all adjusted p>0.246).

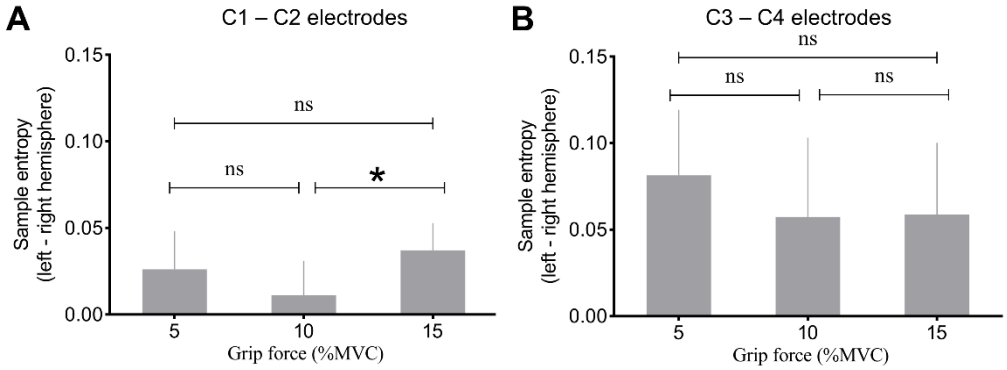

Figure 41: Lateralized entropy for three grip force magnitudes in EEG activity over (A) C1 – C2 electrodes, and (B) C3 – C4 electrodes; bars and eror bars indicate mean and standard error respectively; asterisk indicates adjusted p<0.05 and *ns* indicates no statistical significance

sE in EEG activity within the frontal electrodes showed no modulation with laterality or force magnitude (no Laterality × Force interaction: $F_{(2,14)}$=1.361, p=0.288; no main effect of Laterality: $F_{(1,7)}$=0.014, p=0.910; no main effect of Force: $F_{(2,14)}$=0.578,

p=0.574). The frontal EEG activity showed no modulation with channel and force magnitude (Channel × Force interaction: $F_{(2,14)}$=4.546, p=0.030, η_p^2=0.394; no main effect of channel: $F_{(1,7)}$=0.185, p=0.680; no Laterality × Channel interaction: $F_{(1,7)}$=0.228, p=0.648; post hoc Tukey's test: all adjusted p>0.400; Figure 42). Similarly, EEG activity in parietal electrodes showed no modulation with laterality, nor force (no Laterality × Force interaction: $F_{(2,14)}$=0.436, p=0.655; no main effect of Laterality: $F_{(1,7)}$=0.260, p=0.626; no main effect of Force: $F_{(2,14)}$=0.701, p=0.513; main effect of channel: $F_{(1,7)}$=10.318, p=0.015, η_p^2=0.596; no Channel × Force interaction: $F_{(2,14)}$=0.007, p=0.993; no Laterality × Channel interaction: $F_{(1,7)}$=0.082, p=0.783; post hoc Tukey's test: all adjusted p>0.740; Figure 42).

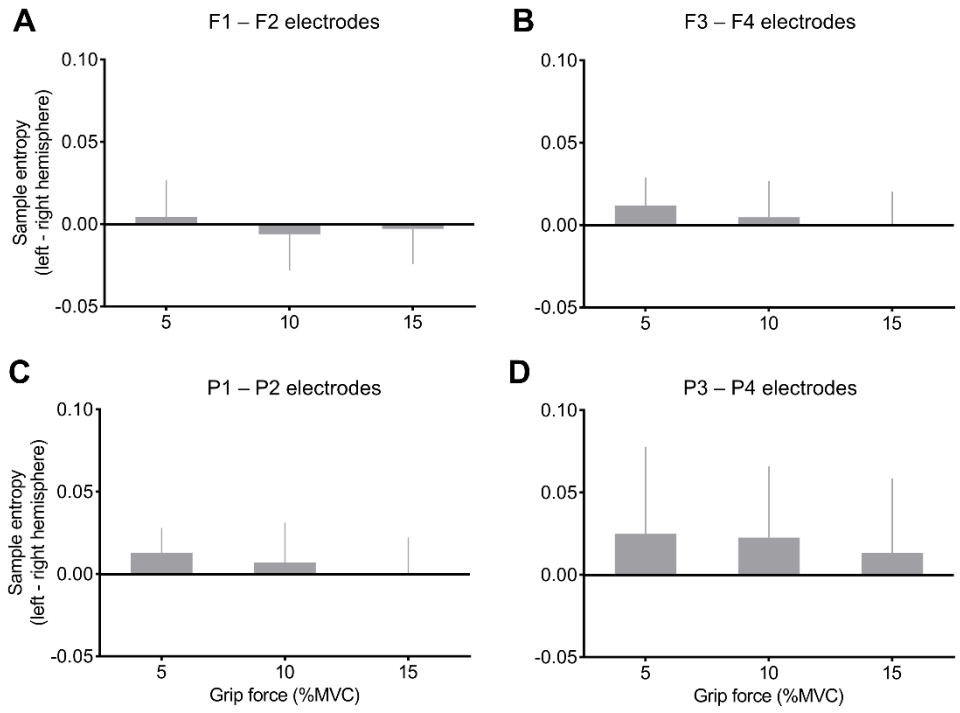

Figure 42: No modulation in sample entropy in EEG activity over the frontal and posterior parietal regions with brain laterality, nor with force magnitudes for (A) F1 – F2, (B) F3 – F4, (C) P1 – P2, and (D) P3 – P4 electrodes; bars and error bars indicate mean and standard error respectively.

4.3.3. No modulation in SD in EEG activity with laterality, channel topography, and force magnitude

The standard deviation (SD) in EEG activity over central electrodes altered with laterality and force magnitude (Laterality × Force interaction: $F_{(2,14)}$=4.358, p=0.034, η_p^2=0.384; no main effect of Laterality: $F_{(1,7)}$=2.680, p=0.146; no main effect of Force: $F_{(2,14)}$=1.037, p=0.380) however, showed no modulation in lateralized activity with grip force magnitude (post hoc Tukey's test for C1 vs. C2 electrodes activity: all adjusted p>0.0710; for C3 vs. C4 electrodes: all adjusted p>0.410). No other contrast detected changes in EEG SD over central electrodes (no main effect of channels, nor associated interaction effects: all F<1.568, all p>0.250).

SD in EEG activity over frontal electrodes altered with channel topography (main effect of Channels: $F_{(1,7)}$=19.701, p=0.003, η_p^2=0.738) however, subsequent analysis showed no modulation in SD of EEG activity across channels (post hoc Tukey's test for F1 vs. F3, and F2 vs. F4 electrode activity: all adjusted p>0.990). No other contrast registered modulation in EEG SD from the frontal electrodes (no main effect, nor interaction effect: all F<2.440, all p>0.130). Similarly, EEG activity recorded over the parietal electrodes showed changes with channel topography (main effect of Channels: $F_{(1,7)}$=12.891, p=0.009, η_p^2=0.648) but no modulation in channel activity during subsequent analysis (post hoc Tukey's test for P1 vs. P3, and P2 vs. P4 electrode activity: all adjusted p>0.850). Other contrasts failed to show modulation with laterality, force, or channel topography (no other main effects, nor interaction: all F<1.700, all p>0.234).

Analysis of sE in EEG activity using bipoles failed to show modulation with laterality, channels, force magnitude (no main effects: all $F<1.640$, all $p>0.238$; nor interaction effects: all $F<1.921$, all $p>0.130$). Due to the identification of bipoles as neighboring electrodes posterior to the electrodes of interest, it is likely that the EEG activity registered within these bipole pairs shared common activation patterns resulting into negligible modulation post bipole computation.

4.4. Discussion

In this study, we investigated the modulation of neural variability measured using EEG during an isometric grip force production task. We found lateralized, force magnitude-dependent modulation of sample entropy in electrical activity recorded over the central electrodes. In contrast, similar modulation was not observed in the electrical activity recorded over the frontal and parietal regions. These findings indicate spatially constrained changes in the regularity of EEG signals during the force production task. On the other hand, assessment of sequence-independent component of neural variability (via SD) showed no modulation with laterality, channel topography, or force magnitude. We discuss these findings in the context of fronto-parietal cortical activity underlying digit force control and their relevance in the development of noninvasive brain-machine interfaces.

4.4.1. Lateralized modulation in EEG variability during digit force control

Neural variability has been previous studied in the context of cognitive tasks involving decision making, face-matching, or attentional cueing paradigms (Mcintosh et al., 2008; Garrett et al., 2011a, 2013b; Grady and Garrett, 2014). In the current study,

we highlight lateralized and force-magnitude dependent modulation in EEG variability over the central electrodes specifically during a force production task in healthy young individuals. Prior neuroimaging work focusing on averaged neural activity has shown hemisphere-specific activation in sensorimotor and premotor cortical activity during force control tasks (Ehrsson et al., 2000b, 2003; Vaillancourt et al., 2003b; Poon et al., 2012; Atique and Francis, 2021). For instance, activation in contralateral primary somatosensory, motor, dorsal and ventral premotor cortices (S1, M1, PMd, and PMv respectively) has been shown to encode force representation in nonhuman primates (Atique and Francis, 2021). Other studies have observed similar spatial activation during the exertion of grip force in humans using fMRI as well as EEG (Ehrsson et al., 2000b, 2003; Vaillancourt et al., 2003b; Poon et al., 2012). Consequently, involvement of contralateral M1, PMd during the force control task could underlie the increase in EEG variability over central contralateral versus ipsilateral hemisphere. Studies probing mechanistic contribution of these regions highlight the processing of visual information specific to digit force scaling within the M1 and PMd cortices (Olivier et al., 2007; Davare et al., 2010; van Polanen and Davare, 2015). The integration of visuomotor information across PMd and M1 is known to facilitate via the reciprocal tracts and phase-locked oscillations during the motor tasks (Churchland et al., 2006b; Hendrix et al., 2009; Atique and Francis, 2021). Given the sensitivity of entropy to sequential interactions within the EEG signal, it is likely that the observed lateralized changes in entropy in electrical activity over central channels could represent the phase-dependent information processing within and between left M1 and PMd.

4.4.2. Influence of cognitive and sensorimotor processes on neural variability

In addition to the lateralized changes in neural variability over central electrodes, we observed non-linear modulation in sE with force magnitude. Similar changes in neural activity has been previously reported in blood oxygen-level dependent (BOLD) signal over the S1, M1, premotor, visual, and cerebellar regions which showed non-linear, higher-order modulation with grip force magnitude (Alahmadi et al., 2016). Non-linear modulation in neural activation during task demands could be arguably traced to neurophysiological and cognitive sources. When presented with varying task demands such as exerting different force levels, intermediate forces could be perceived optimal to direct the metabolic activity depending upon the attentional requirements, visual and proprioceptive processing, and complex sequencing of the underlying neural activity (Alahmadi et al., 2016). Consistent with this notion, a recent study assessing intracortical activity recorded over M1 via implanted multiunit electrodes in patients with tetraplegia showed non-linear influence of volitional state (imagined, observed, or attempted movement) on grip force representation in M1 neural population activity (Rastogi et al., 2020). Moreover, the authors found that neural activity encompassed by the implanted electrodes was particularly sensitive to the volitional states, while showing a subset of this activity also sensitive to the non-linear interaction of volitional state and force levels. Notably, the sensitivity of neural activity to task parameters was variable across participants (Rastogi et al., 2020). Concomitant with these findings, it is possible that the non-linear modulation in neural variability with force levels observed in our study could represent optimal state transitions in force-dependent

cognitive processes either in isolation, or in conjunction with the force level representation in the M1, PMd, or S1 regions. As we observed reduction in lateralized neural variability over central electrodes at 10% MVC, it is possible that a combination of the cognitive and force level representation in the neural variability could be influenced by 'slacking' (i.e., repeating drifts) in grip force, a phenomenon reported to exhibit a relationship with force magnitude that is linear for forces below 10% MVC, and non-linear for forces greater than 10% MVC (Smith et al., 2018).

4.4.3. Neural variability as a critical feature to guide brain-computer interfaces (BCI)

Our study provides experimental evidence to the theoretical framework supporting mechanistic role of neural variability to digit force control. When considered alongside previous studies probing neural variability to understand cognition, we highlight neural variability as a potential feature to aid the development of (non)invasive BCI applications for clinical rehabilitation. An important problem in the BCI literature has been to decode the motor intent to facilitate successful execution of action for patients with sensorimotor deficits e.g., stroke, Parkinson's disease, tetraplegia, or spinal cord injury to name a few (Bradberry et al., 2009; Bhagat et al., 2016; Luu et al., 2017; An et al., 2018; Paek et al., 2019; Moore et al., 2020; Atique and Francis, 2021). Studies focusing on this problem have shown feasibility of decoding the motor intent signals from cortical recordings obtained invasively from nonhuman primates (An et al., 2018; Atique and Francis, 2021) as well as from semi-invasive electrocorticography in humans (Schalk et al., 2007; Sanchez et al., 2008). Importantly, our previous work showed similar success in decoding the motor intent

from noninvasive EEG signals recorded from healthy young individuals, indicating the potential of incorporating EEG signals in noninvasive BCI applications for characterizing motor intent (Bradberry et al., 2010). Our findings pertaining to the neural variability within a trial (current study) as well as across the trials (Rao and Parikh, 2019) support the notion that neural variability could provide additional insights into neural computations prior to, and during movement execution, and could enhance the decoding of motor intent for BCI applications.

With BCI systems equipped to execute the reaching movement using the neural signals, an important challenge faced by the current systems has been to incorporate specialized mechanisms enabling dexterous manipulation of the objects (Bhagat et al., 2016; Luu et al., 2017; An et al., 2018; Paek et al., 2019; Moore et al., 2020; Atique and Francis, 2021). Our recent study investigating reconstruction of grip force trajectories across range of force magnitudes using noninvasive EEG signals showed that spectral power in theta (<5 Hz), alpha (8-12 Hz) and beta bands (14-30 Hz) over the parietal areas was strongly correlated with grip force trajectories (Paek et al., 2019). On the contrary, spectral power in gamma bands (>30 Hz) over the frontal areas showed stronger correlations with the force trajectories (Paek et al., 2019). As our current findings depict non-linear modulation in EEG variability with grip force magnitude that was spatially specific to the central electrode locations but not the frontal and parietal electrode sites, we consider neural variability as a complementary measure to characterize grip force trajectories. Consequently, future studies could consider incorporating neural variability in addition to the currently known features (e.g., spectral power and voltage potentials) for reconstructing the grip force trajectories and

dexterous manipulation. Collectively, our findings highlight the complementary nature of neural variability that is sequence-dependent, spatially specific, and functionally sensitive to the grip force task demands, supporting its potential for augmenting rehabilitation efforts using noninvasive EEG among patients with sensorimotor deficits. In the process, it is important to attribute due consideration to spatial resolution of neuroimaging modality employed to assess neural variability. While it is one of the strengths of the current study to highlight higher-order, nonlinear neural dynamics during digit force control via sensor-space data for noninvasive BCI applications, it should be noted that the sensor-space resolution could be a limiting factor in determining the spatially specific activity over the selected frontal and parietal electrodes. Increasing the spatial resolution could further advance our understanding of the finer interactions among neural ensembles.

Chapter 5. Findings in broader context, and future directions

5.1. Broader applications

Through the first study performed as a part of this dissertation, our findings highlight that during unimanual isometric grip force control, integrity of M1 activity was critical in regulating sequential component of grip force variability at lower forces, especially when visual feedback of the applied and the target force was available. This finding was supported by the observation that sample entropy in grip force for 5 and 15% MVC at all timescales (quantifying sequence-dependent component of grip force variability) increased following cTBS versus sham over M1. Therefore, we reject the null hypothesis that disrupting M1 does not affect sequence-dependent component of grip force variability. In contrast, we observed no change in the standard deviation or coefficient of variation (quantifying sequence-independent components of grip force variability) following cTBS versus sham over M1. We, therefore, failed to reject the null hypothesis that disrupting M1 has no effect on sequence-independent component of grip force variability. From the second study, we observed that sequence-dependent component of fronto-parietal EEG variability showed lateralized, spatially specific, and force magnitude-dependent modulation during grip force control. This finding was supported by the observation that sample entropy in EEG variability was laterally specific and showed non-linear modulation with grip force magnitude for central electrodes placed closer to the midline. Consequently, we reject the null hypothesis that sequence-dependent component of EEG variability does not modulate with grip force magnitude. As we observed no change in standard deviation

of EEG variability over central, parietal, or frontal electrodes, we failed to reject the null hypothesis that sequence-independent component does not modulate with grip force magnitude. Collectively, these findings underscore the mechanistic involvement of not only M1, but a network of neural ensembles spanning the frontal and parietal regions in directing processes essential for efficient grip force control.

Notably, we characterized variability either in motor output (viz. grip force) or in the neural activity (viz. EEG signals) using (a) typical measures such as SD and the coefficient of variation (CV = SD/mean) and (b) sample entropy measure that investigates the degree of regularity in the signal. Our in-depth investigation of the sample entropy at multiple timescales allowed us to investigate systematic interactions across the frequency spectra such that finer (or lower) timescales encompass interactions from a broader band of frequencies (low and high frequencies) whereas coarser (or higher) timescales encompassing narrower band of frequency-interactions (low frequencies) (Costa et al., 2005; Stergiou and Decker, 2011; Kosciessa et al., 2020; Shah-Basak et al., 2020) and understand how these interactions are affected with non-invasive brain stimulation and/or task demands. It has been recently shown that local and inter-cortical functional connectivity during the task could influence the entropy by means of associated neural rhythms (Wang et al., 2018; Shah-Basak et al., 2020). Such local and long-range neural interactions might have contributed to systematic modulation in sample entropy of EEG signals measured over central regions. These findings could represent a combination of task-dependent cognitive and force-related processes. The application of cTBS over M1 in our TMS study might have altered the variability in neural activity intra-M1 and in its associated cortical connections thereby, affecting the regularity in the grip force

application, consistent with (Guerra et al., 2016; Shah-Basak et al., 2020). Overall, our TMS study depicts M1 as a critical node in establishing the regularity in grip forces under the influence of visual feedback.

Taken together, our findings contribute to the broader literature by underscoring mechanistic contribution of fronto-parietal neural processes to digit force control. Moreover, the study of sample entropy measure when compared with SD and CV measures better assisted with the understanding of modulatory effects of TMS as well as provided better understanding of the representation of the task-related dynamics (force levels) in neural networks. These findings could guide future investigations to develop cortical targets for neural plasticity-driven rehabilitation among clinical population. Consistent with our previous work, the neural mechanisms identified in the studies could also provide insights into the functional organization of neural circuits that enable complex behavior such as digit force control. As mentioned before, these findings could potentially inform the BCI literature by incorporating neural variability as a distinguishing feature to assess neural processing, as well as designing interventions that could account for effects of disrupting one cortical region on its associated higher-order behavior.

Through the two studies outlined in this dissertation, we provide robust evidence showing altered behavioral variability following changes in the cortical activation (Aim 1) and determining systematic modulation in neural variability with changes in sensorimotor behavioral task demands (Aim 2). Besides indicating bidirectional relationship between neural and behavioral variability, findings from this dissertation also underscore the critical role of sequence-dependent component of variability in characterizing the neural and behavioral underpinnings of grip force control.

5.2. Potential limitation and future directions

Although noninvasive neuromodulation using cTBS and iTBS protocols have been widely studied, the physiological mechanisms mediating the neuromodulatory effects remain unclear (Huang et al., 2005; Di Lazzaro et al., 2008b, 2008a; Rossi et al., 2009a). Researchers argue about distinct processes, namely the long-term depression (LTD) and long-term potentiation (LTP)-like plasticity underlying the effect of cTBS and iTBS, respectively (Di Lazzaro et al., 2008b, 2008a). Consequently, despite the initially proposed opposite polarity in activation elicited by the two protocols in the literature (cortical inhibition for cTBS, facilitation for iTBS), our study is limited by the currently unknown neural mechanisms elicited by cTBS and iTBS. Nevertheless, consistent findings reported by several studies including those from our group and other labs globally affirm the neuromodulatory effects to last for ~25-30 minutes after administering the cTBS protocol (Huang et al., 2007; Olivier et al., 2007; Ragert et al., 2009; Davare et al., 2010; Rao et al., 2019).

A potential limitation related to neuroimaging using EEG is the unavailability of subject-specific MRI data. The MRI information could equip EEG analysis with higher spatial resolution to conduct source localization for the experiment (Poon et al., 2013). We employed sensor- and bipoles-based approach to assess the fronto-parietal EEG variability. Of note, while increased spatial resolution is desirable, the primary question we were interested in required adequate temporal resolution to quantify the moment-to-moment neural variability using SD and sE-based measures. The temporal resolution in the available EEG dataset is appropriate for the findings presented, and is consistent with the

established framework for EEG processing in multiple studies (Rearick et al., 2001; Cao et al., 2015; Paek et al., 2019).

Future studies could consider (**a**) mapping the spatially constrained modulation in EEG variability by incorporating the subject-specific MRI information. Beyond M1, it is also likely that a wider cortical network could underlie the processing of regularity in grip forces and (**b**) assessing the effects of disrupting M1 activity on the associated nodes, and its influence on the aspects of grip force variability. Lastly, BCI applications as well as clinical rehabilitation studies could consider incorporating identified neural processes to guide interventions aimed at restoring upper extremity fine motor functions among patients with sensorimotor deficits.

References

Aguirre GK, Zarahn E, D'Esposito M (1998) The variability of human, BOLD hemodynamic responses. Neuroimage.

Alahmadi AAS, Samson RS, Gasston D, Pardini M, Friston KJ, D'Angelo E, Toosy AT, Wheeler-Kingshott CAM (2016) Complex motor task associated with non-linear BOLD responses in cerebro-cortical areas and cerebellum. Brain Struct Funct 221:2443–2458.

Allen EA, Pasley BN, Duong T, Freeman RD (2007) Transcranial magnetic stimulation elicits coupled neural and hemodynamic consequences. Science (80-) 317:1918–1921.

Ameli M, Dafotakis M, Fink GR, Nowak DA (2008) Predictive force programming in the grip-lift task: The role of memory links between arbitrary cues and object weight. Neuropsychologia 46:2383–2388.

Ameli M, Kemper F, Sarfeld AS, Kessler J, Fink GR, Nowak DA (2011) Arbitrary visuo-motor mapping during object manipulation in mild cognitive impairment and Alzheimer's disease: A pilot study. Clin Neurol Neurosurg 113:453–458.

An J, Yadav T, Ahmadi MB, Tarigoppula VSA, Francis JT (2018) Near Perfect Neural Critic from Motor Cortical Activity Toward an Autonomously Updating Brain Machine Interface. In: 2018 40th Annual International Conference of the IEEE Engineering in Medicine and Biology Society (EMBC), pp 73–76.

Asaad WF, Rainer G, Miller EK (1998) Neural activity in the primate prefrontal cortex during associative learning. Neuron 21:1399–1407.

Atique MMU, Francis JT (2021) Mirror neurons are modulated by grip force and reward expectation in the sensorimotor cortices (S1, M1, PMd, PMv). Sci Rep 11:1–17.

Baweja HS, Kennedy DM, Vu J, Vaillancourt DE, Christou EA (2010) Greater amount of visual feedback decreases force variability by reducing force oscillations from 0-1 and 3-7 Hz. Eur J Appl Physiol 108:935–943.

Baweja HS, Patel BK, Martinkewiz JD, Vu J, Christou EA (2009) Removal of visual feedback alters muscle activity and reduces force variability during constant isometric contractions. Exp Brain Res 197:35–47.

Bernard JA, Seidler RD (2012) Evidence for motor cortex dedifferentiation in older adults. Neurobiol Aging 33:1890–1899.

Berner J, Schönfeldt-Lecuona C, Nowak D a (2007) Sensorimotor memory for fingertip forces during object lifting: the role of the primary motor cortex. Neuropsychologia 45:1931–1938.

Bestmann S, Krakauer JW (2015) The uses and interpretations of the motor-evoked potential for understanding behaviour. Exp Brain Res 233:679–689.

Bhagat NA, Venkatakrishnan A, Abibullaev B, Artz EJ, Yozbatiran N, Blank AA, French J, Karmonik C, Grossman RG, O'Malley MK, Francisco GE, Contreras-Vidal JL (2016) Design and Optimization of an EEG-Based Brain Machine Interface (BMI) to an Upper-Limb Exoskeleton for Stroke Survivors. Front Neurosci 10:122.

Bilodeau M, Keen DA, Sweeney PJ, Shields RW, Enoka RM (2000) Strength training can improve steadiness in persons with essential tremor. Muscle and Nerve 23:771–778.

Birn RM (2012) The role of physiological noise in resting-state functional connectivity. Neuroimage 62:864–870.

Blennerhassett JM, Carey LM, Matyas TA, Pt B, Carey LM, Matyas TA, Jm AB, Lm C, Ta M (2006) Grip Force Regulation During Pinch Grip Lifts Under Somatosensory Guidance : Comparison Between People With Stroke and Healthy Controls. Arch Phys Med Rehabil 87:418–429.

Bradberry TJ, Gentili RJ, Contreras-Vidal JL (2010) Reconstructing three-dimensional hand movements from noninvasive electroencephalographic signals. J Neurosci 30:3432–3437.

Bradberry TJ, Rong F, Contreras-Vidal JL (2009) Decoding center-out hand velocity from MEG signals during visuomotor adaptation. Neuroimage 47:1691–1700.

Brincat SL, Miller EK (2015) Frequency-specific hippocampal-prefrontal interactions during associative learning. Nat Neurosci 18:576–581.

Bunday KL, Tazoe T, Rothwell JC, Perez MA (2014) Subcortical Control of Precision Grip after Human Spinal Cord Injury. J Neurosci 34:7341–7350.

Burstedt MKO, Flanagan JR, Johansson RS (1999) Control of grasp stability in humans under different frictional conditions during multidigit manipulation. J Neurophysiol 82:2393–2405.

Busa MA, Emmerik REA Van (2016) Multiscale entropy : A tool for understanding the complexity of postural control. J Sport Heal Sci 5:44–51.

Cao L, Hao D, Rong Y, Zhou Y, Li M, Tian Y (2015) Investigating the modulation of brain activity associated with handgrip force and fatigue. Technol Heal Care 23:S427–S433.

Capaday C, Lavoie BA, Barbeau H, Schneider C, Bonnard M (1999) Studies on the corticospinal control of human walking. I. Responses to focal transcranial magnetic stimulation of the motor cortex. J Neurophysiol 81:129–139.

Chaisanguanthum KS, Shen HH, Sabes PN (2014) Motor variability arises from a slow random walk in neural state. J Neurosci 34:12071–12080.

Chen R, Hallett M (1999) The time course of changes in motor cortex excitability associated with voluntary movement. Can J Neurol Sci 26:163–169.

Chen R, Yaseen Z, Cohen LG, Hallett M (1998) Time course of corticospinal excitability

in reaction time and self-paced movements. Ann Neurol 44:317–325.

Chouinard PA, Leonard G, Paus T (2005) Role of the primary motor and dorsal premotor cortices in the anticipation of forces during object lifting. J Neurosci 25:2277–2284.

Christou EEAE (2011) Aging and Variability of Voluntary Contractions. Exerc Sport Sci Rev 39:77–84.

Chu WTV, Sanger TD (2009) Force variability during isometric biceps contraction in children with secondary dystonia dueto cerebral palsy. Mov Disord 24:1299–1305.

Churchland MM, Afshar A, Shenoy K V (2006a) A Central Source of Movement Variability. Neuron 52:1085–1096.

Churchland MM, Santhanam G, Shenoy K V (2006b) Preparatory Activity in Premotor and Motor Cortex Reflects the Speed of the Upcoming Reach. J Neurophysiol 96:3130–3146.

Cohen J (2016) The earth is round (p <. 05). What If There Were No Significance Tests? Class Ed:21–34.

Cohen LG (2000) A window into the role of inhibitory and excitatory mechanisms of perception? J Physiol 529:283.

Cohen LG, Celnik P, Pascual-Leone A, Corwell B, Falz L, Dambrosia J, Honda M, Sadato N, Gerloff C, Catala MD, Hallett M (1997) Functional relevance of cross-modal plasticity in blind humans. Nature 389:180–183.

Cole KJ, Rotella DL (2002) Old age impairs the use of arbitrary visual cues for predictive control of fingertip forces during grasp. Exp Brain Res 143:35–41.

Collins DF, Brooke JD, McIlroy WE (1993) The Independence of Premovement H-Reflex Gain and Kinesthetic Requirements for Task-Performance. Electroencephalogr Clin Neurophysiol 89:35–40.

Costa M, Goldberger AL, Peng C (2005) Multiscale entropy analysis of biological signals. :1–18.

Cumming G, Calin-Jageman RJ (2016) Introduction to the New Statistics: Estimation, Open Science, and Beyond. Routledge.

Dafotakis M, Grefkes C, Eickhoff SB, Karbe H, Fink GR, Nowak DA (2008) Effects of rTMS on grip force control following subcortical stroke. Exp Neurol 211:407–412.

Darling WG, Wolf SL, Butler AJ (2006) Variability of motor potentials evoked by transcranial magnetic stimulation depends on muscle activation. Exp brain Res 174:376–385.

Davare M, Andres M, Clerget E, Thonnard J-LJ-L, Olivier E (2007) Temporal Dissociation between Hand Shaping and Grip Force Scaling in the Anterior Intraparietal Area. J Neurosci 27:3974–3980.

Davare M, Andres M, Cosnard G, Thonnard JL, Olivier E (2006) Dissociating the role of

ventral and dorsal premotor cortex in precision grasping. J Neurosci 26:2260–2268.

Davare M, Kraskov A, Rothwell JC, Lemon RN (2011) Interactions between areas of the cortical grasping network. Curr Opin Neurobiol 21:565–570.

Davare M, Lemon R, Olivier E (2008) Selective modulation of interactions between ventral premotor cortex and primary motor cortex during precision grasping in humans. J Physiol 586:2735–2742.

Davare M, Montague K, Olivier E, Rothwell JC, Lemon RN (2009) Ventral premotor to primary motor cortical interactions during object-driven grasp in humans. CORTEX 45:1050–1057.

Davare M, Parikh PJ, Santello M (2019) Sensorimotor uncertainty modulates corticospinal excitability during skilled object manipulation. J Neurophysiol 121:1162–1170.

Davare M, Rothwell JC, Lemon RN (2010) Causal Connectivity between the Human Anterior Intraparietal Area and Premotor Cortex during Grasp. Curr Biol 20:176–181.

de Freitas PB, Lima KCA (2013) Grip force control during simple manipulation tasks in non-neuropathic diabetic individuals. Clin Neurophysiol 124:1904–1910.

De Luca CJ, Foley PJ, Erim Z (1996) Motor unit control properties in constant-force isometric contractions. J Neurophysiol 76:1503–1516.

Delorme A, Makeig S (2004) EEGLAB: An open source toolbox for analysis of single-trial EEG dynamics including independent component analysis. J Neurosci Methods 134:9–21.

Dennis NA, Hayes SM, Prince SE, Madden DJ, A S, Cabeza R (2009) Effects of Aging on the Neural Correlates of Successful Item and Source Memory Encoding. J Exp Psychol Learn Mem Cogn 34:791–808.

Dettmers C, Lemon RN, Stephan KM, Fink GR, Frackowiak RS (1996) Cerebral activation during the exertion of sustained static force in man. Neuroreport 7:2103–2110.

Devanne H, Lavoie BA, Capaday C (1997) Input-output properties and gain changes in the human corticospinal pathway. Exp brain Res 114:329–338.

Dhawale AK, Smith MA, Olveczky BP (2017) The Role of Variability in Motor Learning. Annu Rev Neurosci 40:479–498.

Di Lazzaro V, Pilato F, Dileone M, Profice P, Oliviero a, Mazzone P, Insola a, Ranieri F, Meglio M, Tonali P a, Rothwell JC (2008a) The physiological basis of the effects of intermittent theta burst stimulation of the human motor cortex. J Physiol 586:3871–3879.

Di Lazzaro V, Pilato F, Saturno E, Oliviero A, Dileone M, Mazzone P, Insola A, Tonali PA, Ranieri F, Huang YZ, Rothwell JC (2005) Theta-burst repetitive transcranial

magnetic stimulation suppresses specific excitatory circuits in the human motor cortex. J Physiol 565:945–950.

Di Lazzaro V, Ziemann U, Lemon RN (2008b) State of the art: Physiology of transcranial motor cortex stimulation. Brain Stimul 1:345–362.

Dideriksen JL, Negro F, Enoka RM, Farina D (2012) Motor unit recruitment strategies and muscle properties determine the influence of synaptic noise on force steadiness. J Neurophysiol 107:3357–3369.

Dinstein I, Heeger DJ, Behrmann M (2015) Neural variability: Friend or foe? Trends Cogn Sci 19:322–328.

Duarte M, Zatsiorsky VM (2002) Effects of body lean and visual information on the equilibrium maintenance during stance. Exp Brain Res 146:60–69.

Duchateau J, Enoka RM (2011) Human motor unit recordings: Origins and insight into the integrated motor system. Brain Res 1409:42–61.

Ehrsson HH, Fagergren A, Forssberg H (2001) Differential fronto-parietal activation depending on force used in a precision grip task: An fMRI study. J Neurophysiol 85:2613–2623.

Ehrsson HH, Fagergren A, Johansson RS, Forssberg H (2003) Evidence for the involvement of the posterior parietal cortex in coordination of fingertip forces for grasp stability in manipulation. J Neurophysiol 90:2978–2986.

Ehrsson HH, Fagergren A, Jonsson T, Westling G, Johansson RS, Forssberg H (2000a) Cortical Activity in Precision- Versus Power-Grip Tasks: An fMRI Study. J Neurophysiol 83:528–536.

Ehrsson HH, Fagergren A, Jonsson T, Westling G, Roland S, Forssberg H, Oran G (2000b) Cortical Activity in Precision- Versus Power-Grip Tasks : An fMRI Study Cortical Activity in Precision- Versus Power-Grip Tasks : An fMRI Study. J Neurophysiol 83:528–536.

Eisen A, Entezari-Taher M, Stewart H (1996) Cortical projections to spinal motoneurons: changes with aging and amyotrophic lateral sclerosis. Neurology 46:1396–1404.

Enoka RM, Christou EA, Hunter SK, Kornatz KW, Semmler JG, Taylor AM, Tracy BL (2003) Mechanisms that contribute to differences in motor performance between young and old adults. J Electromyogr Kinesiol 13:1–12.

Enoka RM, Duchateau J (2017) Rate coding and the control of muscle force. Cold Spring Harb Perspect Med 7:1–12.

Faisal AA, Selen LPJ, Wolpert DM (2008) Noise in the nervous system. Nat Rev Neurosci 9:292–303.

Feeney DF, Mani D, Enoka RM (2018) Variability in common synaptic input to motor neurons modulates both force steadiness and pegboard time in young and older adults. J Physiol 596:3793–3806.

Fellows SJ, Noth J (2003) Grip Force Abnormalities in De Novo Parkinson's Disease. Mov Disord 19:560–565.

Fisk JE, Warr PB (1998) Associative learning and short-term forgetting as a function of age, perceptual speed, and central executive functioning. J Gerontol Psychol Sci 53:112–121.

Flanagan JR, Beltzner MA (2000) Independence of perceptual and sensorimotor predictions in the size- weight illusion. Nat Neurosci 3:737–741.

Fontanini A, Katz DB (2008) Behavioral states, network states, and sensory response variability. J Neurophysiol 100:1160–1168.

Fox MD, Snyder AZ, Vincent JL, Raichle ME (2007) Intrinsic Fluctuations within Cortical Systems Account for Intertrial Variability in Human Behavior. Neuron 56:171–184.

Friendly M, Monette G, Fox J (2013) Elliptical Insights: Understanding Statistical Methods through Elliptical Geometry. Stat Sci 28:1–39.

Fu Q, Zhang W, Santello M (2010) Anticipatory planning and control of grasp positions and forces for dexterous two-digit manipulation. J Neurosci 30:9117–9126.

Gagnon H, Simmonite M, Cassady K, Chamberlain J, Freiburger E, Lalwani P, Kelley S, Foerster B, Park DC, Petrou M, Seidler RD, Taylor SF, Weissman DH, Polk TA (2019) Michigan Neural Distinctiveness (MiND) study protocol: Investigating the scope, causes, and consequences of age-related neural dedifferentiation. BMC Neurol 19:1–17.

Galganski ME, Fuglevand AJ, Enoka RM (1993) Reduced control of motor output in a human hand muscle of elderly subjects during submaximal contractions. J Neurophysiol 69:2108–2115.

Gallen CL, Baniqued PL, Chapman SB, Aslan S, Keebler M, Didehbani N, Esposito MD (2016) Modular Brain Network Organization Predicts Response to Cognitive Training in Older Adults. PLoS One 11:1–17.

Garrett DD, Kovacevic N, McIntosh AR, Grady CL (2010) Blood oxygen level-dependent signal variability is more than just noise. J Neurosci 30:4914–4921.

Garrett DD, Kovacevic N, McIntosh AR, Grady CL (2011a) The importance of being variable. J Neurosci 31:4496–4503.

Garrett DD, Kovacevic N, McIntosh AR, Grady CL (2013a) The modulation of BOLD variability between cognitive states varies by age and processing speed. Cereb Cortex 23:684–693.

Garrett DD, McIntosh AR, Grady CL (2011b) Moment-to-moment signal variability in the human brain can inform models of stochastic facilitation now. Nat Rev Neurosci 12:612.

Garrett DD, McIntosh AR, Grady CL (2014) Brain signal variability is parametrically

modifiable. Cereb Cortex 24:2931–2940.

Garrett DD, Samanez-Larkin GR, MacDonald SWS, Lindenberger U, McIntosh AR, Grady CL (2013b) Moment-to-moment brain signal variability: A next frontier in human brain mapping? Neurosci Biobehav Rev 37:610–624.

Gentner R, Wankerl K, Reinsberger C, Zeller D, Classen J (2008) Depression of human corticospinal excitability induced by magnetic theta-burst stimulation: Evidence of rapid polarity-reversing metaplasticity. Cereb Cortex 18:2046–2053.

Goel R, Nakagome S, Rao N, Paloski WH, Contreras-Vidal JL, Parikh PJ (2019) Fronto-Parietal Brain Areas Contribute to the Online Control of Posture during a Continuous Balance Task. Neuroscience 413:135–153.

Gordon AM, Forssberg H, Johansson RS, Westling G (1991) The integration of haptically acquired size information in the programming of precision grip. Exp brain Res 83:483–488.

Gordon AM, Westling G, Cole KJ, Johansson RS (1993a) Memory representations underlying motor commands used during manipulation of common and novel objects. J Neurophysiol 69:1789–1796.

Gordon M, Cole KJ, Johansson S (1993b) Manipulation of Common and Novel Objects. Brain.

Gorniak SL, Khan A, Ochoa N, Sharma MD, Phan CL (2014) Detecting subtle fingertip sensory and motor dysfunction in adults with type II diabetes. Exp Brain Res 232:1283–1291.

Grady CL, Garrett DD (2014) Understanding variability in the BOLD signal and why it matters for aging. Brain Imaging Behav 8:274–283.

Grady CL, Garrett DD (2018) Brain signal variability is modulated as a function of internal and external demand in younger and older adults. Neuroimage 169:510–523.

Grafton ST (2010) The cognitive neuroscience of prehension: Recent developments. Exp Brain Res 204:475–491.

Guerra A, Pogosyan A, Nowak M, Tan H, Ferreri F, Di Lazzaro V, Brown P (2016) Phase Dependency of the Human Primary Motor Cortex and Cholinergic Inhibition Cancelation during Beta tACS. Cereb Cortex 26:3977–3990.

Haar S, Donchin O, Dinstein I (2017) Individual Movement Variability Magnitudes Are Explained by Cortical Neural Variability. J Neurosci 37:9076–9085.

Hadjiosif AM, Smith MA (2015) Flexible control of safety margins for action based on environmental variability. J Neurosci 35:9106–9121.

Harris & Wolpert (2004) Signal-dependent noise determines motor planning. Nature 428:668–673.

Harris C, Wolpert D (1998) Signal-dependent noise determinesmotorplanning. Nature.

Hendrix CM, Mason CR, Ebner TJ (2009) Signaling of Grasp Dimension and Grasp Force in Dorsal Premotor Cortex and Primary Motor Cortex Neurons During Reach to Grasp in the Monkey. J Neurophysiol 102:132–145.

Herzfeld DJ, Vaswani PA, Marko MK, Shadmehr R (2014) A memory of errors in sensorimotor learning. Science 345:1349–1353.

Hess TM (2005) Memory and aging in context. Psychol Bull 131:383–406.

Heuninckx S, Wenderoth N, Swinnen SP (2008) Systems neuroplasticity in the aging brain: Recruiting additional neural resources for successful motor performance in elderly persons. J Neurosci 28:91–99.

Hirsiger S, Koppelmans V, Mérillat S, Liem F, Erdeniz B, Seidler RD, Jäncke L (2016) Structural and functional connectivity in healthy aging: Associations for cognition and motor behavior. Hum Brain Mapp 37:855–867.

Ho J, Tumkaya T, Aryal S, Choi H, Claridge-Chang A (2019) Moving beyond P values: data analysis with estimation graphics. Nat Methods 16:565–566.

Hohl SS, Chaisanguanthum KS, Lisberger SG (2013) Sensory Population Decoding for Visually Guided Movements. Neuron 79:167–179.

Honeycutt CF, Kharouta M, Perreault EJ (2013) Evidence for reticulospinal contributions to coordinated finger movements in humans. J Neurophysiol 110:1476–1483.

Hu B, Zhang X, Mu J, Wu M, Wang Y (2018) Spasticity assessment based on the Hilbert-Huang transform marginal spectrum entropy and the root mean square of surface electromyography signals: A preliminary study. Biomed Eng Online 17:1–20.

Huang Y-Z, Chen R-S, Rothwell JC, Wen H-Y (2007) The after-effect of human theta burst stimulation is NMDA receptor dependent. Clin Neurophysiol 118:1028–1032.

Huang YZ, Edwards MJ, Rounis E, Bhatia KP, Rothwell JC (2005) Theta burst stimulation of the human motor cortex. Neuron 45:201–206.

Huang YZ, Rothwell JC, Chen RS, Lu CS, Chuang WL (2011) The theoretical model of theta burst form of repetitive transcranial magnetic stimulation. Clin Neurophysiol 122:1011–1018.

Hutchinson S, Kobayashi M, Horkan CM, Pascual-Leone A, Alexander MP, Schlaug G (2002) Age-related differences in movement representation. Neuroimage 17:1720–1728.

Jernigan TLT, Archibald SLS, Fennema-Notestine, C Gamst A, Stout J, Bonner J, Hesselink J, Fennema-notestine C (2001) Effects of age on tissues and regions of the cerebrum and cerebellum. Neurobiol Aging 22:581–594.

Johansson RS, Cole KJ (1992) Sensory-motor coordination during grasping and manipulative actions. Curr Opin Neurobiol 2:815–823.

Johansson RS, Westling G (1988) Programmed and triggered actions to rapid load

changes during precision grip. Exp Brain Res 71:72–86.

Jones KE, Hamilton AF, Wolpert DM (2002) Sources of signal-dependent noise during isometric force production. J Neurophysiol 88:1533–1544.

Kanai R, Rees G (2011) The structural basis of inter-individual differences in human behaviour and cognition. Nat Rev Neurosci 12:231–242.

Kang N, Cauraugh JH (2014) Bimanual Force Variability and Chronic Stroke: Asymmetrical Hand Control Tremblay F, ed. PLoS One 9:e101817.

Katagiri N, Yoshida S, Koseki T, Kudo D, Namba S, Tanabe S, Huang YZ, Yamaguchi T (2020) Interindividual Variability of Lower-Limb Motor Cortical Plasticity Induced by Theta Burst Stimulation. Front Neurosci 14:1–10.

Keel J, Smith M, Wassermann E (2001) A Safety Screening Questionnaire for Transcranial Magnetic Stimulation. Clin Neurophysiol:720.

Kiers L, Cros D, Chiappa KH, Fang J (1993) Variability of motor potentials evoked by transcranial magnetic stimulation. Electroencephalogr Clin Neurophysiol 89:415–423.

Kilner JM, Salenius S, Baker SN, Jackson A, Hari R, Lemon RN (2003) Task-dependent modulations of cortical oscillatory activity in human subjects during a bimanual precision grip task. Neuroimage 18:67–73.

Klein-Flugge MC, Nobbs D, Pitcher JB, Bestmann S (2013) Variability of Human Corticospinal Excitability Tracks the State of Action Preparation. J Neurosci 33:5564–5572.

Ko NH, Laine CM, Fisher BE, Valero-Cuevas FJ (2015) Force variability during dexterous manipulation in individuals with mild to moderate Parkinson's disease. Front Aging Neurosci 7:1–10.

Koch G, Del Olmo MF, Cheeran B, Schippling S, Caltagirone C, Driver J, Rothwell JC (2008) Functional interplay between posterior parietal and ipsilateral motor cortex revealed by twin-coil transcranial magnetic stimulation during reach planning toward contralateral space. J Neurosci 28:5944–5953.

Kosciessa JQ, Kloosterman NA, Garrett DD (2020) Standard multiscale entropy reflects neural dynamics at mismatched temporal scales: What's signal irregularity got to do with it?

Kujirai T, Caramia MD, Rothwell JC, Day BL, Thompson PD, Ferbert A, Wroe S, Asselman P, Marsden CD (1993) Corticocortical inhibition in human motor cortex. J Physiol 471:501–519.

Kwon M, Baweja HS, Christou EA (2011) Age-associated differences in positional variability are greater with the lower limb. J Mot Behav 43:357–360.

Lei Y, Ozdemir RA, Perez MA (2018) Gating of Sensory Input at Subcortical and Cortical Levels during Grasping in Humans. J Neurosci 38:7237–7247.

Lemon RN (2008) Descending pathways in motor control. Annu Rev Neurosci 31:195–218.

Li K, Nataraj R, Marquardt TL, Li ZM (2013) Directional coordination of thumb and finger forces during precision pinch. PLoS One 8.

Li K, Wei N, Yue S, Thewlis D, Fraysse F, Immink M, Eston R (2015) Coordination of digit force variability during dominant and non-dominant sustained precision pinch. Exp Brain Res 233:2053–2060.

Lindberg PG, Roche N, Robertson J, Roby-Brami A, Bussel B, Maier MA (2012) Affected and unaffected quantitative aspects of grip force control in hemiparetic patients after stroke. Brain Res 1452:96–107.

Lisberger SG, Medina JF (2015) How and why neural and motor variation are related. Curr Opin Neurobiol 33:110–116.

Lodha N, Christou EA (2017) Low-frequency oscillations and control of the motor output. Front Physiol 8:1–9.

Lodha N, Misra G, Coombes SA, Christou EA, Cauraugh JH (2013) Increased force variability in chronic stroke: Contributions of force modulation below 1 Hz. PLoS One 8:1–9.

Lukos JR, Ansuini C, Santello M (2007) Choice of contact points during multidigit grasping: effect of predictability of object center of mass location. J Neurosci 27:3894–3903.

Lukos JR, Ansuini C, Santello M (2008) Anticipatory control of grasping: Independence of sensorimotor memories for kinematics and kinetics. J Neurosci 28:12765–12774.

Lukos JR, Cho JY, Santello M (2013) Grasping uncertainty: Effects of sensorimotor memories on high-level planning of dexterous manipulation. J Neurophysiol 109:2937–2946.

Luu TP, He Y, Brown S, Nakagame S, Contreras-Vidal JL (2016) Gait adaptation to visual kinematic perturbations using a real-time closed-loop brain–computer interface to a virtual reality avatar. J Neural Eng 13:036006.

Luu TP, Nakagome S, He Y, Contreras-Vidal JL (2017) Real-time EEG-based brain-computer interface to a virtual avatar enhances cortical involvement in human treadmill walking. Sci Rep 7:1–12.

Marneweck M, Barany DA, Santello M, Grafton ST (2018) Neural representations of sensorimotor memory-and digit position-based load force adjustments before the onset of dexterous object manipulation. J Neurosci 38:4724–4737.

Marneweck M, Grafton ST (2020) Representational Neural Mapping of Dexterous Grasping Before Lifting in Humans. J Neurosci 40:2708–2716.

Masquelier T (2013) Neural variability, or lack thereof. Front Comput Neurosci 7:1–7.

Mcintosh AR, Kovacevic N, Itier RJ (2008) Increased Brain Signal Variability

Accompanies Lower Behavioral Variability in Development. 4.

McIntosh AR, Kovacevic N, Lippe S, Garrett D, Grady C, Jirsa V (2010) The development of a noisy brain. Arch Ital Biol 148:323–337.

Miller JD, Herda TJ, Trevino MA, Sterczala AJ, Ciccone AB (2017) Time-related changes in firing rates are influenced by recruitment threshold and twitch force potentiation in the first dorsal interosseous. Exp Physiol 102:950–961.

Milner TE, Franklin DW, Imamizu H, Kawato M (2007) Central control of grasp: Manipulation of objects with complex and simple dynamics. Neuroimage 36:388–395.

Misiaszek JE (2003) The H-reflex as a tool in neurophysiology: Its limitations and uses in understanding nervous system function. Muscle and Nerve 28:144–160.

Mizuguchi N, Uehara S, Hirose S, Yamamoto S, Naito E (2016) Neuronal Substrates Underlying Performance Variability in Well-Trained Skillful Motor Task in Humans. Neural Plast 2016.

Mojtahedi K, Fu Q, Santello M (2015) Extraction of Time and Frequency Features from Grip Force Rates during Dexterous Manipulation. IEEE Trans Biomed Eng 62:1363–1375.

Moon H, Kim C, Kwon M, Chen YT, Onushko T, Lodha N, Christou EA (2014) Force control is related to low-frequency oscillations in force and surface EMG. PLoS One 9:1–9.

Moore B, Khang S, Francis JT (2020) Noise-Correlation Is Modulated by Reward Expectation in the Primary Motor Cortex Bilaterally During Manual and Observational Tasks in Primates. Front Behav Neurosci 14:1–15.

Moorman JR (2019) Physiological time-series analysis using approximate entropy and sample entropy. :2039–2049.

Mutter SA, Holder JM, Mashburn CA, Luna CM (2019) Aging and the role of attention in associative learning. Psychol Aging 34:215–227.

Nagamori A, Laine CM, Loeb GE, Valero-Cuevas FJ (2021) Force variability is mostly not motor noise: Theoretical implications for motor control.

Nataraj R, Audu ML, Li ZM (2015) Digit mechanics in relation to endpoint compliance during precision pinch. J Biomech 48:672–680.

Neto OP, Baweja HS, Christou EA (2010) Increased voluntary drive is associated with changes in common oscillations from 13 to 60 Hz of interference but not rectified electromyography. Muscle and Nerve 42:348–354.

Newell KM, Carlton LG, Hancock PA (1984) Kinetic analysis of response variability. Psychol Bull 96:133–151.

Nowak DA, Berner J, Herrnberger B, Kammer T, Gron G, Schonfeldt-Lecuona C (2009) Continuous theta-burst stimulation over the dorsal premotor cortex interferes with

associative learning during object lifting. Cortex 45:473–482.

Nowak DA, Koupan C, Hermsdörfer J (2007) Formation and decay of sensorimotor and associative memory in object lifting. Eur J Appl Physiol 100:719–726.

Nunez PL, Srinivasan R (2005) Electric Fields of the Brain: The Neurophysics of EEG, 2nd ed. Oxford University Press.

Oldfield RC (1971) The assessment and analysis of handedness: The Edinburgh inventory. Neuropsychologia 9:97–113.

Olivier E, Davare M, Andres M, Fadiga L (2007) Precision grasping in humans: from motor control to cognition. Curr Opin Neurobiol 17:644–648.

Oliviero A, Profice P, Tonali PA, Pilato F, Saturno E, Dileone M, Ranieri F, Di Lazzaro V (2006) Effects of aging on motor cortex excitability. Neurosci Res 55:74–77.

Osborne LC, Lisberger SG, Bialek W (2005) A sensory source for motor variation. Nature 437:412–416.

Paek AY, Gailey A, Parikh PJ, Santello M, Contreras-Vidal JL (2019) Regression-based reconstruction of human grip force trajectories with noninvasive scalp electroencephalography. J Neural Eng 16:66030.

Parikh PJ, Cole KJ (2012) Handling objects in old age: Forces and moments acting on the object. J Appl Physiol 112:1095–1104.

Parikh PJ, Davare M, McGurrin P, Santello M (2014) Corticospinal excitability underlying digit force planning for grasping in humans. J Neurophysiol 111:2560–2569.

Parikh PJ, Fine JM, Santello M (2019) Choice of Contact Points Modulates Sensorimotor Cortical Interactions for Dexterous Manipulation. bioRxiv:621466.

Parikh PJ, Fine JM, Santello M (2020) Dexterous Object Manipulation Requires Context-Dependent Sensorimotor Cortical Interactions in Humans. Cereb Cortex 30:3087–3101.

Parikh PJ, Santello M (2017) Role of human premotor dorsal region in learning a conditional visuomotor task. J Neurophysiol 117:445–456.

Paus T (2005) Inferring causality in brain images: A perturbation approach. Philos Trans R Soc B Biol Sci 360:1109–1114.

Perellón-Alfonso R, Kralik M, Pileckyte I, Princic M, Bon J, Matzhold C, Fischer B, Šlahorová P, Pirtošek Z, Rothwell J, Kojovic M (2018) Similar effect of intermittent theta burst and sham stimulation on corticospinal excitability: A 5-day repeated sessions study. Eur J Neurosci 48:1990–2000.

Perez MA, Cohen LG (2009) Scaling of motor cortical excitability during unimanual force generation. Cortex 45:1065–1071.

Pitcher JB, Ogston KM, Miles TS (2002) Age and sex differences in human motor cortex

input-output characteristics. J Physiol 546:605–613.

Poon C, Chin-Cottongim LG, Coombes SA, Corcos DM, Vaillancourt DE (2012) Spatiotemporal dynamics of brain activity during the transition from visually guided to memory-guided force control. J Neurophysiol 108:1335–1348.

Poon C, Coombes SA, Corcos DM, Christou EA, Vaillancourt DE (2013) Transient shifts in frontal and parietal circuits scale with enhanced visual feedback and changes in force variability and error. J Neurophysiol 109:2205–2215.

Poston B, Christou EA, Enoka JA, Enoka RM (2008) Timing variability and not force variability predicts the endpoint accuracy of fast and slow isometric contractions. Exp brain Res 6:2166–2171.

Prodoehl J, Corcos DM, Vaillancourt DE (2006) Effects of focal hand dystonia on visually guided and internally guided force control. J Neurol Neurosurg Psychiatry 77:909–914.

Ragert P, Camus M, Vandermeeren Y, Dimyan MA, Cohen LG (2009) Modulation of effects of intermittent theta burst stimulation applied over primary motor cortex (M1) by conditioning stimulation of the opposite M1. J Neurophysiol 102:766–773.

Rao N, Chen Y-T, Ramirez R, Tran J, Li S, Parikh PJ (2019) Persistent Elevation of Electrical Pain Threshold following Continuous Theta Burst Stimulation over Primary Somatosensory Cortex in Humans. bioRxiv.

Rao N, Chen YT, Ramirez R, Tran J, Li S, Parikh PJ (2020) Time-course of pain threshold after continuous theta burst stimulation of primary somatosensory cortex in pain-free subjects. Neurosci Lett 722:134760.

Rao N, Mehta N, Patel P, Parikh PJ (2021) Effects of aging on conditional visuomotor learning for grasping and lifting eccentrically weighted objects. J Appl Physiol 131:937–948.

Rao N, Parikh PJ (2017) Variability in Corticospinal Excitability during Digit Force Planning for Grasping in Humans. Neurosci Meet Plan:Program No. 406.06 Available at: https://www.abstractsonline.com/pp8/index.html#!/4376/presentation/18054.

Rao N, Parikh PJ (2019) Fluctuations in Human Corticospinal Activity Prior to Grasp. Front Syst Neurosci 13:1–15.

Rastogi A et al. (2020) Neural Representation of Observed, Imagined, and Attempted Grasping Force in Motor Cortex of Individuals with Chronic Tetraplegia. Sci Rep 10:1–16.

Rearick MP, Johnston JA, Slobounov SM (2001) Feedback-dependent modulation of isometric force control: An EEG study in visuomotor integration. Cogn Brain Res 12:117–130.

Rossi S et al. (2009a) Safety, ethical considerations, and application guidelines for the use of transcranial magnetic stimulation in clinical practice and research. Clin

Neurophysiol 120:2008–2039.

Rossi S, Hallett M, Rossini PM, Pascual-Leone A (2009b) Safety, ethical considerations, and application guidelines for the use of transcranial magnetic stimulation in clinical practice and research. Clin Neurophysiol 120:2008–2039.

Rossini PM et al. (2015) Non-invasive electrical and magnetic stimulation of the brain, spinal cord, roots and peripheral nerves: Basic principles and procedures for routine clinical and research application: An updated report from an I.F.C.N. Committee. Clin Neurophysiol 126:1071–1107.

Rossini PM, Barker AT, Berardelli A, Caramia MD, Caruso G, Cracco RQ, Dimitrijević MR, Hallett M, Katayama Y, Lücking CH (1994) Non-invasive electrical and magnetic stimulation of the brain, spinal cord and roots: basic principles and procedures for routine clinical application. Report of an IFCN committee. Electroencephalogr Clin Neurophysiol 91:79–92.

Salimi I, Frazier W, Reilmann R, Gordon AM (2003) Selective use of visual information signaling objects' center of mass for anticipatory control of manipulative fingertip forces. Exp brain Res 150:9–18.

Salthouse TA (1985) A theory of cognitive aging. North-Holland.

Sanchez JC, Gunduz A, Carney PR, Principe JC (2008) Extraction and localization of mesoscopic motor control signals for human ECoG neuroprosthetics. J Neurosci Methods 167:63–81.

Schabrun SM, Ridding MC, Miles TS (2008) Role of the primary motor and sensory cortex in precision grasping: a transcranial magnetic stimulation study. Eur J Neurosci 27:750–756.

Schalk G, Kubánek J, Miller KJ, Anderson NR, Leuthardt EC, Ojemann JG, Limbrick D, Moran D, Gerhardt LA, Wolpaw JR (2007) Decoding two-dimensional movement trajectories using electrocorticographic signals in humans. J Neural Eng 4:264–275.

Schmidt RA, et al (1979) Motor-output variability: A theory for the accuracy of rapid motor acts. Psychol Rev 86:415–451.

Schmidt RA, Zelaznik H, Hawkins B, Frank JS, Quinn JT (1979) Psychological Review.

Schneider TR, Buckingham G, Hermsdörfer J (2019) Torque-planning errors affect the perception of object properties and sensorimotor memories during object manipulation in uncertain grasp situations. J Neurophysiol 121:1289–1299.

Seidler RD, Bernard JA, Burutolu TB, Fling BW, Gordon MT, Gwin JT, Kwak Y, Lipps DB (2011) Motor control and Aging: Links to age-related brain structural, functional and biomechanical effects. Neurosci Biobehav Rev 34:721–733.

Shadmehr R, Smith MA, Krakauer JW (2010) Error Correction , Sensory Prediction , and Adaptation in Motor Control.

Shah-Basak PP, Sivaratnam G, Teti S, Francois-Nienaber A, Yossofzai M, Armstrong S,

Nayar S, Jokel R, Meltzer J (2020) High definition transcranial direct current stimulation modulates abnormal neurophysiological activity in post-stroke aphasia. Sci Rep 10:1–18.

Siebner HR, Hartwigsen G, Kassuba T, Rothwell JC (2009) How does transcranial magnetic stimulation modify neuronal activity in the brain? Implications for studies of cognition. Cortex 45:1035–1042.

Siswandari Y, Bode S, Stahl J (2019) Performance monitoring beyond choice tasks: The time course of force execution monitoring investigated by event-related potentials and multivariate pattern analysis. Neuroimage 197:544–556.

Slifkin AB, Newell KM (1999) Noise, information transmission, and force variability. J Exp Psychol Hum Percept Perform 25:837–851.

Slifkin AB, Vaillancourt DE, Newell KM (2000) Intermittency in the control of continuous force production. J Neurophysiol 84:1708–1718.

Small SA, Stern Y, Tang M, Mayeux R (1999) Selective decline in memory function among healthy elderly. Neurology 52:1392–1392.

Smith BW, Rowe JB, Reinkensmeyer DJ (2018) Real-time slacking as a default mode of grip force control: Implications for force minimization and personal grip force variation. J Neurophysiol 120:2107–2120.

Sosnoff JJ, Valantine AD, Newell KM (2006) Independence between the amount and structure of variability at low force levels. Neurosci Lett 392:165–169.

Starr A, Caramia M, Zarola F, Rossini PM (1988) Enhancement of motor cortical excitability in humans by non-invasive electrical stimulation appears prior to voluntary movement. Electroencephalogr Clin Neurophysiol 70:26–32.

Stein RB, Gossen ER, Jones KE (2005) Neuronal variability: Noise or part of the signal? Nat Rev Neurosci 6:389–397.

Stergiou N, Decker LM (2011) Human movement variability, nonlinear dynamics, and pathology: Is there a connection? Hum Mov Sci 30:869–888.

Stevens WD, Hasher L, Chiew KS, Grady CL (2008) A neural mechanism underlying memory failure in older adults. J Neurosci 28:12820–12824.

Svendsen JH, Madeleine P (2010) Amount and structure of force variability during short, ramp and sustained contractions in males and females. Hum Mov Sci 29:35–47.

Teo JTH, Swayne OBC, Cheeran B, Greenwood RJ, Rothwell JC (2011) Human theta burst stimulation enhances subsequent motor learning and increases performance variability. Cereb Cortex 21:1627–1638.

Therrien AS, Lyons J, Balasubramaniam R (2013) Continuous theta-burst stimulation to primary motor cortex reveals asymmetric compensation for sensory attenuation in bimanual repetitive force production. J Neurophysiol 110:872–882.

Therrien AS, Richardson BA, Balasubramaniam R (2011) Continuous theta-burst

stimulation to primary motor cortex reduces the overproduction of forces following removal of visual feedback. Neuropsychologia 49:2941–2946.

Tumer EC, Brainard MS (2007) Performance variability enables adaptive plasticity of 'crystallized' adult birdsong. Nature 450:1240–1244.

Uehara S, Mawase F, Celnik P (2018) Learning Similar Actions by Reinforcement or Sensory-Prediction Errors Rely on Distinct Physiological Mechanisms. :3478–3490.

Vaillancourt DE, Larsson L, Newell KM (2003a) Effects of aging on force variability, single motor unit discharge patterns, and the structure of 10, 20, and 40 Hz EMG activity. Neurobiol Aging 24:25–35.

Vaillancourt DE, Newell KM (2003) Aging and the time and frequency structure of force output variability. J Appl Physiol 94:903–912.

Vaillancourt DE, Slifkin AB, Newell KM (2002) Inter-digit Individuation and Force Variability in the Precision Grip of Young, Elderly, and Parkinson's Disease Participants. Motor Control 6:113–128.

Vaillancourt DE, Thulborn KR, Corcos DM (2003b) Neural Basis for the Processes That Underlie Visually Guided and Internally Guided Force Control in Humans. J Neurophysiol 90:3330–3340.

Vakil E, Agmon-Ashkenazi D (1997) Baseline performance and learning rate of procedural and declarative memory tasks: younger versus older adults. J Gerontol B Psychol Sci Soc Sci 52:P229-34.

Vakorin VA, Mišić B, Krakovska O, McIntosh AR (2011) Empirical and theoretical aspects of generation and transfer of information in a neuromagnetic source network. Front Syst Neurosci 5:96.

van Beers RJ (2009) Motor Learning Is Optimally Tuned to the Properties of Motor Noise. Neuron 63:406–417.

van Polanen V, Davare M (2015) Interactions between dorsal and ventral streams for controlling skilled grasp. Neuropsychologia 79:186–191.

Veldman MP, Maurits NM, Nijland MAM, Wolters NE, Mizelle JC, Hortobágyi T (2018) Spectral and temporal electroencephalography measures reveal distinct neural networks for the acquisition, consolidation, and interlimb transfer of motor skills in healthy young adults. Clin Neurophysiol 129:419–430.

Vernet M, Bashir S, Yoo WK, Perez JM, Najib U, Pascual-Leone A (2013) Insights on the neural basis of motor plasticity induced by theta burst stimulation from TMS-EEG. Eur J Neurosci 37:598–606.

Vieluf S, Temprado J, Berton E, Jirsa VK, Sleimen-malkoun R (2015) Effects of task and age on the magnitude and structure of force fluctuations : insights into underlying neuro-behavioral processes. :1–17.

Voss M, Bays PM, Rothwell JC, Wolpert DM (2007) An improvement in perception of

self-generated tactile stimuli following theta-burst stimulation of primary motor cortex. Neuropsychologia 45:2712–2717.

Wang DJJ, Jann K, Fan C, Qiao Y, Zang YF, Lu H, Yang Y (2018) Neurophysiological basis of multi-scale entropy of brain complexity and its relationship with functional connectivity. Front Neurosci 12:1–14.

White O, Davare M, Andres M, Olivier E (2013) The role of left supplementary motor area in grip force scaling. PLoS One 8:e83812.

Wischnewski M, Schutter DJLG (2015) Efficacy and Time Course of Theta Burst Stimulation in Healthy Humans. Brain Stimul 8:685–692.

Wolbrecht ET, Rowe JB, Chan V, Ingemanson ML, Cramer SC, Reinkensmeyer DJ (2018) Finger strength , individuation , and their interaction : Relationship to hand function and corticospinal tract injury after stroke. Clin Neurophysiol 129:797–808.

Woodruff-Pak DS, Vogel RW, Ewers M, Coffey J, Boyko OB, Lemieux SK (2001) MRI-Assessed Volume of Cerebellum Correlates with Associative Learning. Neurobiol Learn Mem 76:342–357.

Wu HG, Miyamoto YR, Castro LNG, Olveczky BP, Smith M a (2014) Temporal structure of motor variability is dynamically regulated and predicts motor learning ability. Nat Neurosci 17:312–321.

Zach N, Inbar D, Grinvald Y, Bergman H, Vaadia E (2008) Emergence of novel representations in primary motor cortex and premotor neurons during associative learning. J Neurosci 28:9545–9556.

Zhang W, Gordon AM, Fu Q, Santello M (2010) Manipulation after object rotation reveals independent sensorimotor memory representations of digit positions and forces. J Neurophysiol.

Zhang X, Wang D, Yu Z, Chen X, Li S, Zhou P (2017) EMG-Torque Relation in Chronic Stroke: A Novel EMG Complexity Representation with a Linear Electrode Array. IEEE J Biomed Heal Informatics 21:1562–1572.

Zhong JY, Moffat SD (2016) Age-related differences in associative learning of landmarks and heading directions in a virtual navigation task. Front Aging Neurosci 8:1–11.